Estimation of Groundwater Residence Time

Using Bomb-Produced Chlorine-36

April 2008

Yuki TOSAKI

Estimation of Groundwater Residence Time Using Bomb-Produced Chlorine-36

A Dissertation Submitted to
the Graduate School of Life and Environmental Sciences,
the University of Tsukuba
in Partial Fulfillment of the Requirements
for the Degree of Doctor of Philosophy in Science
(Doctoral Program in Geoenvironmental Sciences)

Yuki TOSAKI

Abstract

This study presents a methodology for quantitatively estimating residence time of modern groundwater by using bomb-produced ^{36}Cl. Total deposition of bomb-produced ^{36}Cl is estimated for the Oderbruch region, Germany and the Tsukuba Upland, Japan, from measured ^{36}Cl concentrations in groundwater. The proposed method is then applied to springs around Mt. Fuji, Japan.

The $^{36}Cl/Cl$ distribution in groundwater was investigated in the Oderbruch aquifer. The Oderbruch groundwaters appeared to be affected by saline water. The effect of its mixing was corrected using a two-component mixing model. Simulation of tracer transport for ^{3}H and ^{36}Cl derived scaling factors in the range of 0.3–1.22 (c.f. 2.5 based on the latitudinal distribution model). Estimated time-series variation of $^{36}Cl/Cl$ in the Oder River basin is in satisfactory agreement with the $^{36}Cl/Cl$ ratios in wine samples from the Rheingau, Germany. This suggests that an over-simplified model such as the latitudinal distribution model is not suitable for estimating the fallout pattern of bomb-produced ^{36}Cl. The results also imply that the scaling factor can be obtained by measuring ^{36}Cl in systematically-sampled groundwaters.

Depth profile of $^{36}Cl/Cl$ ratio in groundwater was investigated in the Tsukuba Upland. From the vertical distribution of ^{36}Cl, the total bomb-produced ^{36}Cl fallout over the upland is 2.3×10^{12} atoms/m^2, which corresponds to a scaling factor of 0.96. The ratio of the maximum bomb-peak fallout to the average natural background flux for the estimated local fallout history is consistent with measured data in Nepal. This agreement supports the validity of the obtained scaling factor. The results also confirmed that the local fallout history of ^{36}Cl can be estimated from a groundwater profile.

Residence time of spring waters around Mt. Fuji was estimated using bomb-produced ^{36}Cl.

To estimate time-series variation of $^{36}Cl/Cl$ ratio in the Mt. Fuji area, the Dye-3 fallout data was scaled using a scaling factor obtained for the Tsukuba Upland. Measured $^{36}Cl/Cl$ ratios in spring waters were compared to the predicted time-series variation under the assumption of piston flow. Distribution of spring water residence time is reasonably consistent with previous studies. However, residence time in the western foot obviously disagrees with previous one. This may be due to the difference in the natural background $^{36}Cl/Cl$ ratio among different slopes. It can be caused by the difference in the Cl^- concentration in precipitation.

Condition of the recharge area (i.e. the natural background level of $^{36}Cl/Cl$, chloride concentration in precipitation, and mean annual precipitation) has to be known correctly, otherwise errors may be directly enlarged in estimating residence times. However, the results obtained show the fundamental effectiveness of the method proposed in this study.

Keywords: bomb-produced ^{36}Cl; modern groundwater; residence time; groundwater dating; environmental tracer; accelerator mass spectrometry (AMS)

Contents

List of Tables

List of Figures

Chapter 1 Introduction

1.1 Importance of the knowledge of groundwater residence time

Groundwater is the second smallest among the four main reservoirs of water on the earth (i.e. the oceans, ice, groundwater and the atmosphere), yet is a vast resource of freshwater which is accessible for human use. Excluding frozen freshwater preserved in polar ice caps and continental glaciers, up to 98% of the remaining liquid freshwater is stored in the subsurface as groundwater (e.g. Baumgartner and Reichel, 1975, p. 14; Kayane, 1980, p. 43; Schlesinger, 1997, p. 346). Currently, at least 1.5 billion people in the world depend on groundwater resources for their drinking water (e.g. Alley et al., 2002), and the world's growing population will further increase demand on water supplies.

During the past several decades, groundwater has been extensively used for drinking, agricultural irrigation and industrial purposes. As a consequence, groundwater depletion has become a serious problem throughout the world, e.g. in the North China Plain (Shimada, 2000; Kondoh et al., 2001) and the High Plains of the USA (Tase, 2000). Since the mean residence time (renewal time) of groundwater reservoir is typically long (~1000 yr; e.g. Kayane, 1980, p. 43), groundwater is highly vulnerable to excess use and contamination; if groundwater depletion and contamination occur, aquifers will require considerably long time for its recovery and purification.

Therefore, the knowledge of groundwater residence time as well as groundwater flow system is crucial for the development and sustainable utilization of groundwater resources. Groundwater residence time (or groundwater age) is generally defined as the length of time since a water molecule has been isolated from the atmosphere (Davis and Bentley, 1982). According to the definition by Kazemi et al. (2006, p. 6), however, groundwater residence

time is the period of time for a recharged water molecule to discharge from the aquifer, while groundwater age can be defined at any point in the subsurface. For simplicity, this study does not make a distinction between the two terms ‘residence time’ and ‘age’, and employs the former general definition.

1.2 Use of environmental tracers in groundwater hydrology

Groundwaters are commonly classified into three or four categories by the range of their residence time (Kazemi et al., 2006, p. 9): modern (or young) groundwaters (residence time <50–60 yr), old groundwaters (60–50,000 yr), and very old groundwaters (>50,000 yr). In particular, the definition by Clark and Fritz (1997, pp. 172–173) distinguishes submodern groundwaters (residence time 60–1,000 yr) from old groundwaters.

Various radionuclides, stable isotopes and anthropogenic substances in groundwater can be very effective environmental tracers in the investigation of groundwater residence time and groundwater flow (e.g. Phillips and Castro, 2003; Kazemi et al., 2006). Each tracer used for groundwater dating has its appropriate time scale of application. For example, radiogenic ^{4}He and the long-lived radionuclides ^{36}Cl (half-life 3.01×10^{5} yr), ^{81}Kr (2.29×10^{5} yr) and ^{129}I (1.57×10^{7} yr) can cover the range of very old groundwaters, whereas the radionuclide ^{14}C (half-life 5,730 yr) is the most widely used tracer for dating old groundwaters. In addition to these common tracers, the radionuclides ^{32}Si (half-life ~140 yr) and ^{39}Ar (269 yr) are possible candidates to date submodern groundwaters, though successful applications are few up to the present.

For modern groundwaters, ^{3}H (tritium) has been one of the most useful environmental tracers (e.g. Egboka et al., 1983; Robertson and Cherry, 1989). Since large quantities of ^{3}H were produced during the atmospheric nuclear testing period, ^{3}H concentrations in

precipitation reached a peak at around 1963, resulting in a 'bomb pulse' in the hydrological cycle (e.g. Shimada et al., 1994; Yabusaki et al., 2003). However, due to the short half-life of ^{3}H (12.32 yr; Lucas and Unterweger, 2000), the ^{3}H bomb pulse has been attenuated significantly through radioactive decay and has become increasingly difficult to detect. This fact leads to a need for another environmental tracer (i.e. dating method) applicable in studies of modern groundwaters.

Recently, several alternative tracers have been successfully utilized for dating modern groundwaters: e.g. tritiogenic ^{3}He ($^{3}H/^{3}He$ method) (e.g. Schlosser et al., 1988), CFCs (Chlorofluorocarbons) (e.g. Busenberg and Plummer, 1992), SF_6 (sulfur hexafluoride) (e.g. Busenberg and Plummer, 2000) and ^{85}Kr (e.g. Smethie et al., 1992). Figure 1 shows the variations in atmospheric concentrations or fallout rates of these age-dating tracers including the bomb-derived radionuclides ^{3}H, ^{14}C and ^{36}Cl. Tritiogenic ^{3}He is the decay product of ^{3}H, while CFCs and SF_6 are man-made industrial gases, and the radionuclide ^{85}Kr (half-life 10.76 yr) is a fission product gas released by the reprocessing of fuel rods from nuclear reactors. Among these tracers, tritiogenic ^{3}He and CFCs, especially, are extensively used in groundwater studies.

1.3 Previous studies using chlorine-36

Chlorine-36 (^{36}Cl) is a long-lived radioisotope of chlorine with a half-life of 3.01×10^{5} yr. It decays to ^{36}Ar by β emission (98.10%) and to ^{36}S by electron capture (1.90%) (Firestone and Shirley (eds.), 1996, p. 114). On the contrary, chlorine has two naturally-occurring stable isotopes: ^{35}Cl (natural abundance 75.77%; Firestone and Shirley (eds.), 1996, p. 109) and ^{37}Cl (24.23%; Firestone and Shirley (eds.), 1996, p. 119).

Chlorine has a high electron affinity and exists primarily as the chloride anion (Cl^{-}) in the

environment (Bentley et al., 1986a). It generally does not participate in redox reactions and biochemical processes, and is not absorbed onto mineral surfaces except under low pH condition (Feth, 1981; Hem, 1985). Hence, it moves with water in the natural hydrological cycle without significant chemical interaction.

The simple geochemistry and conservative behavior make chloride an ideal tracer in hydrology (Herczeg and Edmunds, 2000). It also makes sampling for chloride and chlorine isotopes analyses very straightforward. With these advantages, ^{36}Cl has been used as an applied isotopic tracer in solute and water transport experiments in various scales: laboratory scale (e.g. Krupp et al., 1972), lysimeter scale (Saxena et al., 1994; Saxena and Jarvis, 1995), and small catchment scale (Nyberg et al., 1999).

As early as during the 1950s and 1960s, several attempts were made to measure ^{36}Cl in the natural environment: ^{36}Cl in rocks (Davis and Schaeffer, 1955), in saline lakes (Davis and Schaeffer, 1955; Bonner et al., 1961; Bagge and Willkomm, 1966), in rivers and freshwater lakes (Schaeffer et al., 1960; Bonner et al., 1961), in groundwater (Schaeffer et al., 1960; Tamers et al., 1969), in salts on the land surface (Bonner et al., 1961; Tamers et al., 1969), and in salts from deep mines (Tamers et al., 1969). Some of these pioneering studies indicated the presence of bomb-produced ^{36}Cl in precipitation and surface waters (Schaeffer et al., 1960; Bonner et al., 1961), and suggested the usefulness of ^{36}Cl as an environmental tracer (Schaeffer et al., 1960; Davis and DeWiest, 1966). However, the analytical techniques at the time had limited practical application due to the large sample size requirement and insufficient sensitivity; early investigations were accomplished using a screen-wall counter (Davis and Schaeffer, 1955; Schaeffer et al., 1960; Bonner et al., 1961), and subsequent researches applied liquid scintillation counting (Bagge and Willkomm, 1966; Ronzani and Tamers, 1966; Tamers et al., 1969; Roman and Airey, 1981; Florkowski and Schuszler, 1986).

The advent of accelerator mass spectrometry (AMS) in the late 1970s allowed widespread application of ^{36}Cl (Elmore et al., 1979). Application studies in the hydrological research field have been reviewed by Bentley et al. (1986a), Fabryka-Martin et al. (1987), Fontes and Andrews (1994) and Phillips (2000). Because of the long half-life, the main application of ^{36}Cl has been the dating of very old groundwaters in large-scale aquifers, e.g. the Great Artesian Basin of Australia (Bentley et al., 1986b; Torgersen et al., 1991), the Milk River aquifer in Alberta, Canada (Phillips et al., 1986; Nolte et al., 1990, 1991), and the Aquia aquifer in Maryland, USA (Purdy et al., 1987, 1996).

The basic principle of ^{36}Cl decay dating was tested and validated by Bentley et al. (1986b). They showed a decreasing pattern in measured $^{36}Cl/Cl$ ratios along the flow direction of groundwater in the Great Artesian Basin. The groundwater ages derived from ^{36}Cl (~1×10^6 yr) are in satisfactory agreement with hydrodynamic ages. However, the addition of chloride in the subsurface leads to the most common complication. The chloride may originate from dissolution of bedded evaporates, and diffusion of marine-origin chloride out of low permeability units.

In the case of the Milk River aquifer, the groundwater shows deceasing $^{36}Cl/Cl$ ratios from its recharge area toward the distal part of the aquifer. The aquifer also exhibits a notable increase of chloride concentration along the flow direction. Phillips et al. (1986) concluded that the distribution patterns of chloride and the $^{36}Cl/Cl$ ratio were caused by ion filtration, and estimated groundwater ages of ~2×10^6 yr at the distal part. In contrast to their results, subsequent studies estimated the source of salinity to be diffusion from the aquitard (Hendry and Schwartz, 1988), and from low permeability units within the aquifer (Fabryka-Martin et al., 1991); the groundwater ages estimated from ^{36}Cl were reduced to 0.25–0.5 × 10^6 yr and ~1×10^6 yr, respectively. Different interpretations were also given by Nolte et al. (1990,

1991).

Andrews and Fontes (1992) discussed the results of these studies and suggested that subsurface production of ^{36}Cl would generally be dominant compared to atmospheric input of cosmogenic ^{36}Cl. These studies were also reevaluated by Lehmann and Purtschert (1997) and Phillips (2000); they concluded that the ^{36}Cl produced in the subsurface does not dominate under common situations. If the source of chloride in groundwater is adequately accounted for, therefore, ^{36}Cl decay dating is feasible in most aquifers.

Coupled with some dating techniques, groundwater can serve as an archive of past climate variation (Shanley et al., 1998; Edmunds, 2005; Shimada, 2005). From this perspective, ^{36}Cl decay dating provides a time scale for reconstructing paleoclimatic variation (e.g. variation of $\delta^{18}O$) beyond the ^{14}C dating range (>40,000 yr B.P.) (e.g. Shimada et al., 1999). On the contrary, a variation of ^{36}Cl concentration itself indicates paleoclimatic information, e.g. recharge rate, evaporation rate and precipitation (Stute et al., 1993; Andrews et al., 1994; Purdy et al., 1996). Recent applications of ^{36}Cl decay dating include combination use of ^{36}Cl and other age-dating tracers to better constrain the obtained groundwater ages (Patterson et al., 2005), to understand the possibilities and limitations of each dating technique (Lehmann et al., 2003), to validate the ^{81}Kr dating method (Sturchio et al., 2004), and to calibrate or correct the ^{4}He dating method (Mahara et al., 2007; Kulongoski et al., 2008).

For modern groundwaters, bomb-produced ^{36}Cl can provide a potential dating tool covering the last ~50 years (Bentley et al., 1982). Advantages of bomb-produced ^{36}Cl as a hydrological tracer are the facts that the peak is well-defined, and that the long half-life of ^{36}Cl makes decay attenuation negligible on the time scale of several decades to centuries (e.g. Fabryka-Martin et al., 1987; Fontes and Andrews, 1994). The ^{36}Cl bomb pulse has heretofore been used to trace water movement in the unsaturated zone and to estimate infiltration rates

especially in arid and semi-arid regions (Norris et al., 1987; Phillips et al., 1988; Scanlon et al., 1990; Cecil et al., 1992; Scanlon, 1992; Walker et al., 1992; Cook et al., 1994; Liu et al., 1995).

However, there are few studies applying the ^{36}Cl bomb pulse to groundwaters, except for its applications simply as a qualitative indicator of the presence of young water (e.g. Purdy et al., 1987; Andrews et al., 1994). In combination with ^{3}H, the ^{36}Cl bomb pulse has been used to estimate groundwater recharge rate in a fractured rock aquifer (Cook and Robinson, 2002), and to deduce transport parameters (flow velocity and dispersivity) of a sandy aquifer (Balderer et al., 2004). Studies focusing on the application of bomb-produced ^{36}Cl as a dating tool are particularly infrequent. Vogt et al. (1994) attempted to estimate groundwater residence time in perched aquifers by using temporal variation in the $^{36}Cl/Cl$ ratio over three years.

The only available approach for quantitatively investigating the potential use of bomb-produced ^{36}Cl has been the reconstruction of ^{36}Cl fallout rates from $^{36}Cl/Cl$ ratios in groundwater (Corcho Alvarado et al., 2005; Tosaki et al., 2007). The ^{36}Cl fallout rates in Denmark reconstructed by Corcho Alvarado et al. (2005) exceeded the estimates based on the data from the Dye-3 ice core (Synal et al., 1990). They attributed it to storage and recycling of chlorine (including bomb-produced ^{36}Cl) in the biosphere, which has been suggested by recent studies (Cornett et al., 1997; G.M. Milton et al., 1997, 2003; J.C.D. Milton et al., 1997; Scheffel et al., 1999; Blinov et al., 2000). Contrary to their results, the ^{36}Cl fallout rates in Germany reconstructed by Tosaki et al. (2007) showed a consistent pattern with the Dye-3 fallout data. However, no detailed methodological description has been presented in the literature for quantitatively estimating groundwater residence time using bomb-produced ^{36}Cl.

1.4 Purpose and outline of the present study

This study aims to provide a methodology on the estimation of groundwater residence time using bomb-produced ^{36}Cl (^{36}Cl bomb-pulse dating). This is the first attempt to quantitatively utilize bomb-produced ^{36}Cl as a dating tool. The obtained results give insights into requirements and limitations on the application of this method.

The methodology has been developed by referring to previous studies on the ^{36}Cl bomb pulse in ice cores (Chapter 2). The basis of the proposed method was investigated in a river-recharged aquifer in the Oderbruch area, Germany (Chapter 4). Bomb-produced ^{36}Cl was then applied to estimate residence time of spring waters in the Mt. Fuji area, central Japan (Chapter 6). For this application, a reference curve of bomb-produced ^{36}Cl fallout in Japan has been constructed using the depth profile of ^{36}Cl concentration in groundwater of the Tsukuba Upland (Chapter 5).

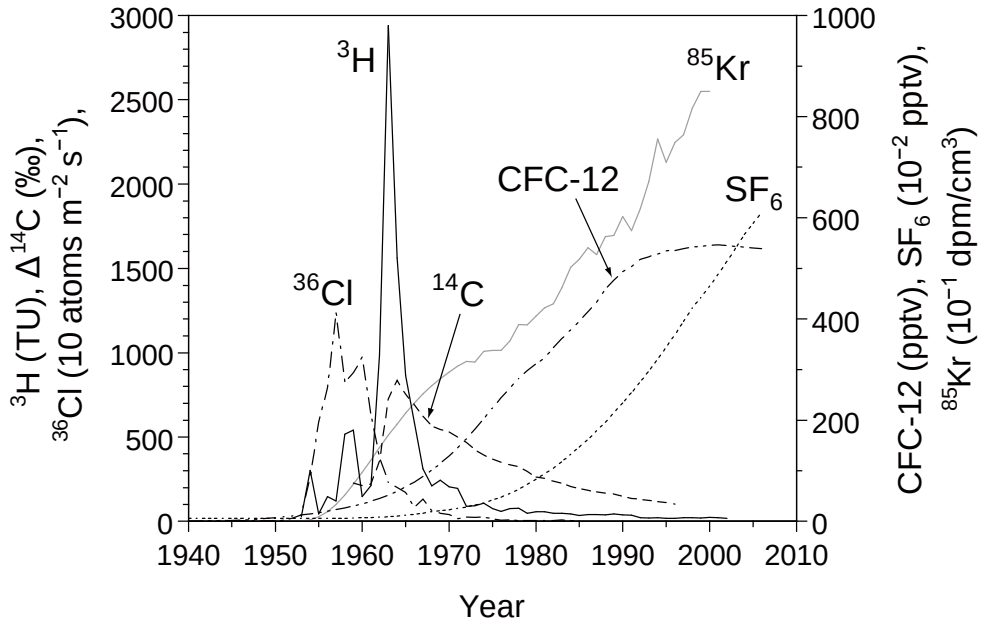

Figure 1 Atmospheric concentrations or fallout rates of environmental tracers used for dating modern groundwaters: ^{36}Cl fallout rates at the Dye-3 site, Greenland (Synal et al., 1990), ^{3}H concentration in precipitation at Ottawa, Canada (IAEA/WMO, 2004), atmospheric Δ^{14}C record at Vermunt, Austria (1959–1983; Levin et al., 1994) and Schauinsland, Germany (1984–1996; Levin and Kromer, 1997), and atmospheric concentrations of CFC-12, SF_6 (USGS CFC Lab) and ^{85}Kr (IAR Freiburg).

Chapter 2 Principle of chlorine-36 dating

2.1 Production and distribution of chlorine-36 in the environment

Chlorine-36 in the environment originates from various sources (Figure 2), which can be broadly classified into two categories: natural production and anthropogenic production. Natural ^{36}Cl is produced in the atmosphere, near the surface and in the subsurface, whereas anthropogenic ^{36}Cl was produced by nuclear weapons testing in the 1950s and has also been released from the activities of nuclear facilities. Mechanisms and characteristics of each production are described in the following subsections.

2.1.1 Natural production in the atmosphere

In the atmosphere, ^{36}Cl is mainly produced through spallation of ^{40}Ar by energetic primary and secondary cosmic rays. Its formation via neutron activation of ^{36}Ar is quantitatively insignificant as suggested from the cross-section measurement by Jiang et al. (1990): ~10% of total atmospheric production (Huggle et al., 1996; Parrat, 1997). Contributions from other nuclear reactions (i.e. spallation of potassium and calcium, and neutron activation of ^{35}Cl) are negligible due to the low abundances of parent isotopes in the atmosphere.

The global mean production rate of ^{36}Cl in the atmosphere has been estimated to be 8.7–22 atoms m^{-2} s^{-1} (Table 1), which is much lower than that of lighter long-lived radionuclides produced from nitrogen (N) and oxygen (O) (i.e. ^{10}Be and ^{14}C). Atmospheric production mainly occurs in the stratosphere with the remainder in the troposphere; the estimated contribution of stratospheric production ranges from 60–70% (Lal and Peters, 1967; Oeschger et al., 1970) to ~90% (Huggle et al., 1996; Parrat, 1997) of total production.

Most of the ^{36}Cl atoms in the stratosphere (~90%) are associated with gaseous HCl (Wahlen et al., 1991).

After production, ^{36}Cl leaves the stratosphere and enters the troposphere with a mean residence time of about 2 years (Synal et al., 1990). The ^{36}Cl produced in the atmosphere is mixed with marine-derived stable chlorine (from sea spray), and falls quickly as wet or dry deposition onto the earth's surface. The mean residence time in the troposphere is expected to be on the order of weeks, according to the estimates for atmospheric aerosols (Turekian et al., 1977; Bleichrodt, 1978; Raisbeck et al., 1981). In addition, measurements of ^{36}Cl in wet-only and bulk precipitation samples showed that dry deposition accounts for ~25% of total ^{36}Cl deposition (Hainsworth et al., 1994).

Because of the shielding effect of the earth's geomagnetic field, production of ^{36}Cl in the stratosphere is strongly dependent on the geomagnetic latitude (Lal and Peters, 1967). Maximum production occurs at the geomagnetic poles where the cut-off rigidity is minimal (e.g. Kodama, 1968). However, subsequent fallout of ^{36}Cl is expected to follow a totally different latitudinal pattern, with greatest deposition at mid-latitudes (Lal and Peters, 1967). This pattern is primarily due to the injection of stratospheric air masses into the troposphere, which occurs mainly at mid-latitudes (Reiter, 1975; Holton et al., 1995).

The variation of ^{36}Cl fallout with latitude calculated by Bentley et al. (1986a) was based on a simplified model proposed by Lal and Peters (1967). Since the global mean production rate used by Bentley et al. (1986a) (16 atoms m^{-2} s^{-1}) included relatively large contribution from neutron activation of ^{36}Ar (5 atoms m^{-2} s^{-1}), Andrews and Fontes (1992) proposed to revise the Bentley et al. model, that is, to use the original Lal and Peters model. However, recent studies calculated the global mean production rate as ~20 atoms m^{-2} s^{-1} (see Table 1). Figure 3 shows the revised Lal and Peters model scaled with a global mean production rate of

20 atoms m^{-2} s^{-1}.

Atmospheric chloride is mainly of oceanic origin, which decreases exponentially with increasing distance from the coast (Eriksson, 1960; Keywood et al., 1997). Therefore, the atomic ratio of ^{36}Cl to total chloride ($^{36}Cl/Cl$) in precipitation or recharging water is largely determined by the latitudinal pattern of atmospheric ^{36}Cl fallout and delivery of marine chloride. The distribution of $^{36}Cl/Cl$ ratio over the continental United States was estimated by Bentley et al. (1986a) using the chloride deposition data from Eriksson (1960). The estimated $^{36}Cl/Cl$ distribution pattern is basically in agreement with measured values for pre-bomb groundwaters (Moysey et al., 2003). Similar approach was applied in the southeastern part of Australia (Davie et al., 1989).

2.1.2 Natural production near the surface

Surface production of ^{36}Cl takes place in the first few meters of the ground surface (also in the ocean surface). The main reactions are spallation of calcium and potassium by energetic secondary neutrons, and thermal neutron activation of ^{35}Cl in surface rocks. Although most types of rock contain only a small amount of ^{35}Cl, the relatively large neutron-activation cross section of ^{35}Cl leads to significant ^{36}Cl production. Since cosmic rays are generally attenuated by the atmosphere and the upper lithosphere, the production rate of ^{36}Cl decreases exponentially with depth, and hence is generally negligible below a few meters depth. The ^{36}Cl production through spallation of ^{40}Ar is relatively insignificant, because argon is not abundant at the surface.

Production of ^{36}Cl mainly occurs within mineral grains; accordingly, weathering reactions are essential processes for such ^{36}Cl to move through the unsaturated zone and enter groundwater. Andrews et al. (1991) and Andrews and Fontes (1992) suggested that the ^{36}Cl

released by weathering is more important than atmospheric input in recharge areas of many aquifers. However, Phillips (2000) reevaluated its contribution and concluded that surface production is insignificant in most temperate regions, except for the area of high elevation.

2.1.3 Natural production in the subsurface

Virtually all ^{36}Cl production in the deep subsurface occurs due to thermal neutron activation of ^{35}Cl. Because of the relatively large cross section of ^{35}Cl, measurable amounts of ^{36}Cl can be produced through the reaction. Neutron activation of ^{36}Ar is infrequent in the subsurface due to the scarcity of argon.

Thermal neutron flux in the deep subsurface arises from the decay of the uranium (U) and thorium (Th) decay series radionuclides. The uranium and thorium decay series produce both direct fission neutrons and secondary neutrons from alpha particle adsorption or neutron emission reactions on light elements such as Al, Na, O, Mg and Si (e.g. Feige et al., 1968). The secondary neutrons are more common than fission neutrons in most rocks (Bentley et al., 1986a).

2.1.4 Anthropogenic production

In addition to the natural production of ^{36}Cl, anthropogenic activities have also produced large quantities of ^{36}Cl in the environment. Significant amounts of ^{36}Cl were produced by thermonuclear testing on small islands or barges; the main sources were the explosions on barges at Bikini and Eniwetok atolls in 1954, 1956 and 1958 (Zerle et al., 1997). Neutrons released from the testing activated ^{35}Cl in seawater (Dyrssen and Nyman, 1955). Part of these bomb-produced ^{36}Cl had reached the stratosphere and spread over the globe.

High concentrations of ^{36}Cl (~6.2×10^8 atoms/L; mean value of 5 samples) were

measured in precipitation collected at Long Island, New York, USA between 1957 and 1960 (Schaeffer et al., 1960). In contrast, subsequent measurements of precipitation samples collected at La Jolla, California, USA in 1979 (Finkel et al., 1980), and at Tucson, Arizona, USA in 1982 (Bentley et al., 1982) showed lower concentrations: 1.8×10^6 atoms/L and $2.6–3.1 \times 10^6$ atoms/L, respectively. These results indicated that the ^{36}Cl concentration in precipitation had decreased by 1–2 orders of magnitude from 1960 to around 1980.

Detailed fallout history of ^{36}Cl has been preserved in ice cores, e.g. from the Dye-3 site, Greenland (65°11'N, 43°50'W) (Elmore et al., 1982; Suter et al., 1987; Synal et al., 1990), showing a ^{36}Cl peak in the late 1950s (~7 years prior to the ^{3}H peak). Figure 4 gives the annual fallout rates of ^{36}Cl for 1945–1985 calculated from measured ^{36}Cl data, ice density, accumulation rates and ice weight by Synal et al. (1990). As the figure shows, the ^{36}Cl fallout rate has increased from 1950, peaked in the late 1950s by 2–3 orders of magnitude, and afterward declined exponentially. The enhanced fallout rate returned to pre-bomb level in around 1985. Ice core records of bomb-produced ^{36}Cl have been obtained for other locations over the globe: the Upper Fremont Glacier, Wyoming, USA (43°N) (Cecil and Vogt, 1997; Cecil et al., 1998, 1999), the Nangpai Gosum Glacier, Nepal (28°N) (Green et al., 2000), the Inilchek Glacier, Kyrgyzstan (42°N) (Green et al., 2004), the Guliya Ice Cap, China (35°N) (Green et al., 2004) and Vostok, Antarctica (79°S) (Delmas et al., 2004).

The latitudinal deposition model for atmospheric cosmogenic nuclides' fallout (Lal and Peters, 1967; Figure 3) is an empirically-developed model according to the observed pattern in stratospheric fallout of fission products from nuclear tests (e.g. ^{90}Sr; Machta, 1959, 1965). Hence, the fallout of bomb-produced ^{36}Cl is also expected to show a similar latitudinal distribution. On the contrary, Phillips et al. (1988) used the observed data for ^{185}W (Lockhart et al., 1959) to estimate the latitudinal pattern of bomb-produced ^{36}Cl fallout. This model,

which was later revised by Phillips (2000), also shows greatest deposition at mid-latitudes. For simplicity, however, the Lal and Peters model has generally been applied to estimate the local bomb-produced ^{36}Cl fallout in most of previous studies (e.g. J.C.D. Milton et al., 1997; Corcho Alvarado et al., 2005).

In addition to latitude, precipitation amount may affect fallout rates of bomb-produced radionuclides (e.g. Peterson, 1970). Monthly ^{36}Cl fallout variation proportional to monthly precipitation amount was actually observed for cosmogenic ^{36}Cl (Knies et al., 1994). Based on Knies et al.'s results, Phillips (2000) proposed a precipitation correction scheme, which uses local deviations in precipitation from mean latitudinal precipitation to normalize measured ^{36}Cl deposition rates.

However, empirical data over the United States by Moysey et al. (2003) did not exhibit a clear correlation between cosmogenic ^{36}Cl flux and precipitation, presumably due to other controlling factors. Given similar precipitation dependence for bomb-produced ^{36}Cl fallout, the application of the precipitation correction proposed by Phiilips (2000) will not necessarily lead to improvement of results. Therefore, this study does not employ the precipitation correction to ^{36}Cl deposition.

Table 2 summarizes the previously measured deposition data of bomb-produced ^{36}Cl, showing a large variation. These values appeared to be influenced by the combination of the above-mentioned factors. The data have been mainly obtained from the depth–concentration profile of ^{36}Cl in soil. As a result, most of these data are from arid and semi-arid regions.

Anthropogenic ^{36}Cl can also be produced locally through neutron activation of ^{35}Cl by underground nuclear tests (Ogard et al., 1988; Phillips et al., 1990) and from the activities of nuclear facilities (Beasley et al., 1992, 1993).

2.2 Decay dating of very old groundwaters

This section briefly describes the basic principle of ^{36}Cl decay dating in order to understand the behavior of ^{36}Cl in groundwater. Once in the aquifer, meteoric ^{36}Cl due to atmospheric production gradually decays with a half-life of 301,000 yr until the establishment of secular equilibrium between decay and subsurface production (Figure 5). At the same time, the addition of chloride from the aquitard may often occur, which has the secular equilibrium ^{36}Cl/Cl ratio.

If these processes are accounted for, the mixing equation is described as follows (Phillips et al., 1986):

$$RC = R_{\mathrm{i}} C_{\mathrm{i}} \mathrm{e}^{-\lambda t} + R_{\mathrm{e}} C_{\mathrm{i}} (1 - \mathrm{e}^{-\lambda t}) + R_{\mathrm{e}} (C - C_{\mathrm{i}}) \tag{1}$$

where R is the ^{36}Cl/Cl ratio, C is the Cl^- concentration, R_{i} and C_{i} are the initial values of ^{36}Cl/Cl and Cl^-, R_{e} is the ^{36}Cl/Cl ratio at secular equilibrium, λ is the decay constant of ^{36}Cl (2.30×10^{-6} yr^{-1}), t is the groundwater age. The first term expresses the radioactive decay of meteoric (cosmogenic) ^{36}Cl, the second term represents the buildup of ^{36}Cl due to subsurface production, and the third term accounts for the addition of chloride in the aquifer.

Rearrangement of Equation (1) leads to the following equation to estimate groundwater residence time:

$$t = \frac{-1}{\lambda} \ln \frac{C(R - R_{\mathrm{e}})}{C_{\mathrm{i}}(R_{\mathrm{i}} - R_{\mathrm{e}})}. \tag{2}$$

This equation does not account for the mixing of subsurface chloride which has the ^{36}Cl/Cl ratio markedly different from R_{e}.

Chlorine-36 content in water is usually expressed in two different ways: the ^{36}Cl

concentration (the number of ^{36}Cl atoms in one liter of water), and the $^{36}Cl/Cl$ ratio (the atomic ratio of ^{36}Cl to stable chlorine). Many processes affect these values: radioactive decay, in situ production, addition of chloride, evaporation or dilution, mixing, and ion filtration. The ^{36}Cl concentration can be affected by evapotranspiration or dilution, subsurface production and radioactive decay, and is not changed by the addition of stable chlorine. On the contrary, the $^{36}Cl/Cl$ ratio is not affected by evapotranspiration or dilution, while it changes with the addition of stable chlorine, subsurface production and radioactive decay. Several types of plots using any two components among the $^{36}Cl/Cl$ ratio, the ^{36}Cl concentration, and the chloride concentration are generally utilized to identify dominant processes affecting the ^{36}Cl content in groundwater (Bird et al., 1991; Davis et al., 1998; Figure 6).

Determination of the initial $^{36}Cl/Cl$ ratio (R_i) and the secular equilibrium $^{36}Cl/Cl$ ratio (R_e) is most essential in ^{36}Cl decay dating. The initial ratio can be determined by measuring long-term precipitation (e.g. Hainsworth et al., 1994; Knies et al., 1994) or shallow groundwater which does not include bomb-produced ^{36}Cl. However, several problems on the determination of the initial value were discussed by Davis et al. (1998). As an example, the ^{36}Cl production rate in the atmosphere is usually assumed to have been constant through time, whereas paleoenvironmental records from ice cores (Baumgartner et al., 1998) and packrat middens (Plummer et al., 1997) suggest that the production rate has undergone some variation.

In contrast, the secular equilibrium ratio can be evaluated from the U and Th contents in rocks comprising the aquifer (Andrews et al., 1986; Lehmann and Loosli, 1991). The knowledge of such information in study areas is therefore necessary when one attempts to apply ^{36}Cl decay dating.

2.3 Bomb-pulse dating of modern groundwaters

Any practical method for estimating groundwater residence time using bomb-produced ^{36}Cl has not given in previous studies. Hence, this study describes and proposes a possible methodology. As most of other age-dating tracers (e.g. CFCs, SF_6 and ^{85}Kr) require their detailed historical concentrations in the atmosphere as a reference, the local fallout history of ^{36}Cl has to be estimated prior to the application of bomb-produced ^{36}Cl.

According to Green et al. (2004), the ^{36}Cl concentration profiles have almost identical shapes for the ice cores from the Dye-3 site (Greenland) (Synal et al., 1990), the Inilchek Glacier (Kyrgyzstan) and the Guiliya Ice Cap (China). It can therefore be assumed that the fallout pattern of bomb-produced ^{36}Cl is essentially uniform at least in the northern hemisphere. The local fallout history of bomb-produced ^{36}Cl can then be estimated by linearly scaling the Dye-3 fallout values (Synal et al., 1990), which is currently the most detailed data on the ^{36}Cl bomb pulse.

Several previous studies used latitudinal correction factors based on the Lal and Peters model (Figure 3) to estimate local fallout rates of bomb-produced ^{36}Cl (e.g. J.C.D. Milton et al., 1997; Corcho Alvarado et al., 2005). In these cases, the Dye-3 fallout data were directly scaled and the difference in latitudinal distributions of bomb-produced ^{36}Cl and cosmogenic ^{36}Cl has not been considered. However, results of ^{36}Cl measurements in several ice cores suggest some differences (Green et al., 2000). Therefore, the present study deals with these two components separately.

The scaling factor (*SF*) defined here is the ratio of bomb-produced ^{36}Cl fallout for a given area to that for the Dye-3 site. It accounts for the difference in fallout rates mainly due to the differences in latitude and precipitation amount. The simplest approach for obtaining a *SF* value is to compare total bomb-produced ^{36}Cl depositions between two sites (i.e. the site of

interest and the Dye-3 site). An estimate of total deposition can be obtained from ice core, soil and groundwater profiles (Table 2).

The ^{36}Cl flux for 1560–1920 AD at the Dye-3 site is 20 ± 6 atoms m^{-2} s^{-1} (Synal et al., 1994), which can be taken as the natural background flux. This value is subtracted from annual values for 1945–1985 (Synal et al., 1990) to obtain yearly values of bomb-produced ^{36}Cl fallout at the Dye-3 site. If a *SF* value is obtained for a given area, the Dye-3 values can be linearly scaled to predict the local fallout history of ^{36}Cl.

To allow comparison with measured ^{36}Cl/Cl ratios of groundwater samples, the ^{36}Cl fallout values has to be converted to the ^{36}Cl/Cl unit. The following mass balance equation can be used to derive the ^{36}Cl/Cl ratio (Andrews et al., 1994; Fontes and Andrews, 1994):

$$R = \frac{F \times 3.156 \times 10^{7}}{P \times 10^{-3} \times C_{\mathrm{p}} \times 6.022 \times 10^{23} / 35.45} \tag{3}$$

where R is the measured ^{36}Cl/Cl ratio, F is the ^{36}Cl fallout (atoms m^{-2} s^{-1}), P is the mean annual precipitation (mm), and C_{p} is the Cl^{-} concentration in the precipitation (mg/L). Similar mass balance relationship holds for the ^{36}Cl concentration as follows (Andrews et al., 1986; Fontes and Andrews, 1994):

$$A = \frac{F \times 3.156 \times 10^{7}}{P}\left(\frac{100}{100 - E}\right) \tag{4}$$

where A is the ^{36}Cl concentration, E is the mean annual evapotranspiration rate (%).

Equation (3) enables the derivation of the tentative ^{36}Cl/Cl time series contributed only from bomb-produced component. Finally, the ^{36}Cl/Cl time-series variation is obtained by adding the the natural background value. It can be determined from the lower limit of

measured $^{36}Cl/Cl$ ratios in groundwater at a given study site, which have not been affected by bomb-produced ^{36}Cl. As a consequence, a time-series variation of ^{36}Cl can be estimated for a study area. If piston flow is reasonably assumed, comparison between the predicted time-series variation and measured $^{36}Cl/Cl$ ratios gives estimates of groundwater residence times.

Table 1
Previously calculated estimates of the global mean production rate of ^{36}Cl in the atmosphere

Production rate (atoms m^{-2} s^{-1})	Reference
11	Lal and Peters (1967)
22	Oeschger et al. (1970)
8.7	O'Brien (1979)
19	Blinov (1988)
11.8	Masarik and Reedy (1995)
19	Huggle et al. (1996)
20	Parrat (1997)
18.8	Masarik and Beer (1999)
16	Lazarev (2003)

Table 2
Measured total depositions of bomb-produced ^{36}Cl in different locations

Location	Latitude	^{36}Cl fallout (10^{12} atoms/m^2)	Precipitation (mm/yr)	Profile	Reference
Dye-3, Greenland	65°N	2.4	500*	Ice core	Synal et al. (1990)
Hanford, WA, USA	47°N	1.1–2.5	160–210	Soil	Prych (1998)
Borden, ON, Canada	44°N	5.75	1,000†	Groundwater	Bentley et al. (1982)
Yucca Mountain, NV, USA	37°N	6.0 ± 1.1	150	Soil	Norris et al. (1987)
Socorro, NM, USA	34°N	0.7–0.9	250*	Soil	Phillips et al. (1988)
Las Cruces, NM, USA	32°N	2.5	230	Soil	Phillips et al. (1988)
Hueco Bolson, TX, USA	31°N	2.5	280	Soil	Scanlon et al. (1990); Scanlon (1992)
Murbko, SA, Australia	34°S	0.4	260	Soil	Cook et al. (1994)
Borrika, SA, Australia	35°S	1.3–2.4	340	Soil	Cook et al. (1994)
Naracoorte Ranges, SA, Australia	36–37°S	1.2–2.3	500–650	Soil	Walker et al. (1992); Cook et al. (1994)

* Data from Phillips (2000).

† Data from J.C.D. Milton et al. (1997).

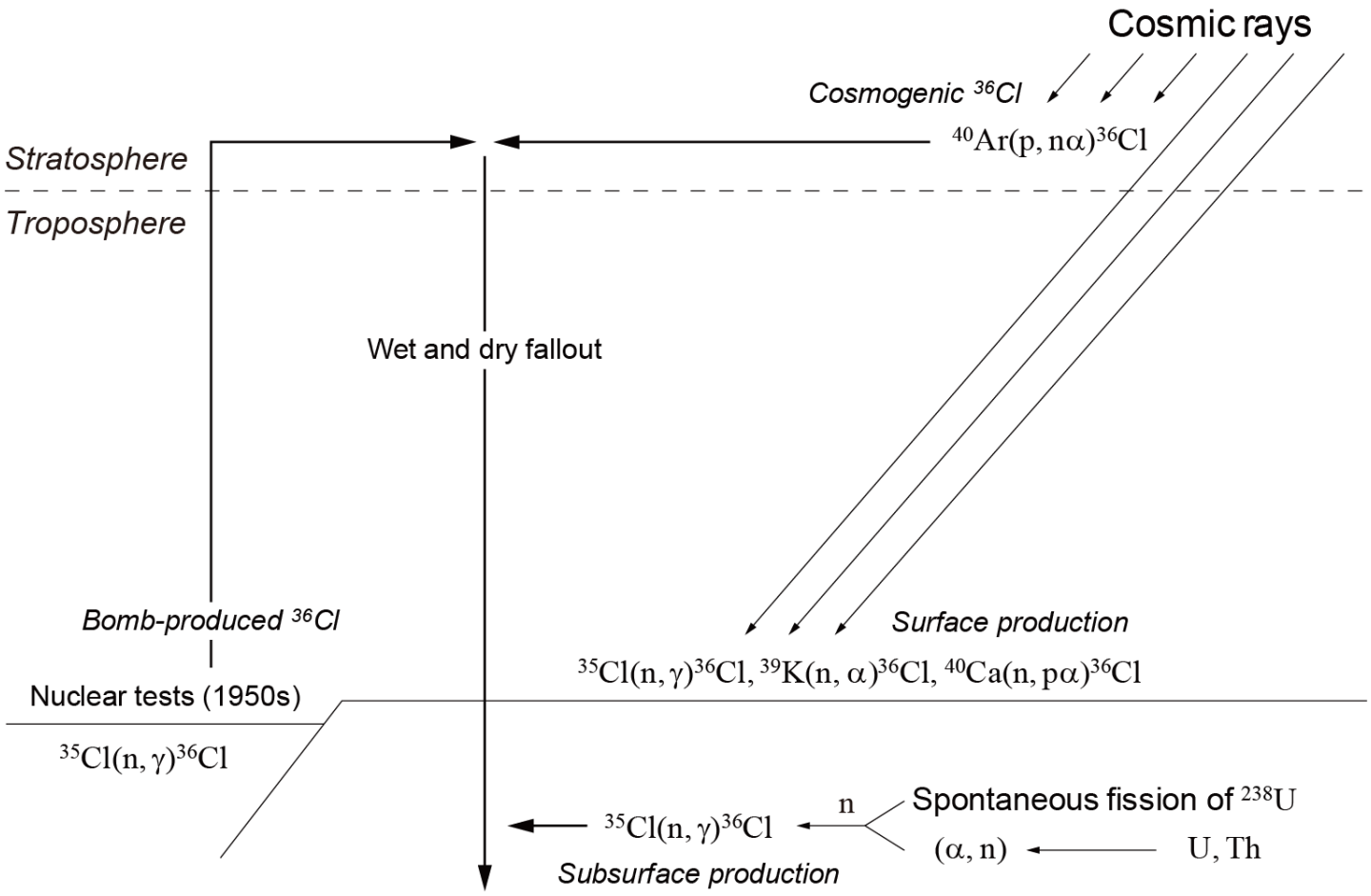

Figure 2 Production of ^{36}Cl in the environment

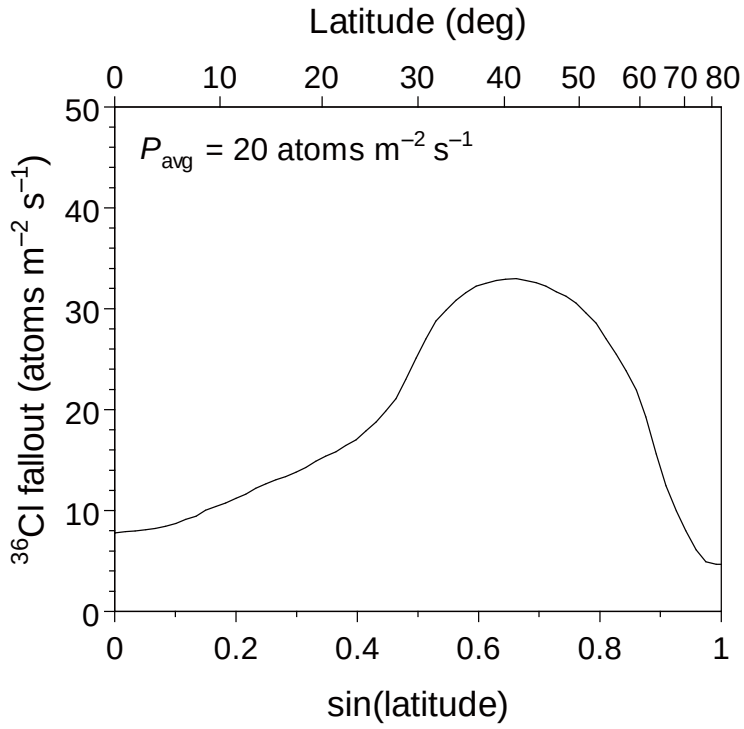

Figure 3 Latitudinal variation of ^{36}Cl fallout. Predicted latitudinal pattern is from Lal and Peters (1967). The global mean production rate (P_{avg}) was assumed to be 20 atoms m^{-2} s^{-1} (see Table 1).

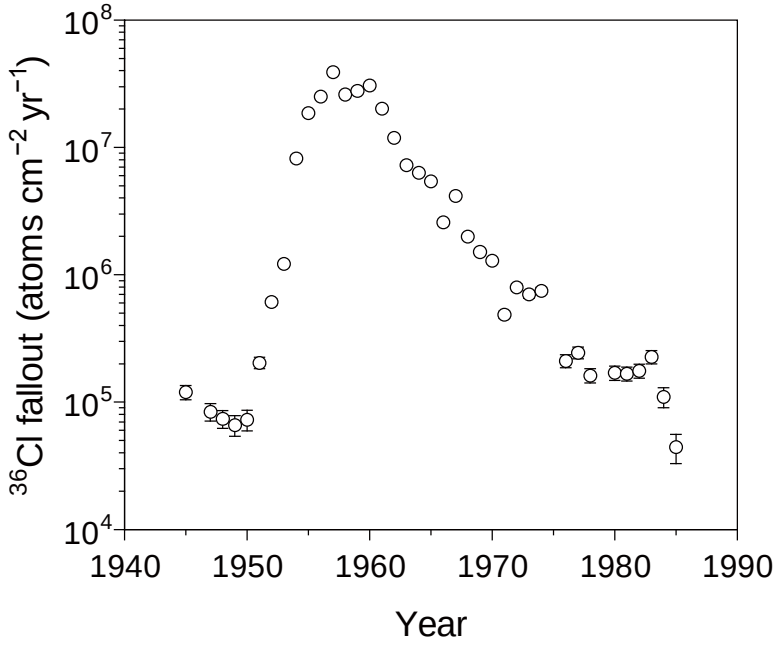

Figure 4 ^{36}Cl fallout history measured at the Dye-3 site, Greenland. Fallout rates of ^{36}Cl were deduced from the Dye-3 ice core profile spanning 1945–1985 (Synal et al., 1990).

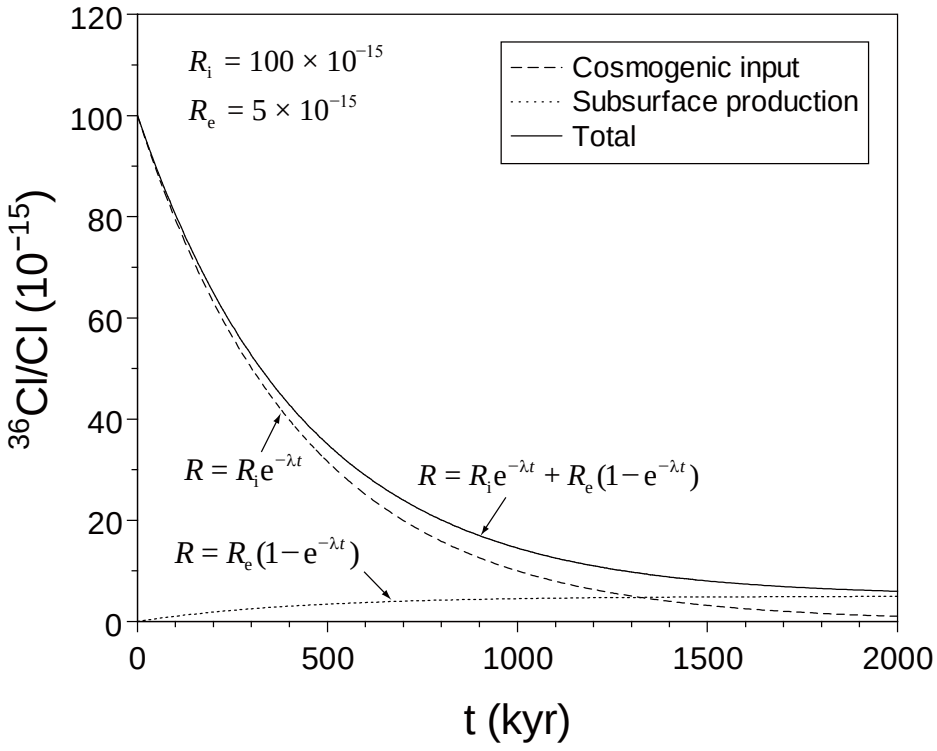

Figure 5 Variation of ^{36}Cl/Cl ratio with time due to decay of cosmogenic input and to subsurface production (modified from Fontes, 1989; Mahara et al., 2006). The values of 100×10^{-15} and 5×10^{-15} were assumed for the initial ^{36}Cl/Cl ratio (R_i) and the secular equilibrium ^{36}Cl/Cl ratio (R_e), respectively.

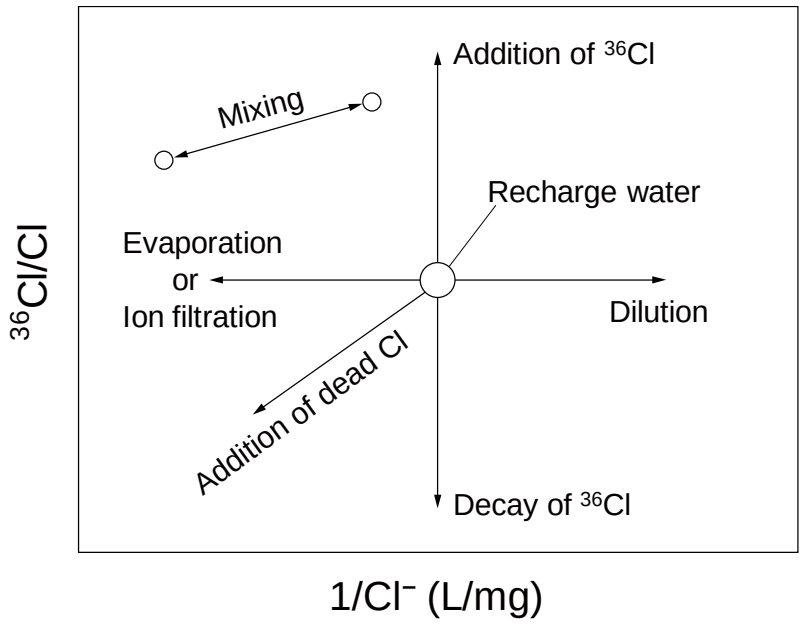

Figure 6 Physical and chemical processes affecting $^{36}Cl/Cl$ ratios and Cl^- concentrations (after Bird et al., 1991; Davis et al., 1998).

Chapter 3 Measurement of chlorine-36

3.1 Sample preparation

For the measurement of ^{36}Cl, water samples were prepared as silver chloride (AgCl). Since the isobar ^{36}S (natural abundance 0.02%; Firestone and Shirley (eds.), 1996, p. 113) severely interferes with the ^{36}Cl measurement by AMS, chemical reduction of sulfur is of major importance in preparing AgCl samples. Removal of sulfur (in the form of SO_4^{2-}) can be achieved by precipitation of $BaSO_4$ (e.g. Conard et al., 1986), by differential elution from an anion exchange resin (Vogt and Herpers, 1988), and by absorption onto a cation exchange resin (in the form of $BaSO_4$) (Jiang et al., 2004). The sample preparation scheme described here (Figure 7) has been developed according to standard procedures (e.g. Conard et al., 1986). The main part of the scheme including sulfur reduction process was performed in an air-conditioned room to prevent additional sulfur contamination and also under dark conditions to avoid the photolytic decomposition of AgCl.

Before the first step shown in the figure, groundwater and precipitation samples with low Cl^- concentration are often required to be concentrated either by evaporative concentration, vacuum distillation (e.g. Conard et al., 1986), or anion exchange (e.g. Vogt et al., 1994). The present study employed an anion exchange column method because it can readily process large-volume samples with minimal risk of contamination from the atmosphere.

An ion exchange system was originally developed in order to further increase the processing efficiency. This system includes a pump (Masterflex No. 7553-80, Cole-Parmer) with four pump heads and anion exchange columns. Each pump head uses Tygon tubing (inner diameter 3.1 mm) to transport the sample into a column. The employment of this system enabled simultaneous processing of four samples, and reduced time for sample

pretreatment.

As an anion exchange column, approximately 20 mL (wet volume) of AG 4-4X anion exchange resin in the free-base form (100–200 mesh; Bio-Rad Laboratories) was used with a 60 mL Bond Elute column (Varian). The resin was cleaned by passing 4 M HNO_3 through the column. After being neutralized with Milli-Q water (resistivity greater than 18 MΩ·cm; Millipore), the resin was conditioned with 0.5 M NH_4OH and 2 M NH_4OH, and was neutralized again with Milli-Q water.

All samples were filtered through 0.20 μm (DISMIC-25cs, Advantec) or 0.45 μm (JHWP04700, Millipore) filters. The Cl^- concentrations of aliquots were determined by ion chromatography. Water samples containing ~1 mg of Cl were prepared for the ^{36}Cl measurement. After filtration, the samples greater than ~150 mL were acidified with 0.6 mL of 13 M HNO_3, and were run through an anion exchange resin. Chlorine was then eluted from the resin with 30 mL of 3 M HNO_3. In contrast, the samples less than ~150 mL were acidified with 0.5 mL of 13 M HNO_3 after filtration. The AgCl can then be directly precipitated from the solution.

The samples were henceforth processed according to the steps shown in Figure 7. The AgCl was precipitated by adding excess $AgNO_3$, and was separated by centrifugation. The AgCl precipitate was once dissolved in 3 M NH_4OH and saturated $Ba(NO_3)_2$ solution was added to the solution. It was allowed to stand overnight in an oven at ~60°C, in order to effectively precipitate SO_4^{2-} as $BaSO_4$. This precipitate was removed by filtration with a 0.20 μm membrane filter, and the filtrate was acidified by the addition of 13 M HNO_3 to precipitate AgCl again.

The sample was purified by repeating precipitation of AgCl with HNO_3 and dissolution in NH_4OH. In order to further exclude remaining impurities, the AgCl precipitate was washed

with Milli-Q water three times and with 99.5% C_2H_5OH twice using ultrasonic vibration. The AgCl was then dried in the oven at 130°C for 3 hours. The overall chemical yield of chlorine was, on the average, about 80%. For subsequent ^{36}Cl-AMS, a benzene solution saturated with fullerene (C_{60}) was added to each sample (~5 μL per 1 mg of AgCl) and the sample was re-dried just before the target pressing.

3.2 Accelerator mass spectrometry

Accelerator mass spectrometry (AMS) is an ultra-sensitive mass spectrometry technique usually based on a tandem Van de Graaff accelerator. Instead of measuring radioactive decay rates, AMS directly counts the number of atoms in a sample and enables measurements of several long-lived radionuclides, e.g. ^{10}Be (half-life 1.36×10^6 yr), ^{14}C (5730 yr), ^{26}Al (7.05×10^5 yr), ^{36}Cl (3.01×10^5 yr) and ^{129}I (1.57×10^7 yr), at very low abundances (10^{-12}–10^{-15}) in extremely small samples (<1 mg).

In the late 1970s, Muller (1977) proposed that long-lived radioisotopes could be separated and directly detected using a cyclotron. It was soon followed by measurements of ^{14}C with tandem Van de Graaff accelerators (Bennett et al., 1977; Nelson et al., 1977; Purser et al., 1977). Shortly afterward, Elmore et al. (1979) successfully detected ^{36}Cl in surface waters and groundwaters by using AMS. This technique was then applied to the measurements of Antarctic ice, rainwater, seawater and meteorites (Nishiizumi et al., 1979; Finkel et al., 1980). Subsequent widespread applications of AMS in numerous scientific research fields, including e.g. archaeology, geology, hydrology and environmental sciences, have been extensively reviewed by Elmore and Phillips (1987), Finkel and Suter (1993), Tuniz et al. (1998), and Fifield (1999).

In the present study, the ^{36}Cl/Cl ratios of the samples were measured with the AMS

system at the Tandem Accelerator Complex, University of Tsukuba (Tsukuba AMS system). The Tsukuba AMS system consists of an original Cs sputtering ion source, the 12UD Pelletron tandem accelerator (National Electrostatics Corporation), and an AMS beam line (Figure 8). Because of the advantage of a high terminal voltage (~11 MV), the system is especially suited for the detection of heavier nuclides including ^{26}Al and ^{36}Cl (Sasa et al., 2007).

At the Tsukuba AMS system, a molecular pilot beam is used to stabilize the terminal voltage of the tandem accelerator; the tri-carbon molecular ion ($^{12}C_3^-$) is used as a pilot beam for ^{36}Cl-AMS (Nagashima et al., 2000; Sasa et al., 2007). Due to the addition of the saturated fullerene solution to each sample, $^{12}C_3^-$ ions are produced in the ion source concurrently with Cl^- ions. Stable $^{35}Cl^-$ ions are measured as a current using a Faraday cup after a 120° magnet just downstream of the ion source, while the $^{36}Cl^-$ ions of interest are pre-accelerated with $^{12}C_3^-$.

Following pre-acceleration, the negative ions with a mass of 36 are injected into the accelerator through a 90° inflection magnet. The negative ions are accelerated by a large positive voltage of 10 MV at the high voltage terminal, where they interact with a carbon foil (1st stripper foil). Collisions with the foil remove electrons from the ions, causing the molecular ions (including $^{12}C_3^-$) to dissociate and producing positive atomic ions (charge changing reaction).

The positive voltage at the terminal, in turn, repels the positive ions, and makes them go through a second stage of acceleration. After passing the accelerator, the ions are bent through a 90° analyzing magnet that selects $^{36}Cl^{9+}$ and $^{12}C^{3+}$ ions. As mentioned previously, the beam current of $^{12}C^{3+}$ measured at an image slit just after the analyzing magnet is used for the terminal voltage stabilization.

The ions pass through a switching magnet and enter the AMS beam line. These ions undergo a second step of charge changing by another carbon foil (2nd stripper foil). The $^{36}Cl^{14+}$ ions are transported to a ΔE–E detector by an electrostatic deflector (energy selector) and a 45° magnet (momentum selector), while ^{12}C ions are deflected from the main beam path.

The detector provides measurements of the energy loss (ΔE) of ions in the counter gas (isobutane), and the residual energy (E). Since ions of different atomic number lose their energy at different rates, the ΔE–E plot permits the separation of the isobar (^{36}S). As shown in Figure 9, $^{36}Cl^{14+}$ ions are clearly distinguished from the $^{36}S^{14+}$ background.

The relative ratio of $^{36}Cl^{14+}/^{35}Cl^{-}$ (counts/μC) derived from such measurements of a sample is normalized to that obtained for a standard sample yielding the $^{36}Cl/Cl$ ratio of the sample as shown by the following equation:

$$R_{\text{sample}} = R_{\text{standard}} \times \frac{RR_{\text{sample}}}{RR_{\text{standard}}} \tag{5}$$

where R_{sample} and R_{standard} are the $^{36}Cl/Cl$ ratios for the sample and that for the standard, respectively, and RR_{sample} and RR_{standard} are the relative ratios of $^{36}Cl^{14+}$ to $^{35}Cl^{-}$ (counts/μC) for the sample and that for the standard, respectively. The standard samples used in this study are the diluted NIST ^{36}Cl standards ($^{36}Cl/Cl = 1.000 \times 10^{-11}$ or 4.47×10^{-11}; Sharma et al., 1990; Nagashima et al., 2004).

The $^{36}Cl/Cl$ ratio of the sample is then subjected to the background correction using the ratio of a chemical blank prepared from NaCl reagent. The overall precision of the system is better than 5%, and the background level of $^{36}Cl/Cl$ measurement is $\sim 5 \times 10^{-15}$. The obtained $^{36}Cl/Cl$ ratio of the sample includes statistical error derived from uncertainties (1σ) of the

sample, the standard and the blank.

In this study, the ^{36}Cl data are basically used in the form of $^{36}Cl/Cl$ ratios; these ratios are used in further discussion rather than ^{36}Cl concentrations in order to minimize the possible influences of dilution and/or evaporation processes on the interpretation of the results.

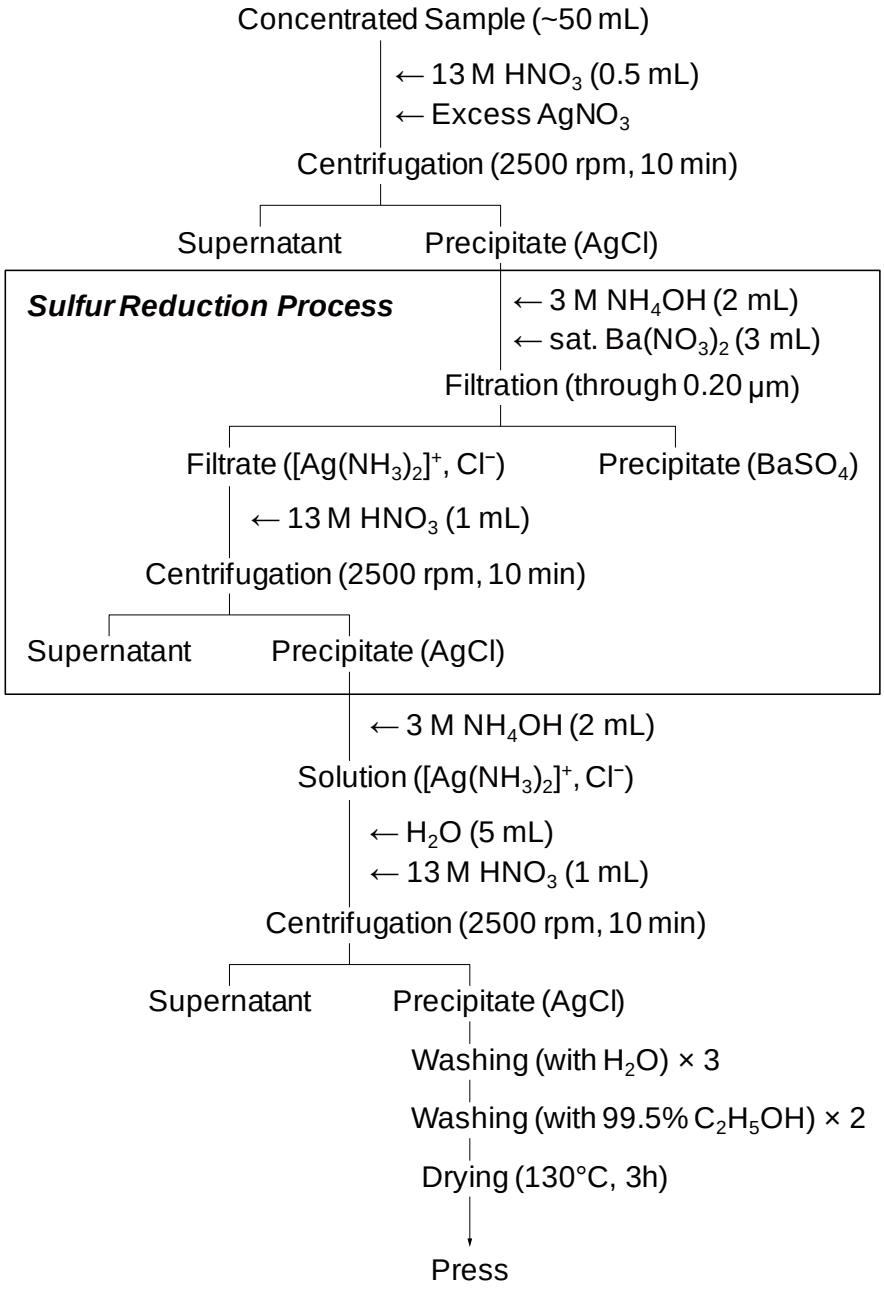

Figure 7 Sample preparation scheme for ^{36}Cl-AMS.

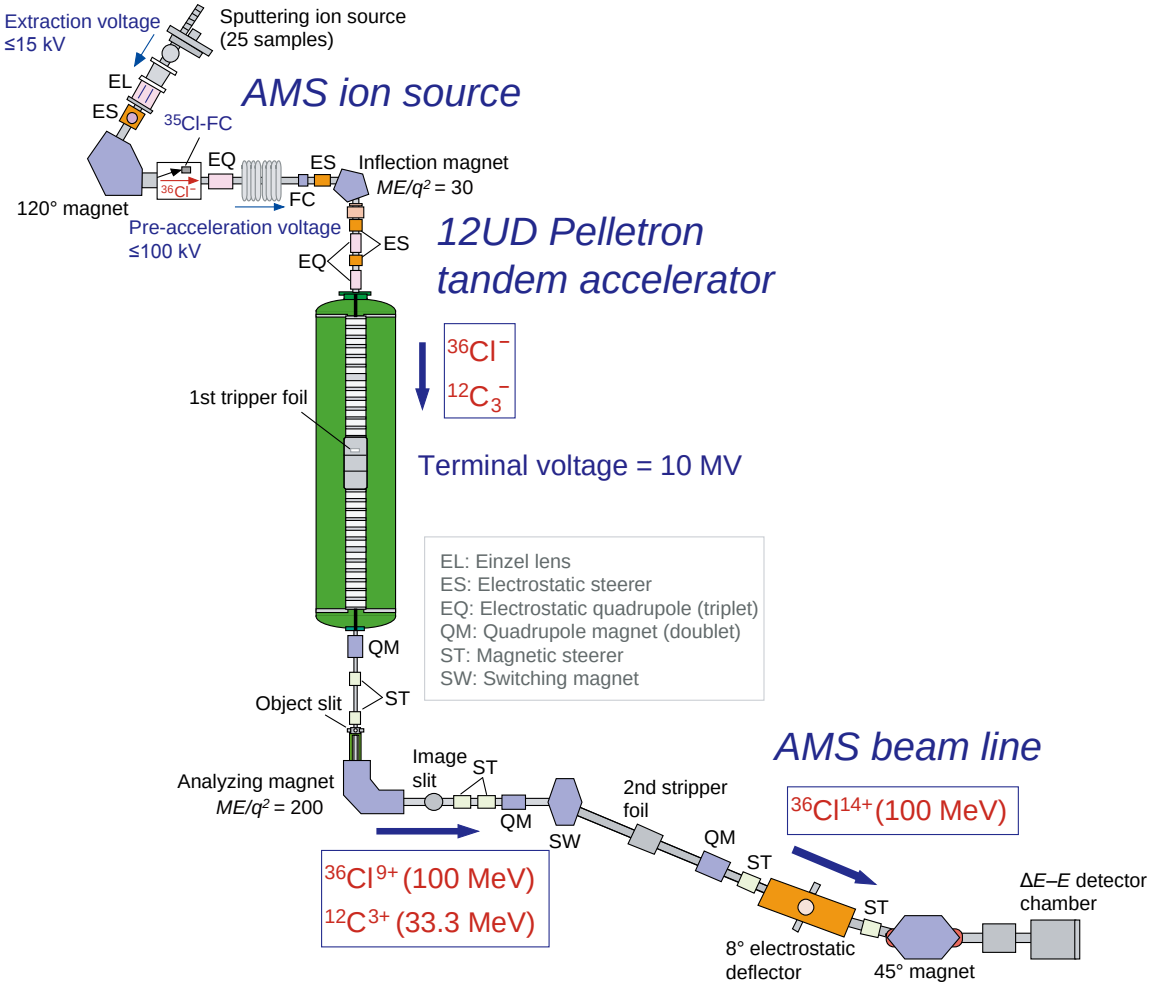

Figure 8 Schematic diagram of the Tsukuba AMS system.

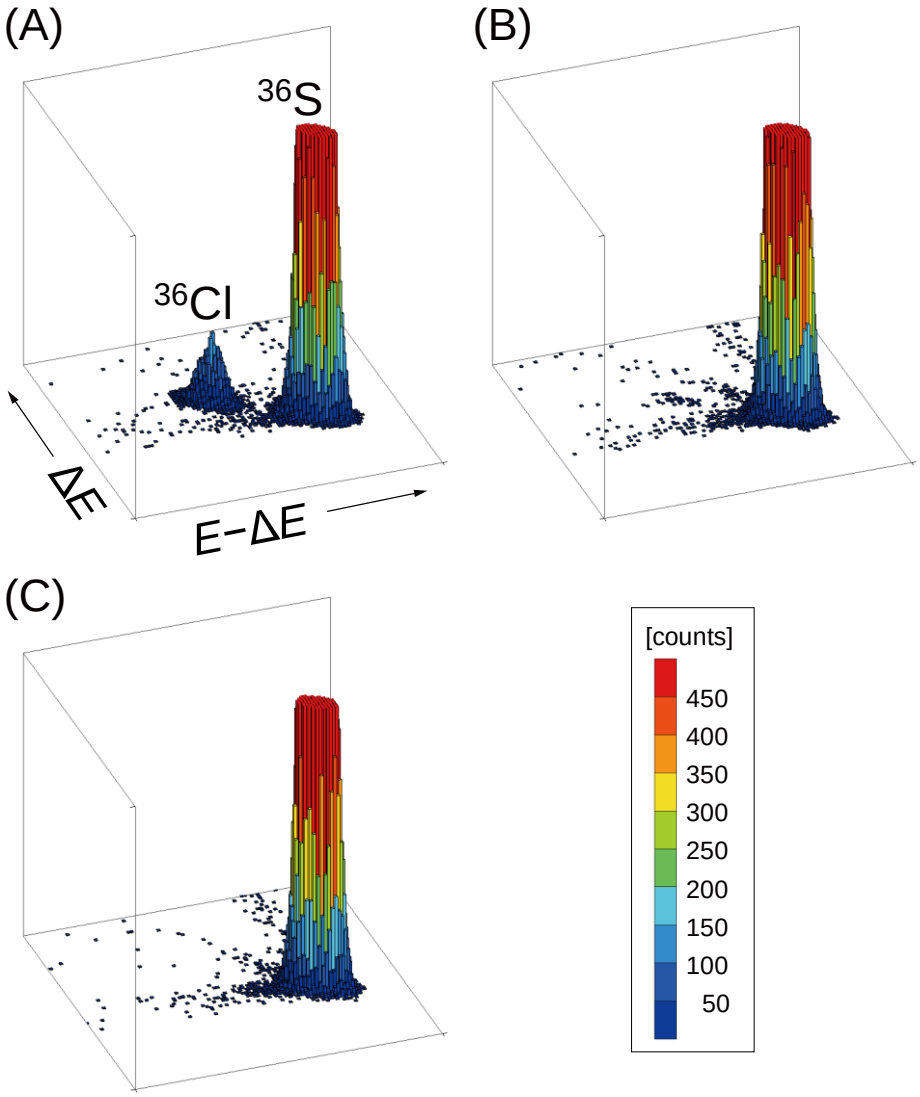

Figure 9 Two-dimensional spectra of energy loss versus residual energy showing the separation of ^{36}Cl from ^{36}S. (A) Standard sample (^{36}Cl/Cl = 1 × 10^{-11}). (B) River water sample (Oder, ^{36}Cl/Cl = 5 × 10^{-14}). (C) Blank sample (^{36}Cl/Cl = 4 × 10^{-15}).

Chapter 4 Distribution of bomb-produced chlorine-36 in groundwater

4.1 Study area

The Oderbruch is a large polder (reclaimed land) area which is located in the northeastern part of Germany (Figure 10). At the east side of the area, the Oder River flows northward on the border between Germany and Poland into the Baltic Sea. The Oder River begins in the Oder Mountains of the Czech Sudeten in the eastern part of Czech Republic. The Oderbruch has a dry climate characterized by a mean annual precipitation of 434 mm (1951–1980) (Massmann, 2002) and a high evapotranspiration rate (greater than precipitation).

Hydrogeology and groundwater chemistry of the Oderbruch area have been intensely investigated (Massmann, 2002; Massmann et al., 2003, 2004; Sültenfuß and Massmann, 2004). Surface elevation of the investigated area is 2–3 m above sea level. The area lies mainly below the river water level, and the river base is highly permeable because it consists of coarse sand and gravel. Consequently, river water is permanently infiltrating into the shallow aquifer as shown in Figure 11.

The aquifer consists of fine to medium-sized sands and the thickness is about 20–30 m on the average. It is underlain by a glacial till (thickness ~120 m) and overlain by an alluvial loam (thickness 0.4–4.0 m). Along the river banks of the area, the aquifer is confined up to about 3 km inland (Figures 10 and 11) and recharged by river water infiltration only.

4.2 Sampling and analyses

Groundwater sampling points are located along the major groundwater flow direction in the confined areas (Figure 10). At each point, groundwater samples were obtained from piezometers at two depths (5–7 m and 19–21 m below ground surface). These depths

correspond to upper and lower parts of the aquifer (Figure 11). The samples obtained in March 2006 include 16 groundwater samples and one river water sample from the Oder River.

In addition to ^{36}Cl analysis, major anions (Cl^-, SO_4^{2-}, NO_3^-) were measured by an ion chromatography (Ion Analyzer IA-100, Dkk-Toa). Dissolved silica (SiO_2) concentrations were determined with an ICP-AES system (ICAP-757, Nippon Jarrell-Ash) at the Chemical Analysis Division, Research Facility Center for Science and Technology, University of Tsukuba. All samples for ion chromatography and ICP-AES analyses were filtered through a 0.20 μm membrane filter.

4.3 Water chemistry

Table 3 presents the results of major anion concentration analysis. Concentrations of major cations (Na^+, K^+, Mg^{2+}, Ca^{2+}) and bicarbonate (HCO_3^-) were also included in the table (G. Massmann, pers. comm.).

As shown in Figure 12, the Cl^- concentrations decrease from ~120 mg/L to ~20 mg/L with increasing distance from the Oder River. One possible cause of the decrease is mixing between the groundwater and infiltrating water from the surface. Although the aquifer is essentially confined up to the point No. 8 (Figure 10), the groundwater can be recharged to some extent by infiltration through the unsaturated zone (50–70 mm/yr; Massmann, 2002).

The Cl^- concentration in the infiltrating water would be 2.1–9.5 mg/L. These values were calculated from 434 mm of mean annual precipitation (Massmann, 2002) with 0.34–1.1 mg/L of Cl^- concentration (southern Germany; Scheffel et al., 1999), and 50–70 mm of mean annual recharge rate (Massmann, 2002). The mixing rate of the infiltrating water would be 85–90%, when the infiltration is responsible for all of the reduction in Cl^- concentrations.

However, the mean annual recharge rate (50–70 mm) is very small compared to the thickness of the aquifer (~20 m; Figure 11). Accordingly, the mixing of 85–90% of the infiltrating water should not have occurred. Other phenomena such as change in Cl^- concentration of the Oder River may have caused the variation.

The possible mixing rate of the infiltrating water would be ~18% as calculated from 70 mm/yr of recharge rate for 50 years (as discussed later) and 20 m of the thickness of the aquifer. In this case, Cl^- derived from the infiltrating water is only 0.4–1.7% of total Cl^- in the groundwater. This contribution would not cause serious effect to the original $^{36}Cl/Cl$ ratio. Therefore, any influence of the infiltrating water does not appear to be a significant driver of the observed variations of the $^{36}Cl/Cl$ ratios.

Figure 13 describes the distribution of SiO_2 concentrations. Especially for the deep wells, SiO_2 concentrations steadily increase with the distance from the Oder River. It suggests again that the contribution of the infiltrating water is of minor importance. Hence, the variation of Cl^- concentration may have been caused by temporal variation of Cl^- concentration in the river water.

An increasing trend of Cl^- concentration has been observed in the upper part of the Oder River (Absalon and Matysik, 2007). This trend was possibly caused by the inflow of saline waters from coal mine drainage (due to the dewatering of mines) in the territories of Poland and the Czech Republic (Absalon and Matysik, 2007). The Cl^- concentration in the upper Oder River has reached the maximum of 1,600 mg/L over a distance of about 200 km (Helios Rybicka, 1996). The mixing of saline waters is, hence, the most likely cause of the Cl^- concentration variation in the groundwater. This influence has to be accounted for in the following analysis of $^{36}Cl/Cl$ distribution.

In addition, variable SiO_2 concentrations for the upper part of the aquifer (Figure 13)

suggest a relatively complex flow pattern. On the contrary, a rather simple flow pattern can be expected for the lower part, from steadily increasing SiO_2 concentrations along the distance from the Oder River. Distribution of hydraulic head estimated from a hydraulic model by Massmann (2002) supports these conditions. Hence, further analysis and discussion focus on the lower part of the aquifer.

4.4 Distribution of bomb-produced chlorine-36 in groundwater

Table 4 lists measured ^{36}Cl data along with $^{3}H/^{3}He$ data from G. Massmann (pers. comm.). Figure 14 shows the $^{36}Cl/Cl$ ratios and the initial tritium concentrations (sum of ^{3}H and tritiogenic ^{3}He) plotted against the distance from the Oder River. As can be seen from the figure, the $^{36}Cl/Cl$ ratios and the initial tritium concentrations showed similar variations with the distance from the Oder River (i.e. along the major groundwater flow direction). High values were clearly observed up to ~3 km away from the Oder River, which were derived from the ^{36}Cl and ^{3}H bomb pulses.

The range of time scale investigated was provided by the results of $^{3}H/^{3}He$ dating. In this case, the groundwater residence time indicates the length of time after infiltration of river water. The $^{3}H/^{3}He$ ages were calculated as follows (Tolstikhin and Kamenskiy, 1969):

$$t = \frac{T_{1/2}}{\ln 2} \ln\left(1 + \frac{[^{3}He_{trit}]}{[^{3}H]}\right) \quad (6)$$

where t is the $^{3}H/^{3}He$ age (yr), $T_{1/2}$ is the half-life of ^{3}H (12.32 yr), $[^{3}H]$ is the ^{3}H concentration (TU), and $[^{3}He_{trit}]$ is the tritiogenic ^{3}He concentration (TU). According to the results, the residence times of these groundwater samples range from a few years to ~50 years (G. Massmann, pers. comm.; Table 4).

In order to account for the mixing effect of saline water as mentioned in the previous section, the following two-component mixing model was employed:

$$R = \frac{C_A C_B (R_B - R_A)}{C(C_A - C_B)} + \frac{C_A R_A - C_B R_B}{C_A - C_B} \quad (7)$$

where R and C are the $^{36}Cl/Cl$ ratio and the Cl^- concentration in water after mixing, respectively, R_A and C_A are the $^{36}Cl/Cl$ ratio and the Cl^- concentration in water A, respectively, and R_B and C_B are the $^{36}Cl/Cl$ ratio and the Cl^- concentration in water B, respectively. In the present case, water A is the original water before mixing, and water B is saline water. Rearrangement of Equation (7) leads to the following equation:

$$R_A = \frac{RC(C_A - C_B) - R_B C_B (C_A - C)}{C_A (C - C_B)}. \quad (8)$$

The $^{36}Cl/Cl$ ratio of the original water (R_A) can be estimated from Equation (8). The C_A was assumed to be in the range of 5–20 mg/L. The minimum value of 5 mg/L was calculated from the assumed Cl^- concentration in precipitation of 1 mg/L (cf. 0.34–1.1 mg/L; southern Germany; Scheffel et al., 1999) and estimated evapotranspiration rate of 80% (as described later). The maximum value of 20 mg/L is according to the lowest Cl^- concentration among the samples (Table 3). The $^{36}Cl/Cl$ ratio in the present river water, $(5.4 \pm 0.5) \times 10^{-14}$, was used as R_B, assuming it reflects the $^{36}Cl/Cl$ ratio in saline waters. The C_B was assumed to be 10,000 mg/L.

Figure 15 shows the calculation results for the lower part of the aquifer. Since the $^{36}Cl/Cl$ ratio of 1D, $(4.6 \pm 0.4) \times 10^{-14}$, is lower than the assumed R_B, it was excluded from the calculation. For the samples 6D, 7D and 8D, the calculated Cl^- concentrations would be

reliable, since their lower Cl^- concentrations indicate less influence from saline waters (Table 3). Conversely, higher concentrations for the remaining samples suggest that the calculation can lead to erratic results. The natural background $^{36}Cl/Cl$ ratio can be estimated to be in the range of 0.8–1.5 × 10^{-13} from the corrected $^{36}Cl/Cl$ ratio of the sample 8D (Figure 15).

4.5 One-dimensional transport model simulation

In order to relate the measured ^{36}Cl concentrations in groundwater to the fallout history of bomb-produced ^{36}Cl, the distribution and transport of tracers in groundwater were simulated according to the approach described in Balderer et al. (2004). This analysis employed the following analytical solution of a one-dimensional advection–dispersion equation (e.g. Bear, 1979, p. 266):

$$C(x,t) = \frac{C_0 / n_e}{(4\pi D_l t)^{1/2}} \cdot \exp\left[-\frac{(x - v_a t)^2}{4 D_l t} \right] \tag{9}$$

where t is the length of time after the input of tracer, x is the transport distance of tracer along the groundwater flow path, $C(x, t)$ is the tracer concentration at a distance x at time t, C_0 is the input tracer concentration, v_a (= $v_r \times n_e$) is the advective flow velocity (Darcy velocity), v_r is the real velocity (linear velocity), n_e is the effective porosity, D_l (= $\alpha \times v_r$) is the longitudinal dispersion coefficient, and α is the longitudinal dispersivity.

The input functions for ^3H and ^{36}Cl in river water at the time of infiltration were deduced using the following exponential mixing model (Maloszewski and Zuber, 1982):

$$C_{\text{out}}(t) = \int_0^\infty C_{\text{in}}(t - \tau) g(\tau) \exp(-\lambda \tau) \mathrm{d}\tau \,, \tag{10}$$

$$g(\tau) = \frac{1}{T^*} \exp\left(-\frac{\tau}{T^*} \right) \tag{11}$$

where t is the time, $C_{out}(t)$ and $C_{in}(t)$ are the output and input tracer concentrations, respectively, τ is the integration variable representing the transit time distribution resulting from different flow times, $g(t)$ is the transit time distribution function (response function), T^* is the mean transit time of tracer, and λ is the decay constant for radioactive tracers. The response function is defined as the output distribution resulting from an instantaneous injection of the tracer at the input (recharge area). The only or the main parameter of each response function is the mean transit time of tracer (T^*).

The period of calculation is from 1945 to 2006. Raw input data used in the analysis are the ^{3}H concentrations in precipitation at Hof, central Germany, near the Czech border. Yearly values from 1962 to 1997 were obtained by averaging monthly data for each year (IAEA/WMO, 2004), whereas the values for 1953–1961 were estimated using the linear correlation with the data at Ottawa, Canada for 1962–1997 (IAEA/WMO, 2004). For the periods 1945–1952 and 1998–2006, concentrations were assumed to be 8.8 TU (^{3}H concentration in the present river water; Table 4). After subtraction of the natural background level (8.8 TU), bomb-derived concentrations were used as $C_{in}(t)$ in Equation (10) (Figure 16).

In the case of ^{36}Cl, concentrations in recharging water were estimated from the fallout history at the Dye-3 site, Greenland (Synal et al., 1990) by using Equation (4). For mean annual precipitation (P) and mean annual evapotranspiration rate (E), approximate values were estimated using precipitation and evaporation distribution maps (P = 600 mm, E = 80%; Baumgartner and Reichel, 1975, Supplement p. 5, Europe (West) P and E). Subtraction of the natural background (3.5×10^6 atoms/L) derived input values of bomb-produced ^{36}Cl (Figure

16). This natural background concentration was calculated from Equation (4) with the natural background flux of meteoric ^{36}Cl at the Dye-3 site (20 atoms m^{-2} s^{-1}; Synal et al., 1994).

In a similar study in the Danube River basin (Balderer et al., 2004), the value '3 yr' was used as the mean transit time of tracer (T^*). This value had been estimated from the time series of ^{3}H concentration in the Danube River (Rank et al., 1996). The same value can be assumed in this study, because of the similarity in situations, such as the distance along the flow path from the upper part of the river to the infiltration point in the Oderbruch area. Then $C_{out}(t)$ values for the two tracers were calculated from Equation (10) (Figure 17).

The output values of exponential mixing were then used as the input functions for the one-dimensional advection–dispersion transport model (C_0 in Equation (9)). The effective porosity (n_e) used here is 0.2 according to Massmann (2002). Superposition of each concentration from 1-yr input values generated total tracer concentrations at a distance x at time t. Addition of the natural background concentrations led to the simulated tracer concentrations.

Optimal values for v_r and α were determined by fitting the simulated ^{3}H concentrations to measured data. Since an α value of 10 m was presented by Massmann (2002) for the investigated aquifer, markedly small values (by about one order of magnitude) were not adopted. As a result, the deduced parameters are v_r = 300 m/yr and α = 3 m. With regard to ^{36}Cl, output concentrations were converted to the ^{36}Cl/Cl ratio assuming conservation of chloride during the transport.

Figure 18 illustrates the results of the model simulation compared with the measured data. In the case of ^{3}H, the simulated concentrations are lower than the measured concentrations around the peak value. This is possibly due to the fact that the raw input data used here (^{3}H concentrations in precipitation) are simple arithmetic means of monthly values for each year.

The lack of several monthly data may have also induced some errors especially near the bomb peak period.

These parameters were then used to simulate the distribution of ^{36}Cl/Cl ratios in the aquifer. The Dye-3 data used as inputs were scaled by multiplying a factor. Simulated tracer concentrations were fitted to the three reliable measured values (6D, 7D and 8D as mentioned previously) by changing a factor for the input data. The analysis using the corrected ^{36}Cl/Cl ratios for C_A = 20 mg/L in Equation (8) (Figure 15) led to a scaling factor (*SF*) of 0.30 (Figure 18). The calculation for C_A = 5 mg/L increased the resultant *SF* value from 0.30 to 1.22 (Figure 18).

4.6 Estimation of ^{36}Cl/Cl time series

The time-series variation of ^{36}Cl/Cl in the Oder River basin can be estimated with the obtained *SF* values of 0.30–1.22. As described in Section 2.3, the fallout history of bomb-produced ^{36}Cl at the Dye-3 site (Synal et al., 1990, 1994) was scaled with the obtained *SF* values. The fallout values were then converted to the ^{36}Cl/Cl ratio using Equation (3). The mean annual precipitation (*P*) used here is 434 mm (Massmann, 2002), and C_p was assumed to be 1 mg/L. The natural background ^{36}Cl/Cl ratio was assumed as 5×10^{-14}, which is the mean ^{36}Cl/Cl ratio for the pre-bomb period in the Rheingau region, western Germany (Priller et al., 1990). Figure 19 shows the estimated time-series variation of ^{36}Cl/Cl ratio in the Oder River basin.

4.7 Discussion

In Figure 19, the estimated time-series variation of ^{36}Cl/Cl ratio is compared with the ^{36}Cl/Cl ratios of the wine samples from the Rheingau region spanning 1930–1980 (Priller et

al., 1990). Also included in the figure is an estimated curve with a *SF* value of 2.3 based on the latitudinal distribution model by Lal and Peters (1967). Priller et al.'s results have been interpreted as reflecting the $^{36}Cl/Cl$ ratios of soil waters in each sampled year. Hence, the wine values include the effect of water residence time in the vineyard soil as well as variation of ^{36}Cl fallout itself. In light of this effect, an estimated curve using a *SF* value between 0.30 and 1.22 will be in satisfactory agreement with the data from the wine samples. While the curve with the *SF* value of 2.3 obviously exceeds the wine values.

In river-recharged aquifers like the Oderbruch aquifer, chloride in groundwater originates from a vast recharge area in the river basin. Hence, chloride of other than meteoric origin (i.e. artificial origin) may often influence chloride concentration in groundwater. In these cases, influence of chloride addition is rather difficult to quantify accurately. Results would be therefore accompanied by a certain range of uncertainty.

Even allowing for uncertainty in chloride concentration, the measured wine data fall in the range of estimated results from simulating the distribution of ^{36}Cl in the aquifer. In contrast, the application of the Lal and Peters (1967) model leads to higher *SF* values, which seem to overestimate the actual time-series variation of $^{36}Cl/Cl$. This suggests that such an over-simplified model is not suitable for estimating the fallout pattern of bomb-produced ^{36}Cl. The results may also imply that the local *SF* value can be obtained by measuring ^{36}Cl in systematically-sampled groundwaters.

Most of the previous estimates of total bomb-produced ^{36}Cl fallout have been obtained from the ^{36}Cl concentration profile in soil in arid or semi-arid regions (Table 2). In temperate regions, however, the ^{36}Cl bomb pulse had already passed through the unsaturated zone into groundwater. Therefore, groundwater is the only available archive of bomb-produced ^{36}Cl fallout. Total fallout of bomb-produced ^{36}Cl has been obtained from groundwater in favorable

conditions (e.g. Bentley et al., 1982).

As shown in this study, simulation of tracer transports (^{36}Cl and ^{3}H) in a simple groundwater system can also allow estimation of bomb-produced ^{36}Cl fallout. Estimation of the ^{36}Cl/Cl time series by using such archives in a given region, in turn, will enable bomb-produced ^{36}Cl to be applied as a dating tool for groundwater in the region.

4.8 Summary

The ^{36}Cl/Cl distribution in groundwater was investigated in the Oderbruch aquifer, northeastern Germany. The groundwater is recharged by the Oder River, which appeared to be affected by saline waters from mining activities. After correcting the mixing effect using the two-component mixing model, a one-dimensional advection–dispersion equation was employed to simulate the distributions of ^{3}H and ^{36}Cl in groundwater. The parameters determined through the distribution of ^{3}H were used to simulate the ^{36}Cl distribution. Simulated values were fitted to the corrected ^{36}Cl/Cl ratios by changing the factor for the Dye-3 data used as inputs. This analysis derived *SF* values in the range of 0.3–1.22. The time-series variation of ^{36}Cl/Cl in the Oder River basin was estimated using these factors and compared with the ^{36}Cl/Cl ratios in wine samples from the Rheingau region, western Germany.

These are in satisfactory agreement, whereas the application of the well-known latitudinal dependence of nuclides' fallout tends to overestimate the time series. This suggests that such an over-simplified model is not suitable for estimating the fallout pattern of bomb-produced ^{36}Cl. The results may also imply that the local *SF* value can be obtained by measuring ^{36}Cl in systematically-sampled groundwaters. Simulation of tracer transports (including ^{36}Cl) in a simple groundwater system can lead to estimation of local bomb-produced ^{36}Cl fallout (and a

scaling factor). If the $^{36}Cl/Cl$ time series is predicted in a given region by using a *SF* value, residence time of groundwater can be estimated from bomb-produced ^{36}Cl.

Table 3

Chemical composition of the Oderbruch groundwaters

Sample	Sample type	Distance (m)	Na^{+}* (mg/L)	K^{+}* (mg/L)	Mg^{2+}* (mg/L)	Ca^{2+}* (mg/L)	Cl^{-} (mg/L)	SO_4^{2-} (mg/L)	NO_3^{-} (mg/L)	HCO_3^{-}* (mg/L)	SiO_2 (mg/L)
Oder	River water	0	64.2	6.7	13.5	78	116.4	98.9	15.6	158	11.9
1S	Shallow groundwater	181	57.6	7.3	13.0	77	110.0	104.9	0.0	170	10.2
2S	Shallow groundwater	766	52.4	0.7	9.5	85	99.5	98.6	0.0	183	18.4
3S	Shallow groundwater	1134	32.2	1.4	6.9	65	68.7	34.5	0.0	208	21.5
4S	Shallow groundwater	1719	76.0	32.5	30.0	220	187.1	387.1	0.0	323	17.5
5S	Shallow groundwater	2142	32.3	2.4	12.4	98	73.4	129.6	0.0	207	18.2
6S	Shallow groundwater	2558	18.7	1.8	11.5	126	47.7	164.3	2.8	247	23.4
7S	Shallow groundwater	2984	14.7	2.4	1.5	97	31.6	112.7	0.0	256	20.7
8S	Shallow groundwater	3551	19.4	2.1	8.0	75	21.3	0.7	0.0	335	23.7
1D	Deep groundwater	181	67.0	6.3	12.0	73	115.8	90.7	0.0	180	10.5
2D	Deep groundwater	766	63.0	8.1	13.0	83	115.8	107.0	0.0	186	11.8
3D	Deep groundwater	1134	59.5	7.2	12.9	80	102.4	101.5	0.0	188	12.7
4D	Deep groundwater	1719	65.0	6.3	11.8	86	113.7	109.4	0.0	186	14.6
5D	Deep groundwater	2142	40.0	4.5	12.5	105	93.3	126.9	0.0	206	17.1
6D	Deep groundwater	2558	27.5	2.4	9.5	85	55.7	104.1	0.7	243	18.6
7D	Deep groundwater	2984	16.6	2.6	12.4	105	41.8	136.9	0.0	249	20.7
8D	Deep groundwater	3551	19.1	2.8	8.8	80	28.9	34.2	0.0	303	22.6

* Concentrations of cations and bicarbonate ion from G. Massmann (pers. comm.).

Table 4

^{36}Cl and ^{3}H data for the Oderbruch groundwaters

Sample	Sample type	Distance (m)	Cl^- (mg/L)	$^{36}Cl/Cl$ (10^{-15})	^{36}Cl (10^6 atoms/L)	^{3}H* (TU)	$^{3}He_{trit}$* (TU)	$^{3}H/^{3}He$ age* (yr)
Oder	River	0	116.4	54 ± 5	107 ± 11	8.8 ± 0.1	–	0
1S	Shallow groundwater	181	110.0	52 ± 5	98 ± 10	8.8 ± 0.1	1.8 ± 0.5	3
2S	Shallow groundwater	766	99.5	114 ± 9	193 ± 15	13.5 ± 0.2	59.7 ± 0.5	30
3S	Shallow groundwater	1134	68.7	143 ± 8	167 ± 9	8.7 ± 0.2	82.1 ± 0.6	42
4S	Shallow groundwater	1719	187.1	202 ± 11	642 ± 34	13.2 ± 0.1	67.2 ± 0.3	32
5S	Shallow groundwater	2142	73.4	231 ± 11	288 ± 13	13.7 ± 0.1	73.5 ± 0.1	33
6S	Shallow groundwater	2558	47.7	216 ± 11	175 ± 9	5.6 ± 0.4	35.1 ± 0.5	36
7S	Shallow groundwater	2984	31.6	167 ± 7	89 ± 4	1.8 ± 0.2	9.8 ± 0.2	34
8S	Shallow groundwater	3551	21.3	100 ± 6	36 ± 2	0.6 ± 0.0	6.9 ± 0.5	45
1D	Deep groundwater	181	115.8	46 ± 4	91 ± 8	8.8 ± 0.1	0.9 ± 0.3	2
2D	Deep groundwater	766	115.8	62 ± 4	122 ± 8	8.8 ± 0.2	3.2 ± 0.2	6
3D	Deep groundwater	1134	102.4	63 ± 4	110 ± 6	8.8 ± 0.1	3.5 ± 0.5	6
4D	Deep groundwater	1719	113.7	61 ± 6	117 ± 12	8.7 ± 0.2	12.8 ± 0.1	16
5D	Deep groundwater	2142	93.3	148 ± 13	235 ± 20	11.9 ± 0.4	52.4 ± 0.1	30
6D	Deep groundwater	2558	55.7	196 ± 11	186 ± 10	11.9 ± 0.2	74.3 ± 0.4	35
7D	Deep groundwater	2984	41.8	209 ± 12	148 ± 9	4.9 ± 0.1	32.8 ± 0.2	36
8D	Deep groundwater	3551	28.9	71 ± 5	35 ± 3	0.4 ± 0.0	3.3 ± 0.0	42

1 TU (tritium unit) means one ^{3}H atom in 10^{18} ^{1}H atoms.

* Concentrations of ^{3}H and $^{3}He_{trit}$, and $^{3}H/^{3}He$ ages from G. Massmann (pers. comm.).

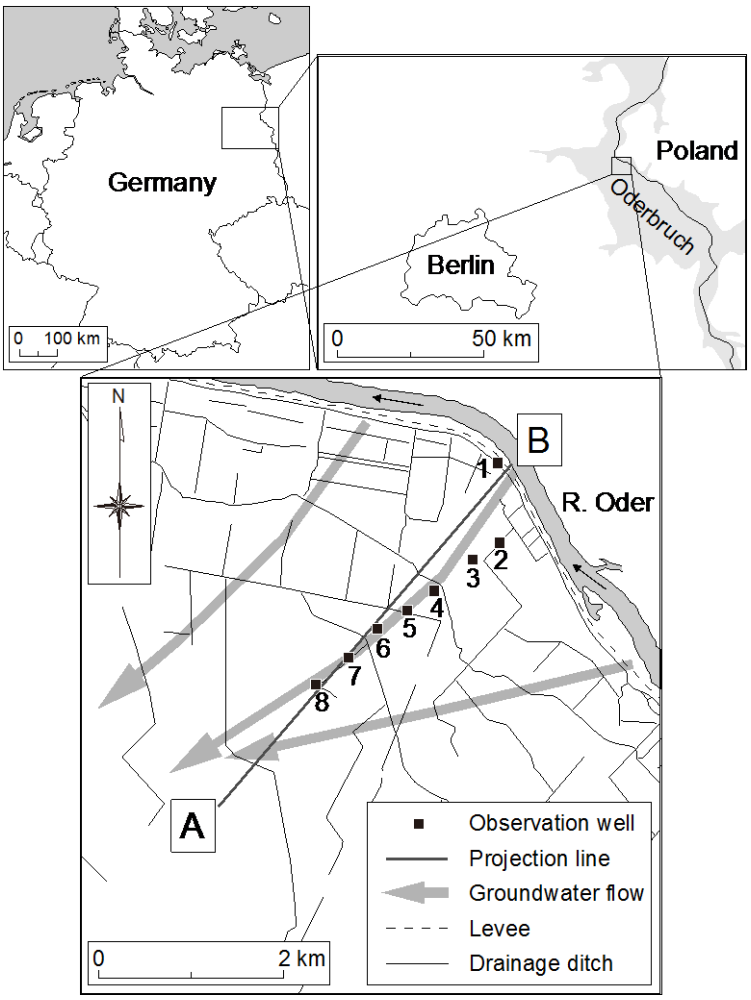

Figure 10 Location of the Oderbruch polder and groundwater sampling points (modified from Sültenfuß and Massmann, 2004). Also indicated is groundwater flow direction based on a hydraulic model by Massmann (2002).

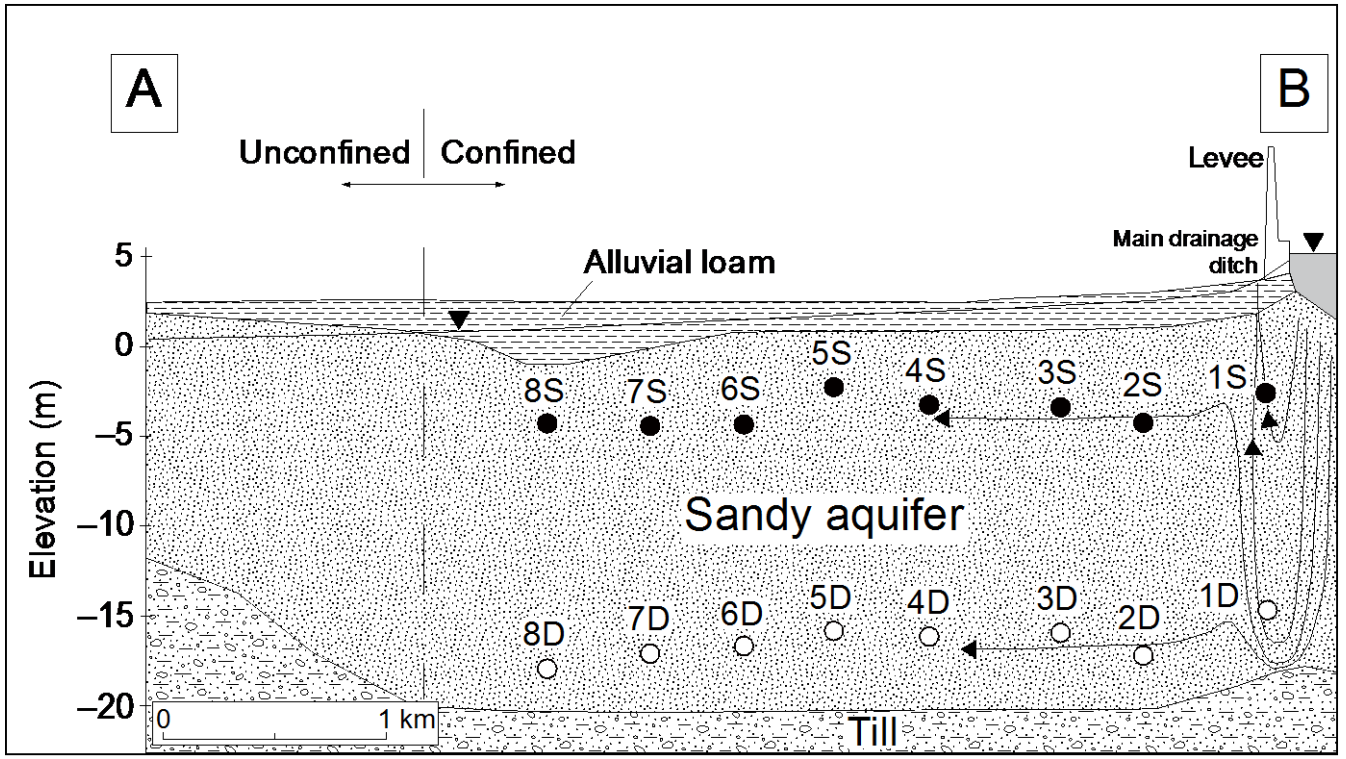

Figure 11 Cross section through the aquifer with major hydrological units (modified from Sültenfuß and Massmann, 2004). This section is along the projection line shown in Figure 10, and the figure has been vertically exaggerated for clarity. The arrows in the aquifer show groundwater flow paths (after Massmann, 2002). Closed and open circles indicate the depths of filter screens of shallow and deep piezometers, respectively.

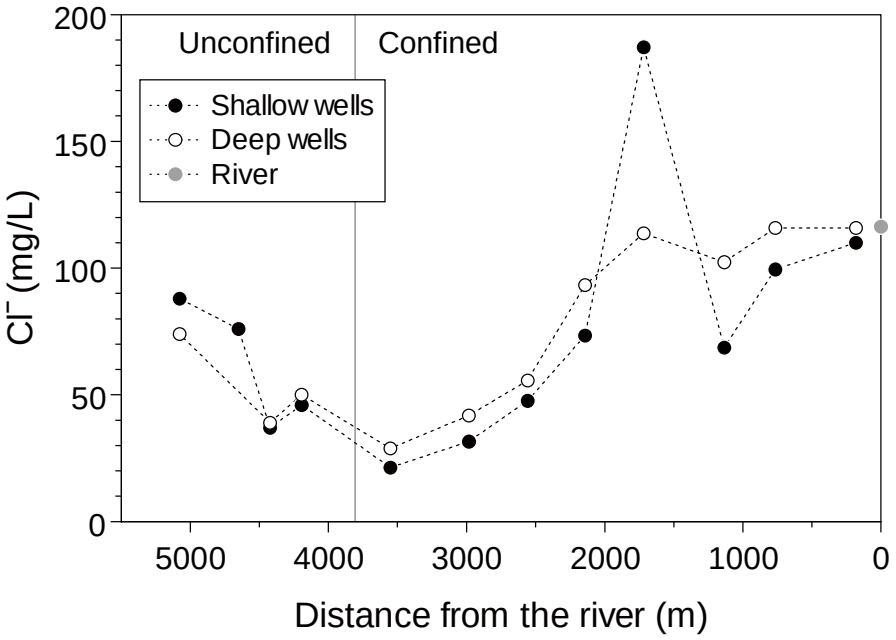

Figure 12 Variation of Cl^- concentration along the distance from the Oder River. Chloride concentrations in the unconfined groundwater are from G. Massmann (priv. comm.).

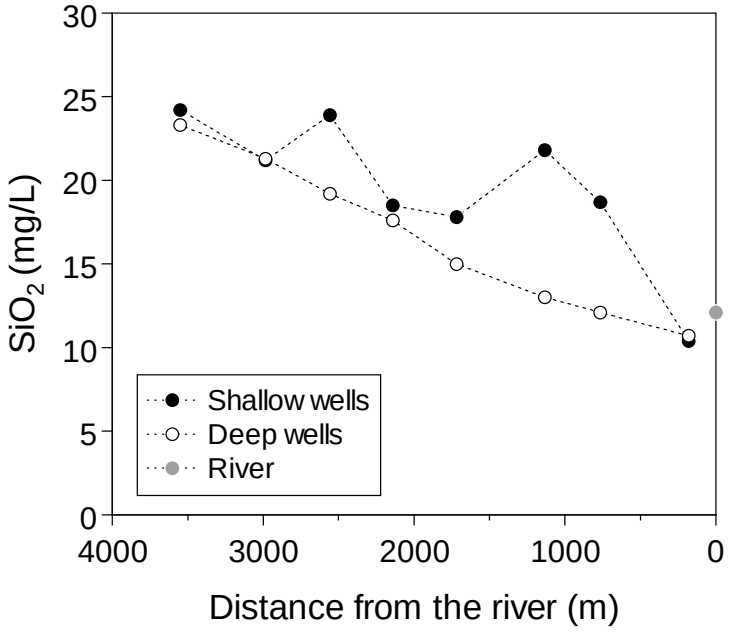

Figure 13 Variation of SiO_2 concentration along the distance from the Oder River.

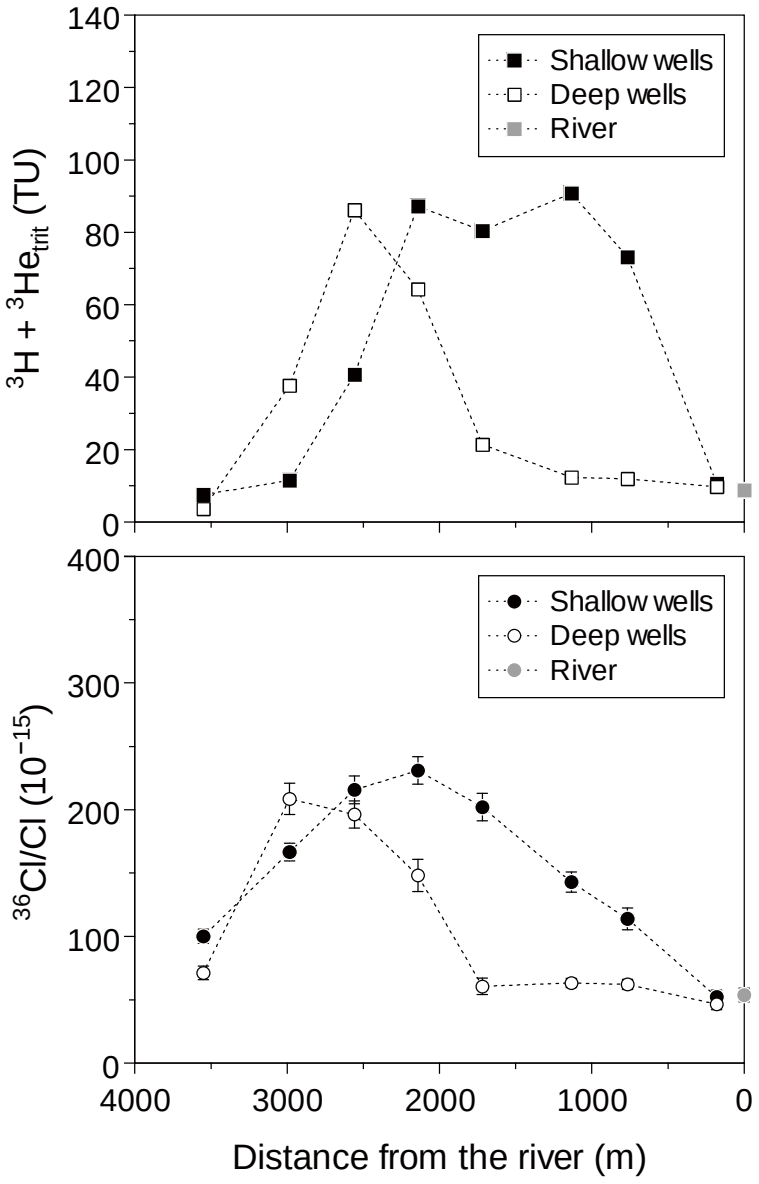

Figure 14 Variation of $^3H + {}^3He_{trit}$ concentration and $^{36}Cl/Cl$ ratio along the distance from the Oder River. The sum of ^3H and $^3He_{trit}$ concentrations is equal to the initial ^3H tritium concentration at the time of recharge.

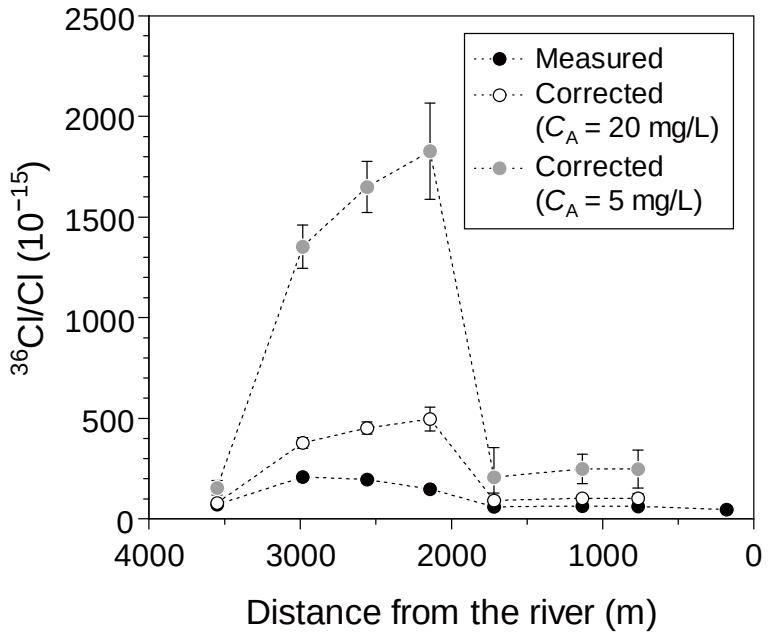

Figure 15 Calculated Cl^- concentrations using the two-component mixing model. Calculations focused on the groundwaters from the lower part of the aquifer.

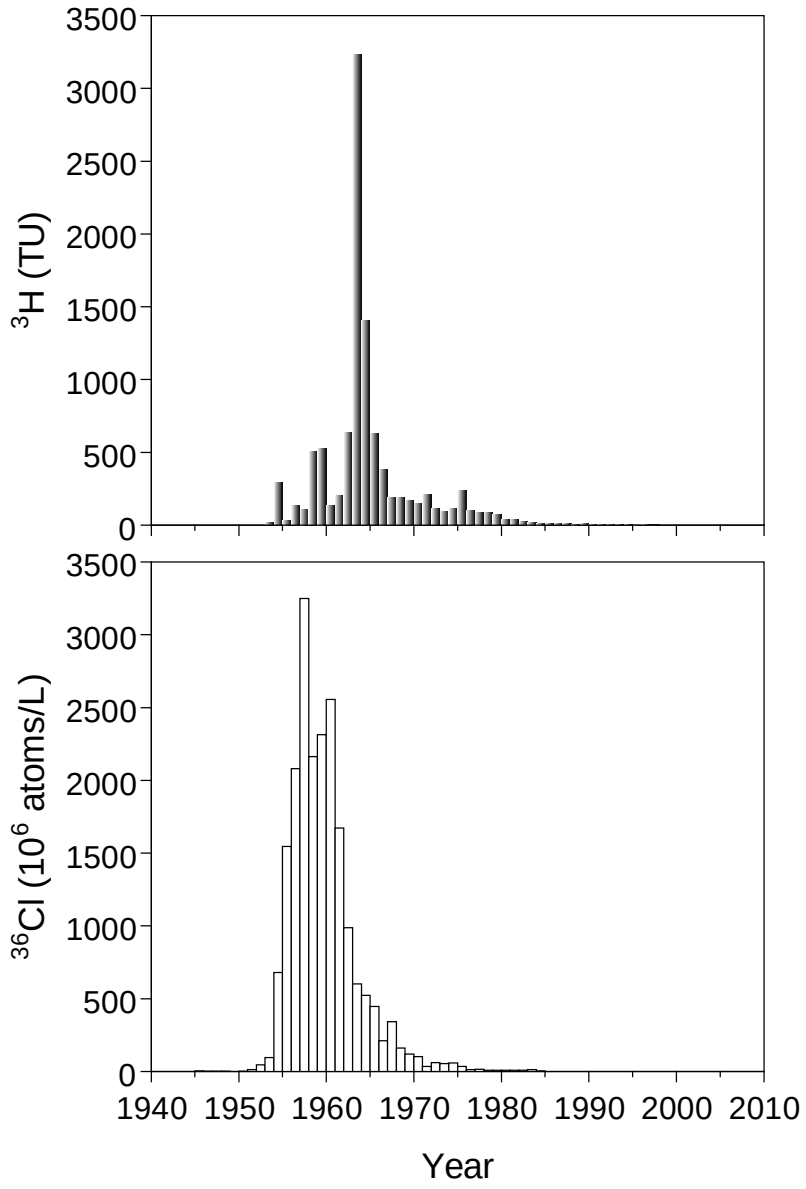

Figure 16 Input functions of ^{3}H and ^{36}Cl for the exponential mixing model.

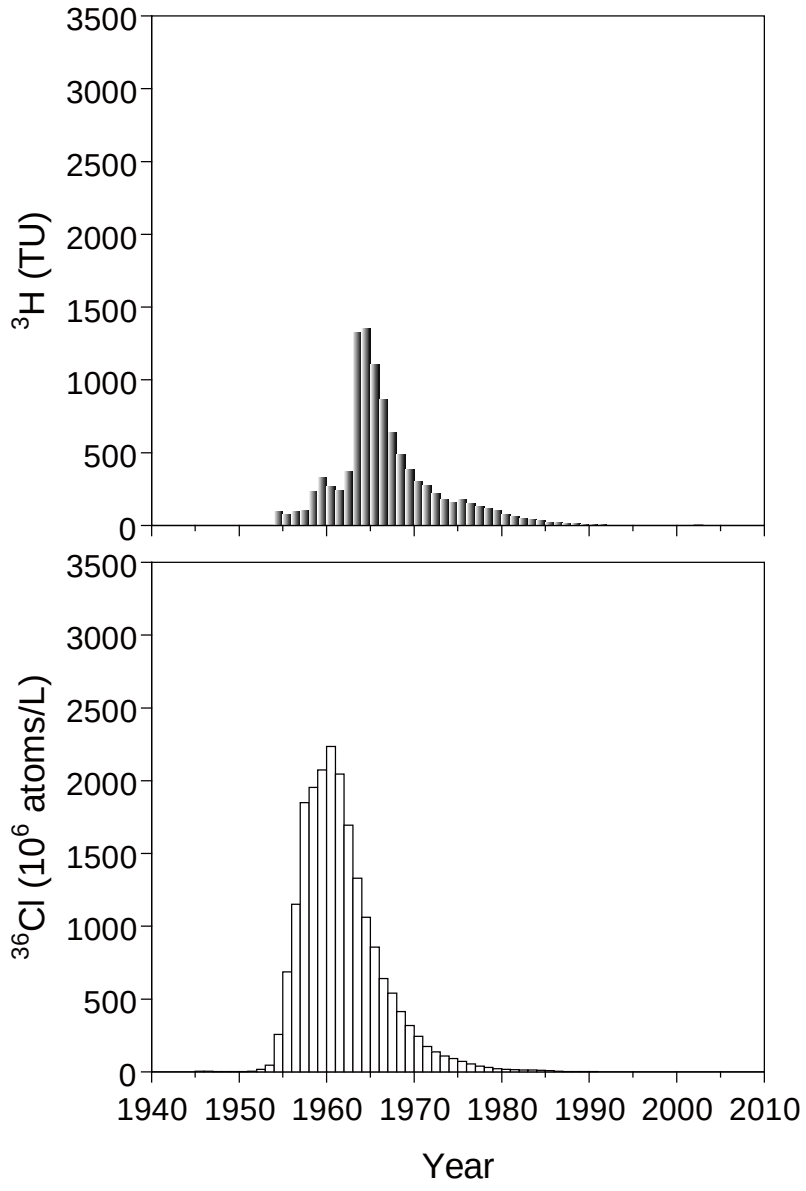

Figure 17 Input functions of ^{3}H and ^{36}Cl for the one-dimensional advection–dispersion transport model simulation.

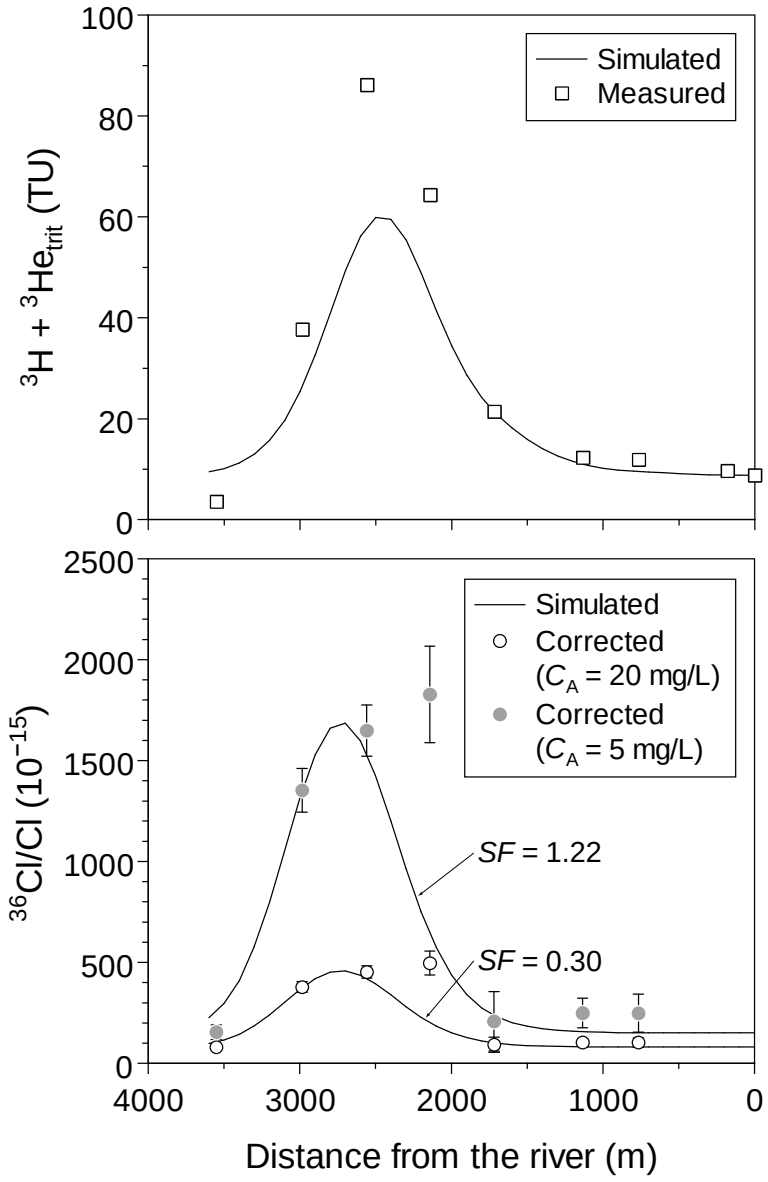

Figure 18 Results of the one-dimensional advection–dispersion transport model simulation.

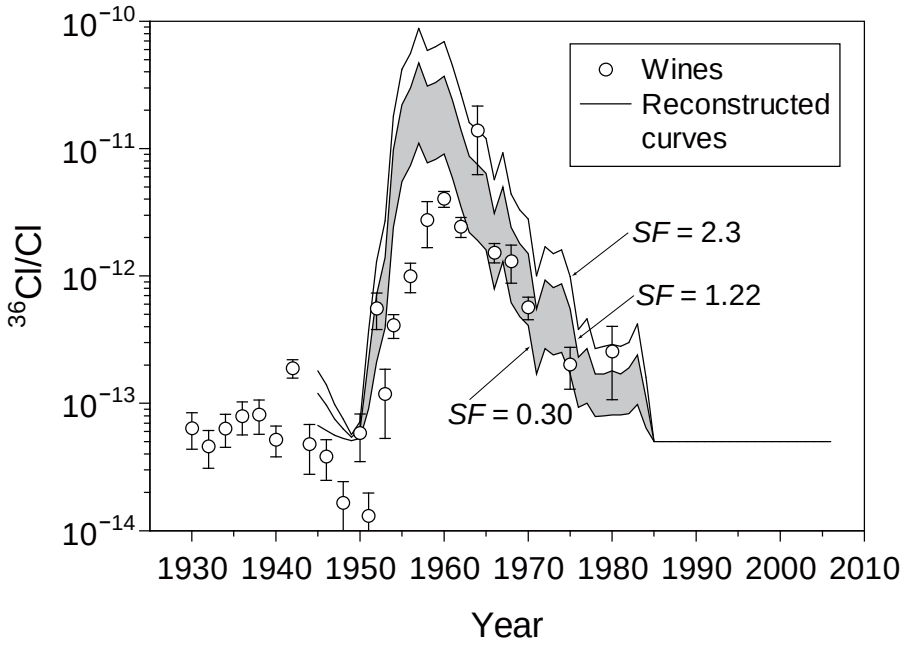

Figure 19 Estimated time-series variation of ^{36}Cl/Cl ratio in the Oder River basin compared with the ^{36}Cl/Cl ratios in wine samples from the Rheingau region, Germany (Priller et al., 1990).

Chapter 5 Estimation of local fallout history of chlorine-36 from the depth profile of groundwater

5.1 Study area

The groundwater sampling and monthly bulk precipitation sampling were conducted at two separate sites in the central part of the Tsukuba Upland (approximately 60 km northeast of Tokyo) in the Kanto region, central Japan (Figure 20). The climate of the area is humid temperate, with an annual precipitation of 1235.6 mm and an annual mean temperature of 13.5°C (average values for 1971–2000; data from the Aerological Observatory at Nagamine near the groundwater sampling site).

The Tsukuba Upland is a Pleistocene upland surrounded by the Sakura River and Lake Kasumigaura on the east, the Tone River on the south, and the Kokai River on the west. At the northeast of the upland, the Tsukuba Mountains (including Mt. Tsukuba, elevation 877 m) extend north and south. Although the upland surface is dissected by small rivers, the elevation typically falls in the range of 20–30 m for the most part (Unozawa et al., 1988).

Geologic information on the upland and its surrounding areas has been described in detail by Unozawa et al. (1988). Basement rocks in the area consist of granitic and metamorphic rocks forming the Tsukuba Mountains. They are overlain by the Kazusa Group sediments of Pliocene to middle Pleistocene age. The overlying Shimosa Group sediments of middle to late Pleistocene age mainly constitute the upland. It consists of six formations (i.e. the Jizodo Formation, the Yabu Formation, the Kamiizumi Formation, the Kamiiwahashi Formation, the Kioroshi Formation and the Joso Formation in ascending stratigraphic order), with the upland surface covered by the Kanto Loam Formation, which is derived from volcanic ash.

The geologic columns for the groundwater sampling site were previously given in

Unozawa et al. (1988) for 0–62.5 m, and in Taguchi (1981) for 0–300 m (Figure 21). Underlying the surface soil are a loam layer (1.5–2.5 m; the Kanto loam), a clay layer (2.5–9 m; the Joso clay, which is the upper most part of the Joso Formation), a sand layer (9–30 m), a fine sand layer (30–47.5 m), and a sand & gravel layer (47.5–55 m) in descending order.

The groundwater table is generally observed within the Kanto loam or the Joso clay. The lower part of the sand layer (ca. 20–30 m) and the sand & gravel layer (ca. 45–55 m) act as shallow confined aquifers; the latter belongs to dominant aquifers in the area (Unozawa et al., 1988). Several sand or gravel aquifers, respectively confined by clay layers, are additionally observed at greater depth down to ~300 m (ca. 80–110 m, 130–145 m and 230–245 m) (Taguchi, 1981).

According to Yasuhara et al. (1991), the Joso clay exhibits remarkably low saturated hydraulic conductivity compared to the overlying Kanto loam (by 2–4 orders of magnitude) and the upper part of the underlying sands (by 3–5 orders of magnitude). The Joso clay, therefore, may have a great influence on the downward flow of groundwater.

Conversely, previous studies have revealed that the hydraulic head of the groundwater decreases with depth (Kayane and Li, 1983; Shimada et al., 1990), to ~55 m (Yasuhara et al., 1990). This observation suggests that the upland surface is essentially acting as a recharge area. Therefore, vertical groundwater movement especially in the central part of the upland can be expected at least for the upper 55 m. Since small rivers dissecting the upland surface are gaining streams for the most part (Unozawa et al., 1988), the shallow aquifers can be assumed to be recharged only from the surface.

5.2 Sampling and analyses

The observation wells of the Geological Survey of Japan (GSJ), the National Institute of

Advanced Industrial Science and Technology (AIST) were used for depth-profile sampling of groundwater. The wells are located on the premises of the GSJ in the central part of the Tsukuba Upland (Figure 20). The six wells used in this study include three deep wells for continuous groundwater level monitoring (Taguchi, 1981).

Groundwater samples were collected using a bailer sampler in February 2004. Each sample mostly corresponds to the upper four layers below the Kanto loam (i.e. the Joso clay, the sands, the fine sands, and the sands & gravels) and the two deep aquifers (Figure 21). Since the two deeper wells (Nos. 5 and 6) have multiple screens, the corresponding samples were collected around the top screens. Due to the spatial variability of the layer's thickness, the well No. 1 is actually screened in the upper-most part of the sands (just beneath the Joso clay). However, when the downward groundwater flow is dominant, it may be reasonable to assume that the sample taken from the well corresponds to the Joso clay.

Monthly bulk precipitation samples were collected from April 2004 at the roof of the Natural Sciences Building, University of Tsukuba. The precipitation sampler used in this study consists of a PE funnel (diameter 15 or 21 cm), a HDPE bottle (3 or 5 L) and a specially developed glassware with a ping-pong ball, which prevents evaporative loss of the sample (Kazahaya and Yasuhara, 1994; Shimada et al., 1994).

The analyses for chloride (Cl^-) concentration and $^{36}Cl/Cl$ ratio were carried out in the laboratory. The samples for Cl^- and ^{36}Cl analyses were filtered through a 0.20 μm membrane filter. The Cl^- concentrations of aliquots were measured by ion chromatography analysis (QIC Analyzer, Dionex; Ion Analyzer IA-100, Dkk-Toa).

5.3 Vertical distribution of chlorine-36 in groundwater

Table 5 summarizes the measured ^{36}Cl data and Figure 21B illustrates the depth profile of

$^{36}Cl/Cl$ ratio in the groundwater. The obtained results clearly show the influence of bomb-produced ^{36}Cl in the upper ~50 m; the highest $^{36}Cl/Cl$ ratio is about one order of magnitude greater than the natural background level. This vertical distribution agrees with the depth profiles of ^{3}H concentrations (Figure 21C).

It is also consistent with the previous observation in the central part of the upland by Kayane and Li (1983), who reported no detectable ^{3}H in the groundwater at depths greater than 36 m in 1982. In contrast, Yasuhara et al. (1990) calculated the downward groundwater flux through the Joso clay as 27 mm/yr based on Darcy's law; it leads to a mean residence time of 30–50 yr in the upper part of the underlying sand layer. The highest $^{36}Cl/Cl$ ratio observed in the sand layer is also consistent with their estimation.

As can be seen from Figure 21, ^{3}H concentrations had gradually decreased from 1999 to 2003 due to both radioactive decay and groundwater flow, while $^{36}Cl/Cl$ ratios showed distinct difference from the natural background level (by one order of magnitude) in 2004. This suggests the potential usefulness of bomb-produced ^{36}Cl as a tracer in modern groundwater as described in previous studies (Bentley et al., 1982; Balderer et al., 2004; Tosaki et al., 2007).

It can be surmised that the deeper the sample, the greater the uncertainty about the corresponding recharge area. Thus, the deepest sample (No. 6; 233.2–244.6 m) was excluded from further discussion. The natural background $^{36}Cl/Cl$ ratio was then estimated as 1×10^{-13} from the result of the sample No. 5 (Figure 21). This is supported by the $^{36}Cl/Cl$ ratio for a sample from a shallow well screened in the Kanto loam (0.7–2.0 m): $(1.19 \pm 0.48) \times 10^{-13}$ in October 2003; the well is located in the Terrestrial Environment Research Center, University of Tsukuba, which is about 6 km northwest from the sampling site at the GSJ.

5.4 Estimation of total bomb-produced chlorine-36 fallout

In a similar way like soil profiles (e.g. Prych, 1998), the total bomb-produced ^{36}Cl fallout in the Tsukuba Upland can be estimated by integrating bomb-produced ^{36}Cl observed in the profile (grayed area in Figure 21). The following equations were used to calculate the total bomb-produced ^{36}Cl fallout:

$$D = \sum (A_{\mathrm{bomb},i} \times h_i \times n_i \times 10^3), \tag{12}$$

$$A_{\mathrm{bomb},i} = (R_i - R_\mathrm{b}) \times \frac{C_i \times 10^{-3} \times 6.022 \times 10^{23}}{35.45} \tag{13}$$

where D is the total bomb-produced ^{36}Cl fallout (atoms/m^2), $A_{\mathrm{bomb},\,i}$ is the concentration of bomb-produced ^{36}Cl (atoms/L), h_i is the thickness of the layer (m), n_i is the porosity (%), R_i is the measured ^{36}Cl/Cl ratio, R_b is the natural background ^{36}Cl/Cl ratio, and C_i is the Cl^- concentration (mg/L).

In the calculation, the obtained values were assumed to be representative for the total thickness of the corresponding four layers below the Kanto loam, and the porosity was assumed to be identical to the effective porosity (for unconsolidated materials; e.g. Todd and Mays, 2005, p. 37). The porosity used for the Joso clay was 62%, which is the arithmetic mean of the 19 measured values over the Tsukuba Upland by Yasuhara et al. (1991). For other layers, representative values were adopted from Morris and Johnson (1967): 39% for sand (as medium sand), 43% for fine sand, and 34% for sand & gravel (as fine gravel). The natural background ^{36}Cl/Cl ratio was set to 1×10^{-13} as mentioned in the previous section.

Consequently, Equation (12) gives the total bomb-produced ^{36}Cl fallout of 2.1×10^{12} atoms/m^2. Because the ^{36}Cl deposited onto the ground may be partly lost with surface waters,

2.1×10^{12} atoms/m^2 would be the minimal estimate. General surface runoff rate in Pleistocene upland and alluvial lowland region is ~20% (e.g. Kotoda, 1968; Miyake, 1978), whereas surface runoff rate measured in an experimental field at the central part of the Tsukuba Upland is ~5% (Itadera and Shimada, 1992). Here it was assumed that 10% of ^{36}Cl is lost by surface runoff. Total bomb-produced ^{36}Cl fallout of 2.3×10^{12} atoms/m^2 was obtained after incorporation of this loss. Dividing this value by 2.4×10^{12} atoms/m^2 (fallout at the Dye-3 site; Synal et al., 1990), a *SF* value of 0.96 was obtained for the Tsukuba Upland (c.f. 2.5 based on the simplified latitudinal fallout distribution model by Lal and Peters, 1967).

It should be noted that the screen length of well No. 2 is wide (11 m) and the thickness of the corresponding sand layer is 21 m (Figure 21). This indicates that the highest ^{36}Cl/Cl ratio in the profile is fairly representative of the layer. Therefore, the calculation described in this section will not lead to erratic results.

5.5 Natural background flux of meteoric chlorine-36

Table 6 and Figure 22 present the results of ^{36}Cl measurement for monthly precipitation samples (from April 2004 to July 2007, except for December 2005, June 2006 and July 2006). Figure 22 shows a clear seasonal variation in ^{36}Cl flux with peaks in the spring (April or May). Similar spring maximum has been observed in other locations (Hainsworth et al., 1994; Knies et al., 1994) and for other cosmogenic radionuclides, e.g. ^{7}Be (e.g. Viezee and Singh, 1980) and ^{10}Be (e.g. Raisbeck et al., 1979). As pointed out in previous studies, the seasonal pattern would be attributed to annual variation of tropopause height (Staley, 1962). According to Staley (1962), the tropopause begins to rise rapidly in April or May at mid-latitudes (especially about 30–40°N). As the tropopause rises, stratospherically produced

^{36}Cl is transported into the troposphere and washed out from the atmosphere after about one week. This mechanism would explain the observed results.

Yearly-averaged ^{36}Cl fluxes are 33, 29, and 33 atoms m^{-2} s^{-1} for April 2004–March 2005, April 2005–March 2006, and April 2006–March 2007, respectively: 31 ± 2 atoms m^{-2} s^{-1} for 3 years. This value is in good agreement with the expected value from the latitudinal dependence of ^{36}Cl fallout with recent estimates of the global mean production rate (Figure 3). Therefore, recycling of bomb-produced ^{36}Cl as methyl chloride (CH_3Cl) from the biosphere (Scheffel et al., 1999) is not evident in the present study area. From the observed results, the natural background flux of meteoric ^{36}Cl is estimated to be 30 atoms m^{-2} s^{-1} in the Tsukuba Upland.

5.6 Estimation of local fallout history

The local fallout history of ^{36}Cl in the Tsukuba Upland was estimated by using the obtained *SF* value of 0.96. The procedure is essentially similar to that described in Section 2.3, except for the conversion to the ^{36}Cl/Cl ratio. The fallout history of bomb-produced ^{36}Cl at the Dye-3 site (Synal et al., 1990, 1994) was scaled with 0.96 for the Tsukuba Upland. Then the natural background ^{36}Cl flux of 30 atoms m^{-2} s^{-1} was added to obtain the local fallout history of ^{36}Cl. Figure 23 shows the estimated fallout history for the Tsukuba Upland, compared with the original Dye-3 data.

5.7 Discussion

In order to allow comparison of the estimated fallout history with several measured data for ice cores at different locations, the ratios of the bomb-peak fallout (F_{max}) to the natural background flux (F_b) of meteoric ^{36}Cl were calculated. Table 7 lists previously reported

F_{max}/F_b ratios for the two mid-latitude sites and the Dye-3 site. The F_{max}/F_b ratio for the Dye-3 site was recalculated from F_{max} of 3.9×10^7 atoms cm^{-2} yr^{-1} (Synal et al., 1990) and F_b of 20 atoms m^{-2} s^{-1} (Synal et al., 1994), instead of using the value '310' given in Green et al. (2000).

It is worth noting that the F_{max}/F_b value determined with the scaling factor of 0.96 reasonably agrees with data from Nepal (Table 7). Supposing that the bomb-produced ^{36}Cl fallout and cosmogenic ^{36}Cl fallout depend similarly on the amount of precipitation (Phillips, 2000), the F_{max}/F_b ratio would be controlled by latitude or local effects. The estimated F_{max}/F_b value for the Tsukuba Upland can be comparable to data from Nepal, because of relatively-near localities.

Concerning the Upper Fremont Glacier, the depth–concentration profile of ^{36}Cl exhibits a somewhat different shape from that of other sites (e.g. the Dye-3 site, the Inilchek Glacier and the Guiliya Ice Cap) (Cecil et al., 1999). This may suggest local effects or post-depositional disturbance of investigated ice layers. Therefore, it should be excluded from the direct comparison of F_{max}/F_b values.

The agreement of the estimated F_{max}/F_b value for the Tsukuba Upland and data from Nepal supports the validity of the obtained *SF* value. The obtained results also confirmed that the local fallout history of ^{36}Cl can be estimated from a groundwater profile as indicated by Bentley et al. (1982).

5.8 Summary

The depth profile of $^{36}Cl/Cl$ ratio in groundwater was investigated in the Tsukuba Upland of central Japan. The obtained results clearly show the influence of bomb-produced ^{36}Cl; the highest $^{36}Cl/Cl$ ratio is about one order of magnitude greater than the natural background

ratio (1×10^{-13}). The vertical distribution of ^{36}Cl is consistent with previous observations using ^{3}H and Darcy's law. From the profile, the total bomb-produced ^{36}Cl fallout in the upland is 2.3×10^{12} atoms/m^2 after the correction for surface runoff (c.f. 2.4×10^{12} atoms/m^2 at the Dye-3 site, Greenland) and a scaling factor of 0.96 was obtained (c.f. 2.5 based on the simplified latitudinal fallout distribution model).

The local fallout history of ^{36}Cl was estimated based on the Dye-3 data (scaled with a factor of 0.96 for the Tsukuba Upland) and the mean ^{36}Cl flux, produced in the atmosphere from cosmic rays and measured 30 atoms m^{-2} s^{-1} in the upland. The ratio of the maximum bomb-peak fallout (F_{max}) to the average natural background flux (F_b) of meteoric ^{36}Cl is consistent with that of measured data in Nepal. This agreement supports the validity of the obtained *SF* value. The obtained results also confirmed that the local fallout history of ^{36}Cl can be estimated from a groundwater profile.

Table 5

^{36}Cl and ^{3}H data for the Tsukuba groundwaters

Well No.	Screen depth (m)	Cl^- (mg/L)	$^{36}Cl/Cl$ (10^{-15})	^{36}Cl (10^6 atoms/L)	^{3}H (TU)‡		
					1998	1999	2003
1	6.75–7.00	6.4	820 ± 38	89.2 ± 4.1	5.6	5.0	3.1
2	21.0–32.0	5.7	1166 ± 76	113.8 ± 7.4	22.7	16.8	11.0
3	38.0–39.5	15.9	570 ± 31	154.2 ± 8.5	5.0	5.3	3.7
4	45.1–56.5	4.0	135 ± 45	9.2 ± 3.1	0.4	–	–
5	82.4–109.0*	3.5	100 ± 24	5.9 ± 1.4	<0.4	–	–
6	233.2–244.6†	4.3	205 ± 42	14.9 ± 3.1	<0.4	–	–

* Also screened in a deeper aquifer (136.5–140.3 m).

† Also screened in deeper layers (255.6–259.4 m and 264.9–272.5 m).

‡ Concentrations of ^{3}H from M. Yasuhara (pers. comm.).

Table 6

^{36}Cl data for precipitation samples collected in Tsukuba

Sample	Precipitation* (mm)	Cl^- (mg/L)	$^{36}Cl/Cl$ (10^{-15})	^{36}Cl (10^6 atoms/L)	^{36}Cl flux (atoms m^{-2} s^{-1})
Apr-04	61	3.0	25 ± 6	1.30 ± 0.31	30 ± 7
May-04	149	0.6	107 ± 20	1.17 ± 0.22	65 ± 12
Jun-04	89	0.7	50 ± 6	0.58 ± 0.08	20 ± 3
Jul-04	143	1.0	42 ± 6	0.68 ± 0.10	36 ± 6
Aug-04	95	1.0	38 ± 6	0.65 ± 0.11	23 ± 4
Sep-04	167	0.9	26 ± 4	0.40 ± 0.07	26 ± 4
Oct-04	471	0.6	38 ± 9	0.37 ± 0.08	66 ± 15
Nov-04	94	1.0	14 ± 3	0.23 ± 0.06	8 ± 2
Dec-04	61	2.5	20 ± 3	0.84 ± 0.14	19 ± 3
Jan-05	94	0.7	47 ± 7	0.55 ± 0.08	19 ± 3
Feb-05	41	1.2	33 ± 5	0.65 ± 0.11	11 ± 2
Mar-05	77	1.1	37 ± 6	0.70 ± 0.12	20 ± 3
Apr-05	86	1.0	60 ± 8	1.00 ± 0.14	33 ± 5
May-05	74	1.2	70 ± 10	1.46 ± 0.21	40 ± 6
Jun-05	53	0.6	115 ± 8	1.08 ± 0.08	22 ± 2
Jul-05	153	1.5	24 ± 4	0.62 ± 0.09	35 ± 5
Aug-05	231	1.1	44 ± 14	0.81 ± 0.25	70 ± 22
Sep-05	53	2.5	33 ± 4	1.41 ± 0.19	29 ± 4
Oct-05	181	0.8	30 ± 4	0.42 ± 0.06	28 ± 4
Nov-05	42	0.9	34 ± 4	0.53 ± 0.07	8 ± 1
Dec-05	1	5.9	–	–	–
Jan-06	49	0.7	84 ± 7	1.01 ± 0.09	19 ± 2
Feb-06	85	1.4	29 ± 4	0.70 ± 0.10	25 ± 4
Mar-06	61	1.5	40 ± 5	1.01 ± 0.11	23 ± 3

(*continued on next page*)

Table 6
(*continued*)

Sample	Precipitation* (mm)	Cl^- (mg/L)	$^{36}Cl/Cl$ (10^{-15})	^{36}Cl (10^6 atoms/L)	^{36}Cl flux (atoms m^{-2} s^{-1})
Apr-06	90	1.5	69 ± 6	1.76 ± 0.16	61 ± 6
May-06	108	1.1	74 ± 6	1.34 ± 0.11	54 ± 5
Jun-06	124	0.5	–	–	–
Jul-06	227	0.2	–	–	–
Aug-06	54	1.6	44 ± 5	1.23 ± 0.15	49 ± 6
Sep-06	164	1.0	32 ± 4	0.53 ± 0.07	33 ± 5
Oct-06	222	0.3	42 ± 5	0.22 ± 0.02	18 ± 2
Nov-06	112	1.2	32 ± 3	0.65 ± 0.06	28 ± 3
Dec-06	166	0.4	40 ± 5	0.28 ± 0.03	17 ± 2
Jan-07	32	1.6	66 ± 6	1.80 ± 0.15	22 ± 2
Feb-07	45	1.8	19 ± 4	0.58 ± 0.12	11 ± 2
Mar-07	46	4.8	13 ± 2	1.04 ± 0.17	18 ± 3
Apr-07	109	1.3	56 ± 6	1.28 ± 0.14	54 ± 6
May-07	172	1.1	88 ± 8	1.64 ± 0.15	106 ± 10
Jun-07	54	0.8	116 ± 8	1.52 ± 0.11	32 ± 2
Jul-07	218	0.4	57 ± 5	0.40 ± 0.03	32 ± 3

* Calculated from the amount of samples collected.

Table 7

Ratios of the maximum flux to the average natural background flux for the ^{36}Cl bomb pulse at different locations

Location	Latitude	Method	F_{max}/F_b	Reference
Tsukuba, Japan	36°N	Estimated	396	This study
Dye-3, Greenland	65°N	Measured	618	Synal et al. (1990, 1994)
Upper Fremont, WY, USA	43°N	Measured	21	Green et al. (2000)
Nangpai Gosum, Nepal	28°N	Measured	416	Green et al. (2000)

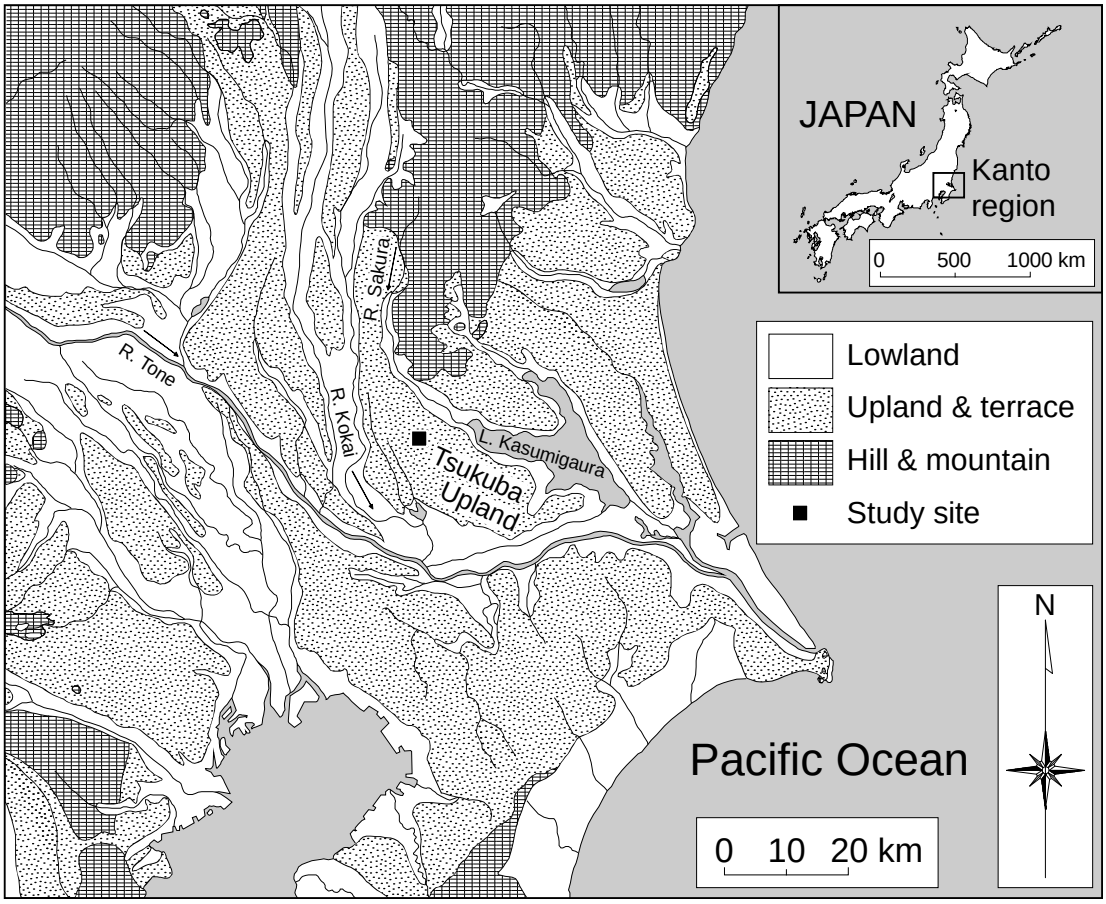

Figure 20 Location of the sampling site in the Tsukuba Upland (after Unozawa et al., 1988).

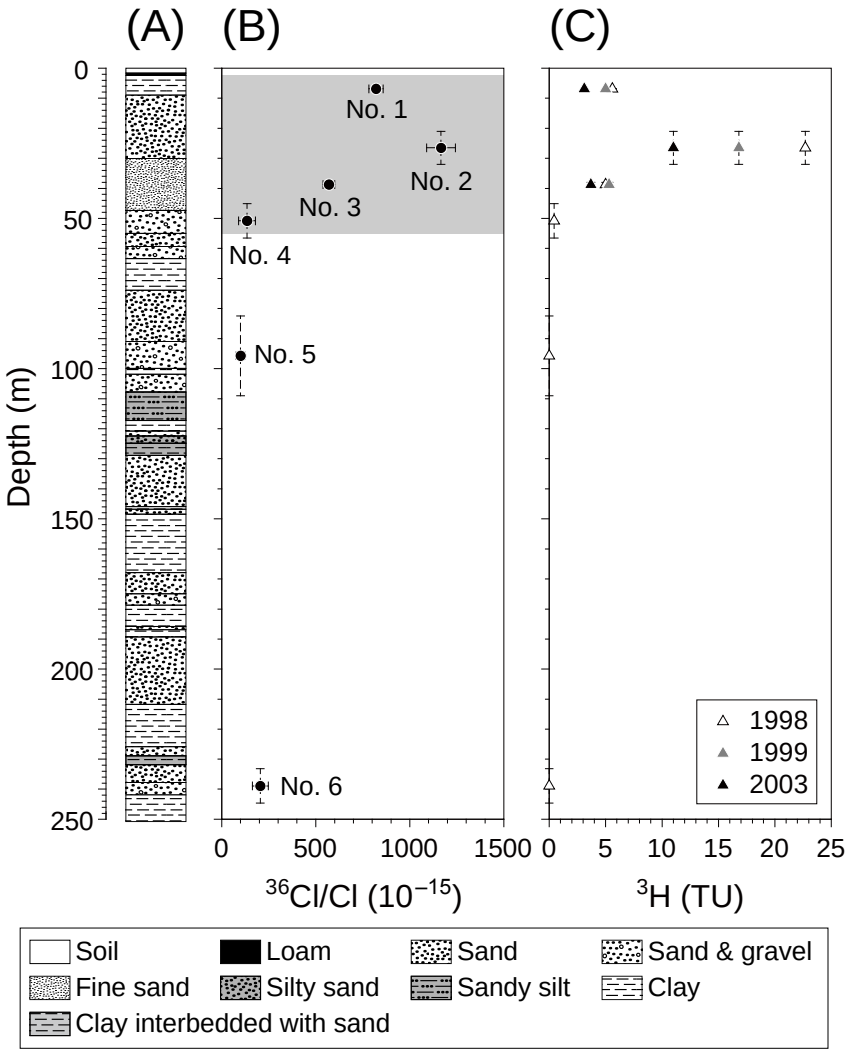

Figure 21 Depth profiles of (B) ^{36}Cl/Cl ratio and (C) ^{3}H concentrations in the groundwater of the Tsukuba Upland. Vertical error bars indicate widths of each screen. (A) A geologic column for the sampling site (after Taguchi, 1981; Unozawa et al., 1988).

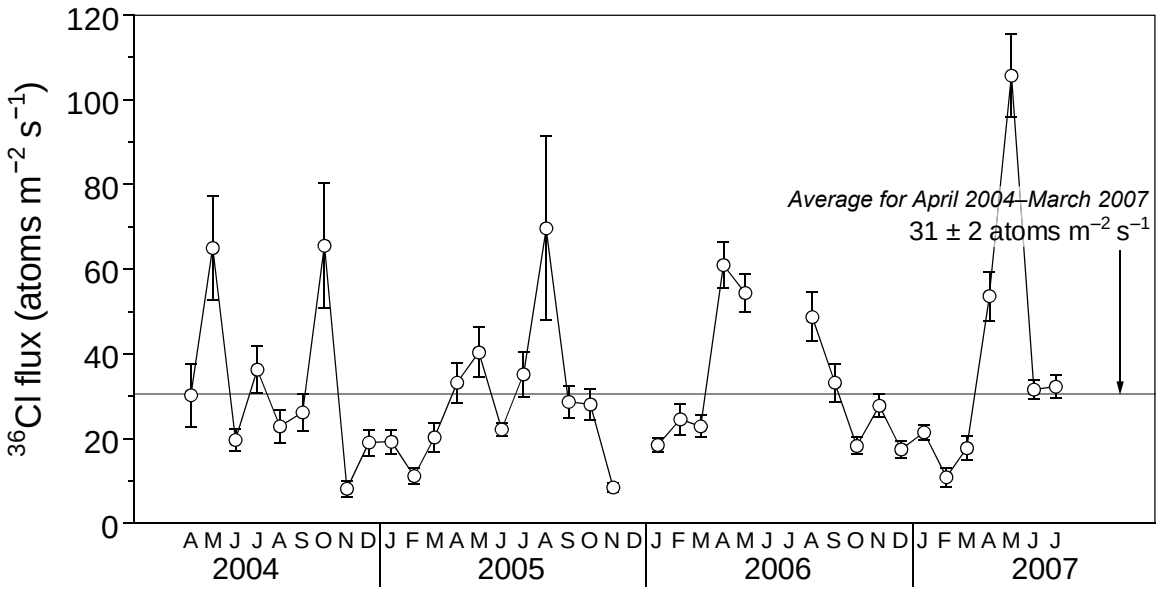

Figure 22 ^{36}Cl flux variation in monthly bulk precipitation samples collected in Tsukuba.

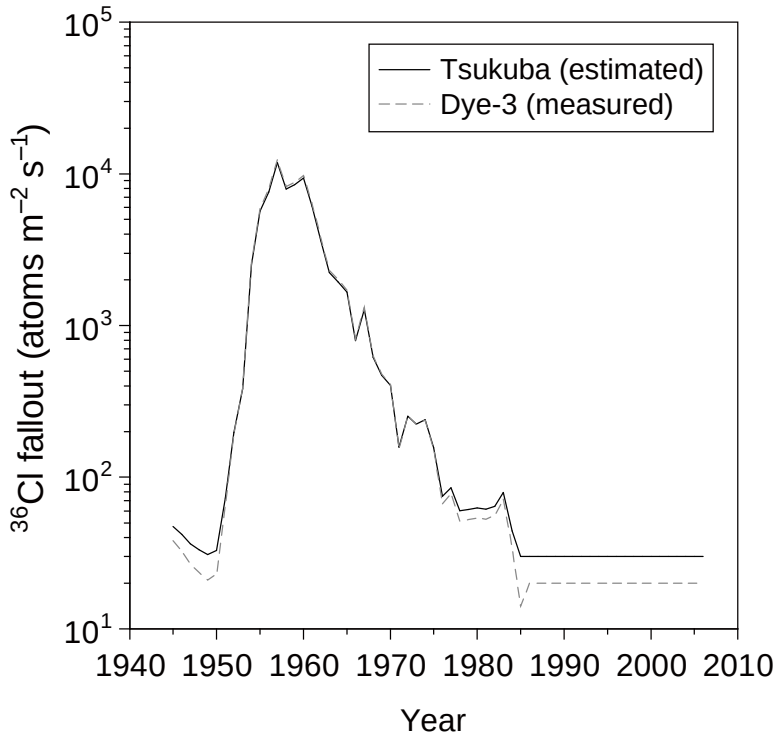

Figure 23 Estimated ^{36}Cl fallout history in the Tsukuba Upland, compared with measured data at the Dye-3 site, Greenland (Synal et al., 1990).

Chapter 6 Residence time of spring waters around Mt. Fuji, Japan

6.1 Study area

The Mt. Fuji area, ~150 km southwest from the Tsukuba Upland, was selected for applying ^{36}Cl bomb-pulse dating of groundwater. Having an elevation of 3,776 m, Mt. Fuji is one of the largest composite stratovolcano in Japan. Geological structure of this volcano has been extensively investigated as described in Tsuya (1968), Tsuya et al. (1988) and Miyaji et al. (1992).

Mt. Fuji primarily consists of alternating basaltic lava flows and coarse-grained pyroclastic rocks (e.g. Tsuya et al., 1988). It can be structurally divided into three parts (i.e. Komitake, Older Fuji and Younger Fuji volcanoes in ascending order) based on the geological and petrological investigations of volcanic ejecta (Tsuya, 1940). Underlying basement rocks are mainly Neogene marine sediments belonging to the Misaka Group (e.g. Miyaji et al., 1992). Figure 24 illustrates the general surface geology of Mt. Fuji and its vicinity.

Eruptive history of Mt. Fuji can be outlined as described subsequently (e.g. Tsuya et al., 1988; Miyaji et al., 1992). Komitake volcano started its activity in the middle Pleistocene with the eruption of andesite lava flows. According to tephrochronological studies (Machida, 1964), Older Fuji volcano began to form about 100,000 yr ago (Machida, 2007). Its activities are characterized by repeated eruption of tephra (volcanic ash) and basaltic lava flows (including mudflows mainly derived from pyroclastic flows and debris avalanches. The following activities of Younger Fuji volcano started in the late Pleistocene with the effusion of enormous lava flows. After a subsequent relatively dormant period during the early Holocene, Younger Fuji volcano became active again about 6,000 yr ago to form the present

Mt. Fuji (Machida, 2007).

The surface of Quaternary volcanoes is generally covered with high-porosity sediments and the resulting high permeability permits them to hold large groundwater reservoirs. The same characteristics are true for Mt. Fuji, which has a number of springs on the foot as well as Fuji Five Lakes on the northern foot (e.g. Yamamoto, 1995, 1996). These water bodies originate from the groundwater in Mt. Fuji recharged by precipitation at the area of high elevation. Annual precipitation over the Mt. Fuji area ranges from 1500–2000 mm on the northern slope to 2750–3000 mm on the eastern slope (Kizawa et al., 1969, p. 143; Yamamoto, 1970); Mt. Fuji receives a total volume of ~2 × 10^9 m^3 of precipitation over a year (Kurata, 1966; Kizawa et al., 1969, p. 141; Yamamoto, 1970).

Most of the springs are located at the distal part of the lava flows which were formed in the early Holocene. This is because alternate lava layers consisting of rapidly-cooled cracked parts and slowly-cooled solidified parts serve as multiple confined aquifers (Tsuchi, 1992). Such groundwater stored in Mt. Fuji has been an important water resource in the region. Due to the extensive use of groundwater, however, its depletion (including depletion of springs especially in the southeastern foot) and salinization (in the southern coastal part) has become a serious problem in 1960s (e.g. Ozaki, 1978; Mitsui, 1982; Ikeda, 1995).

Early hydrogeological data in the Mt. Fuji area were summarized by Kurata (1966) and Yamamoto (1970, 1971). For understanding the basic hydrological processes in Mt. Fuji, Yamamoto (1970) compiled early data and presented a basic mathematical model on the groundwater in Mt. Fuji. Yamamoto (1970) also proposed a hydrological classification of Mt. Fuji: upper recharging zone (>2,000 m), intermediate flowing zone (700–2,000 m), and lower spring zone (<700 m) (Yamamoto, 1995). Subsequent studies provided characteristics of springs distributed on the foot (Ino, 1976, 1987; Yamamoto et al., 1981), and also of interest

was groundwater in the southern foot (Ikeda, 1982, 1989; Nagae, 1984). In 1990s, a comprehensive study was designed to reveal groundwater flow system in Mt. Fuji, which includes investigations on stable isotopic composition (Yasuhara et al., 1995, 1997, 2007), chemical composition (Sato et al., 1997), and water temperature (Sato and Suzuki, 1996) of spring waters and groundwaters. Additionally, intensive investigations by Tsuchi (1992, 2001, 2002, 2007) including boring surveys considerably revealed the mechanisms of springs and groundwater flow in Mt. Fuji.

In parallel, previous studies have also focused on the residence time of groundwater in Mt. Fuji. Most of the previous estimates have been based on ^{3}H concentrations. Table 8 lists ^{3}H concentrations previously reported for major springs on the foot of Mt. Fuji, except for the springs on the northern foot. In the pioneering works during 1960s and 1970s (Takahashi et al., 1969; Ochiai and Kawasaki, 1970, 1972a, b), groundwaters (including springs) in shallow aquifers (i.e. older lava flows of Younger Fuji volcano) generally exhibited high ^{3}H concentrations derived from atmospheric nuclear tests; estimated residence times are several years. In contrast, groundwaters in deep aquifers (i.e. mudflow deposits of Older Fuji volcano) showed low ^{3}H concentrations; they estimated residence times of 20–30 years.

Yoshioka et al. (1993) showed relatively high ^{3}H concentration (~38 TU; measured in 1983) for the springs at the eastern foot. It is obviously higher than that found in the southeastern part (Table 8), and estimated residence times are ~30 yr using an exponential type model. By using the $^{3}H/^{3}He$ dating method (measured at Kakitagawa in 1988), Mahara et al. (1993) deduced the groundwater age of ~10 yr in the southeastern foot. On the contrary, Tsuchi (1992) interpreted ^{3}H concentration of 6.2 TU in the southern foot (measured at Wakutamaike in 1988) as indicating residence time of ~50 yr, while the estimated residence time was revised to ~15 yr in later studies (Tsuchi, 2001, 2002, 2007).

6.2 Sampling and analyses

Water samples collected in August 2006 and March 2007 include 28 spring water samples distributed over the Mt. Fuji area (Figure 25), excluding the northern foot. Additionally two groundwater samples were obtained from artesian flowing wells on the foot of Mt. Ashitaka. Electrical conductivity (EC), pH and temperature were measured in the field. Samples were analyzed for major ions, silica (SiO_2), stable isotopes (D and ^{18}O) and ^{36}Cl in the laboratory. Bicarbonate (HCO_3^-) concentrations were determined by titration with dilute H_2SO_4 solution. Other major ions (Na^+, K^+, Mg^{2+}, Ca^{2+}, Cl^-, SO_4^{2-}, NO_3^-) were measured by ion chromatography analysis (Ion Analyzer IA-100, Dkk-Toa). Dissolved SiO_2 concentrations were determined with an ICP-AES system. All samples for ion chromatography analysis and ICP-AES were filtered through a 0.20 μm membrane filter. Stable isotopic ratios ($\delta^{18}O$ and δD) were measured with a mass spectrometer (MAT252, Thermo Finnigan).

6.3 Stable isotopic composition and water chemistry

Results of $\delta^{18}O$ and δD analyses are listed in Table 9. Figure 26 shows the spatial distribution of $\delta^{18}O$ values in spring waters and groundwaters. As shown in the figure, investigated springs and groundwaters can be classified into five regions (i.e. eastern, southeastern, southern and western foots of Mt. Fuji, and foot of Mt. Ashitaka) using the altitude effect on $\delta^{18}O$ values. Except for the area around Mt. Ashitaka, the classification is basically after Kurata (1966) and Yamamoto (1970).

The southeastern foot of Mt. Fuji is located around the distal part of the Mishima lava flow (Figure 24) and is surrounded by the eastern foot of Mt. Ashitaka (1458 m) and the western outer rim of the crater in Mt. Hakone (~1100 m). As shown in Figure 26, the $\delta^{18}O$ values of the springs in the southeastern foot (from −8.5 to −8.1‰; Nos. 8–11) are lower than

those distributed around Mt. Ashitaka (from −7.4 to −7.8‰; Nos. 7 and 12–14). Similar isotopic characteristics have previously been reported by Yoshioka et al. (1993). This indicates that these springs on the southeastern foot mainly originate from areas of higher elevation than Mts. Ashitaka and Hakone, i.e. the foot of Mt. Fuji through the Mishima lava flow. In the eastern foot, the springs Nos. 1 and 2 have higher $\delta^{18}O$ values than other springs. Considering the locations of these springs, they would originate from the foot of Mt. Hakone or lower mountains.

Figure 27 shows the chemical composition of spring waters using stiff diagrams. The spring waters in the Mt. Fuji area are dominantly Ca-HCO_3 type as previously observed (Yoshioka et al., 1993; Sato and Suzuki, 1996; Sato et al., 1997). Some spring waters are more enriched in Na^+ than the general composition (e.g. No. 26). Increase in concentrations of Na^+ with groundwater flow has been observed for groundwater in other areas (e.g. the Nobi Plain; Sugisaki and Shibata, 1961; Mori, 1985). Such trend might be resulted from cation exchange reactions between Ca^{2+} in groundwater and Na^+ in the aquifer matrix materials (e.g. Chapelle and Knobel, 1983; Edmunds and Walton, 1983), and it suggests longer residence time.

Several spring waters from the southern foot exhibits high NO_3^- concentration (Figure 27). Most of these spring waters have higher $\delta^{18}O$ values than nearby springs. This implies that their recharge elevation is relatively low and that they originate from shallow aquifers. These waters would have been affected by nitrate from agricultural sources (e.g. fertilizer in tea plantation), and are possibly under the influence of anthropogenic Cl. Therefore, the samples with high NO_3^- concentration (>10 mg/L) were excluded from further analyses (e.g. Davis et al., 2003).

6.4 Residence time of spring waters estimated from bomb-produced chlorine-36

Measured $^{36}Cl/Cl$ ratio is presented in Figure 28 and listed in Table 9. The $^{36}Cl/Cl$ ratios range from 4.3×10^{-14} to 4.12×10^{-13}. Relatively high values were found in the eastern part. In order to estimate residence time of these waters, time-series variation of $^{36}Cl/Cl$ in the Mt. Fuji area was estimated using a scaling factor of 0.96 obtained in the previous chapter for the Tsukuba Upland. Yearly values of bomb-produced ^{36}Cl fallout at the Dye-3 site were scaled using the factor of 0.96 for the Mt. Fuji area. The fallout values were converted to the $^{36}Cl/Cl$ ratio using Equation (3).

Typical annual precipitation in the Mt. Fuji area, 2500 mm (e.g. Kizawa et al., 1969, p. 143; Yamamoto, 1970), was used as P. From the results of a previous study, mean recharge elevations for the springs at south, east and west slopes are 1100–2000 m, 1250–2200 m and 1600–2250 m, respectively (Yasuhara et al., 1995, 2007). Therefore, the mean value of four measured Cl^- concentrations at 780–2390 m in the investigated slopes (0.6 mg/L; Hiyama et al., 1995) was used as C_p. This value is reasonably consistent with previous data: 0.67 mg/L (average for June 1989–November 1989) at 1100–1150 m on the southern foot (Inoue et al., 1993), and 0.75 mg/L (average for September 1990–July 1992) at 1300 m on the eastern foot (Maruta et al., 1993). Annual Cl^- deposition flux calculated from assumed P and C_p (42.3 meq m^{-2} y^{-1}) also agrees with an observed value at 1300 m on the eastern foot during July 2006–July 2007 (38.9–40.9 meq m^{-2} y^{-1}; Funakura et al., 2007). The natural background $^{36}Cl/Cl$ ratio in the Mt. Fuji area was then added to the obtained R values. It was assumed to be 5×10^{-14} from the lower limit of measured $^{36}Cl/Cl$ ratios shown in Figure 29B. Figure 29A shows the estimated $^{36}Cl/Cl$ values obtained for the Mt. Fuji area.

As reported in previous studies (e.g. Tsuchi, 1992), most spring waters around Mt. Fuji originate from confined aquifers between lava layers or from the aquifer lying over the Older

Fuji mud flow, which has low permeability. Piston flow would be therefore a reasonable approximation in this area. Based on this assumption, residence times of spring waters can be estimated by comparing Figure 29A and Figure 29B. Considering the earlier results in 1960s (Table 8), which showed elevated level of tritium, most of the spring waters would have been recharged in the post-bomb period. Hence, estimated residence times were obtained using the post-peak part of the curve shown in Figure 29A. One exception is the spring No. 26, which showed low $\delta^{18}O$ value relative to the values for nearby springs. It would have been recharged in higher part of the slope. Its low $^{36}Cl/Cl$ ratio, $(5.3 \pm 0.7) \times 10^{-14}$, additionally suggests that it was recharged in the pre-bomb period.

Figure 30 shows distribution of estimated residence time for spring waters and groundwaters. Spring water residence times estimated for the eastern foot of Mt. Fuji (25–35 yr) are generally longer than those for other foots. In contrast, spring waters with short residence time were found in the southeastern foot (<20 yr). Springs in the southern foot exhibited variable residence times.

6.5 Discussion

Estimated residence times of less than 20 yr for the southeastern foot are consistent with previous results of ~10 yr by the $^{3}H/^{3}He$ dating method (Mahara et al., 1993). Residence times of 25–35 yr estimated for the eastern foot are also in agreement with the fact that higher ^{3}H concentrations (~38 TU) were measured in the eastern foot than those of the southeastern foot in 1983 (Table 8; Yoshioka et al., 1993). While, residence time of 25–30 yr obtained for the western foot obviously disagrees with the result by Ochiai (1995), which indicated bomb-derived ^{3}H in 1969 (137.3 TU; Table 8).

Four samples from the western foot have $^{36}Cl/Cl$ ratios of $\sim 1 \times 10^{-13}$ (Figure 28), which is

more than twice of the assumed natural background level (5×10^{-14}). However, the spring No. 30 shows especially low dissolved ion concentrations, which suggest its short residence time. One reasonable explanation for the disagreement in residence times may be that the natural background level of $^{36}Cl/Cl$ for the western foot is higher than that for other foots under investigation. This can be caused by the difference in the Cl^- concentration in precipitation; lesser stable chloride supply leads to the higher $^{36}Cl/Cl$ ratio (Bentley et al., 1986a). The springs located on the western foot has greater recharge elevation (1600–2250 m) than the springs on other foots (see the previous section; Yasuhara et al., 1995, 2007). Their results support the explanation mentioned here.

Another possible cause of the disagreement is that piston flow is not a reasonable assumption for some of the springs. If exponential mixing is the dominant process, residence times would be reduced to ~8 yr in the western foot. At present, however, available data are not enough for further discussing this issue.

Although the springs located on the southeastern foot mainly originate from the groundwater of Mt. Fuji, mixing of groundwater from Mt. Ashitaka or Mt. Hakone has been suggested (Yoshioka et al., 1993; Yasuhara et al., 2007). Measurement of chloride deposition around Mt. Fuji by Togo et al. (1995, 1997) indicated that the southeastern foot receives greater chloride with airborne salts. Then, the groundwater from the foots of Mt. Ashitaka and Mt. Hakone should contain higher concentrations of chloride. Relatively high Cl^- concentrations in the spring waters on the southeastern foot may be the result of such mixing effect. Therefore, the estimated residence times for the southeastern foot may include some errors.

Estimated residence time for the spring No. 26 (>55 yr) can be related to the fact that the spring is located along the Agoyama Fault (Tsuchi, 2002). It suggests that this spring water

originates from groundwater in deeper aquifers including the mudflow deposits of Older Fuji volcano. This is reasonably consistent with observation in the field that this spring actually discharges from the opposite side of the direction of Mt. Fuji.

Figure 31 shows obtained $^{36}Cl/Cl$ ratios plotted against SiO_2 and HCO_3^- concentrations, which generally serve as indicators of groundwater residence time. No clear relationship was found between SiO_2 concentrations and $^{36}Cl/Cl$ ratios (Figure 31A), whereas Figure 31B shows reasonable correlation between HCO_3^- concentrations and $^{36}Cl/Cl$ ratios. From the figure, the samples with higher $^{36}Cl/Cl$ ratio generally have greater HCO_3^- concentration. The spring No. 26 has the highest HCO_3^- concentration among the springs in the southern foot. Increasing trend in HCO_3^- concentration along groundwater flow direction has been found in the southern foot (Ikeda, 1982, 1989). Figure 31B may provide support for the interpretation that investigated groundwaters are recharged in post-bomb period.

In this study, investigated groundwaters were mainly interpreted as post-bomb waters according to the previous ^3H data in 1960s. However, combined use with other residence time indicators is necessary to distinguish the pre-peak and post-peak waters. Measurement of ^3H may be still effective for this purpose, since there is a time lag between the ^{36}Cl bomb peak and the ^3H peak by ~7 yr (Figure 1). In addition, HCO_3^- can be a supporting indicator of residence time as shown in Figure 31B.

Condition of the recharge area (i.e. the natural background level of $^{36}Cl/Cl$, chloride concentration in precipitation, and mean annual precipitation) has to be known correctly, otherwise errors may be directly enlarged in estimating residence times. However the results obtained in the Mt. Fuji area show the fundamental reasonability of the method using bomb-produced ^{36}Cl to estimate groundwater residence time.

6.6 Summary

Residence time of spring waters around Mt. Fuji was estimated using bomb-produced ^{36}Cl. To estimate time-series variation of $^{36}Cl/Cl$ ratio in the Mt. Fuji area, the Dye-3 fallout data was scaled using a scaling factor obtained for the Tsukuba Upland in the previous chapter. After being converted to the $^{36}Cl/Cl$ ratio, the natural background $^{36}Cl/Cl$ ratio estimated from the lower limit of measured values was added to derive the time-series variation. Measured $^{36}Cl/Cl$ ratios in spring waters were compared to the estimated time-series variation under the assumption of piston flow.

Distribution of spring water residence time is reasonably consistent with previous studies. However, residence time in the western foot obviously disagrees with previous one. This may be due to the difference in the natural background $^{36}Cl/Cl$ ratio among different slopes. It can be caused by the difference in the Cl^- concentration in precipitation. Mean recharge elevation for each foot estimated in a previous study supports the explanation.

Condition of the recharge area (i.e. the natural background level of $^{36}Cl/Cl$, chloride concentration in precipitation, and mean annual precipitation) has to be known correctly, otherwise errors may be directly enlarged in estimating residence times. However, the results obtained in this study show the fundamental effectiveness of the method proposed in this study.

Table 8

Previously measured ^{3}H concentrations in major springs on the foot of Mt. Fuji

Spring	Date	^{3}H (TU)	Reference
Southeastern foot			
Suisen-en	May 21, 1965	71 ± 7	Takahashi et al. (1969)
Kakitagawa	May 23, 1965	76.0	Ochiai and Kawasaki (1970)
Kohamaike	May 23, 1965	80.0	Ochiai and Kawasaki (1970)
Suisen-en	May 23, 1965	73.0	Ochiai and Kawasaki (1970)
Kakitagawa	Jul. 21, 1965	77 ± 8	Takahashi et al. (1969)
Kakitagawa	Aug. 8, 1967	69.2	Ochiai and Kawasaki (1970, 1972a)
Kohamaike	Aug. 8, 1967	116.3	Ochiai and Kawasaki (1970, 1972a)
Kakitagawa	Jul. 12, 1969	124.3	Ochiai (1995)
Suisen-en	Jul. 12, 1969	117.9	Ochiai (1995)
Kohamaike	Jul. 6, 1983	0 ± 3	Yoshioka et al. (1993)
Suisen-en	Jul. 6, 1983	5 ± 5	Yoshioka et al. (1993)
Kakitagawa	Jul. 7, 1983	12 ± 3	Yoshioka et al. (1993)
Maruike	Jul. 7, 1983	8 ± 3	Yoshioka et al. (1993)
Fujiyusuichi	Jul. 7, 1983	7 ± 4	Yoshioka et al. (1993)
Ichibancho	Nov. 9, 1988	9.1 ± 0.5	Mahara et al. (1993)
Kakitagawa	Nov. 10, 1988	7.4 ± 0.5	Mahara et al. (1993)
Ichibancho	Nov., 1990	6.2	Masuda et al. (1994)
Kakitagawa	Nov., 1990	6.4	Masuda et al. (1994)
Maruike	Nov., 1990	6.7	Masuda et al. (1994)
Kakitagawa	1993 or 1994	5.6 ± 0.2	Kakiuchi (1995)
Kakitagawa	Aug. 22, 1995	5.0 ± 0.4	Tsuchi (2001, 2002)
Kohamaike	Aug. 22, 1995	5.4 ± 0.4	Tsuchi (2001, 2002)
Maruike	Aug. 22, 1995	5.5 ± 0.4	Tsuchi (2001, 2002)

(*continued on next page*)

Table 8
(*continued*)

Spring	Date	^{3}H (TU)	Reference
Eastern foot			
Iwanami	Aug. 9, 1967	68.9	Ochiai and Kawasaki (1970)
Iwanami	Jul. 8, 1983	14 ± 9	Yoshioka et al. (1993)
Nakashimizu	Jul. 8, 1983	38 ± 12	Yoshioka et al. (1993)
Numata	Jul. 8, 1983	11 ± 12	Yoshioka et al. (1993)
Southern foot			
Wakutamaike	Jul. 12, 1969	126.2	Ochiai (1995)
Harada	Jul. 12, 1969	119.8	Ochiai (1995)
Wakutamaike	Oct. 19, 1988	6.2 ± 0.2	Tsuchi (1992)
Aomi	Jul. 12, 1993	5.1 ± 0.4	Tsuchi (1996)
Wakutamaike	Jul. 12, 1993	4.5 ± 0.4	Tsuchi (1996)
Yodoshi	Jul. 12, 1993	5.5 ± 0.4	Tsuchi (1996)
Kansekien	1993 or 1994	6.1 ± 0.2	Kakiuchi (1995)
Wakutamaike	1993 or 1994	4.7 ± 0.2	Kakiuchi (1995)
Western foot			
Inokashira	Jul. 11, 1969	137.3	Ochiai (1995)
Inokashira (1)	1991	8.7 ± 0.4	Nakai (1996)
Inokashira (2)	1991	8.1 ± 0.4	Nakai (1996)
Inokashira	1993 or 1994	6.8 ± 0.2	Kakiuchi (1995)
Shiraito	1993 or 1994	5.9 ± 0.2	Kakiuchi (1995)
Shiraito	Jan. 12, 1994	6.2 ± 0.4	Tsuchi (1996)
Foot of Mt. Ashitaka			
Hirayama	Jul. 7, 1983	7 ± 9	Yoshioka et al. (1993)
Mizujinja	Jul. 7, 1983	2 ± 3	Yoshioka et al. (1993)
Keigashima	Jul. 8, 1983	0 ± 8	Yoshioka et al. (1993)

Table 9
^{36}Cl and stable isotopic data for the Mt. Fuji spring waters and groundwaters

No.	Name	Date	$\delta^{18}O$ (‰)	δD (‰)	Cl^- (mg/L)	$^{36}Cl/Cl$ (10^{-15})	^{36}Cl (10^6 atoms/L)
1	Yubune	Mar. 5, 2007	−7.9	−49	2.8	70 ± 6	3.3 ± 0.3
2	Kuwaki	Mar. 6, 2007	−8.1	−50	2.5	314 ± 16	13.5 ± 0.7
3	Nimaibashi	Aug. 24, 2006	−9.9	−66	2.1	412 ± 16	14.8 ± 0.6
4	Nakashimizu	Aug. 24, 2006	−8.9	−57	2.5	105 ± 9	4.4 ± 0.4
5	Numata	Aug. 23, 2006	−9.5	−62	2.6	201 ± 12	8.8 ± 0.5
6	Futagosuijin	Aug. 24, 2006	−9.4	−62	2.2	202 ± 14	7.4 ± 0.5
7	Hirayama	Aug. 23, 2006	−7.7	−48	5.7	99 ± 8	9.6 ± 0.8
8	Komoike	Aug. 21, 2006	−8.1	−52	7.5	68 ± 9	8.7 ± 1.2
9	Suisen-en	Aug. 21, 2006	−8.2	−53	6.9	70 ± 9	8.2 ± 1.1
10	Fujiyusuichi	Aug. 21, 2006	−8.2	−52	7.7	51 ± 8	6.6 ± 1.0
11	Kakitagawa	Aug. 21, 2006	−8.5	−55	6.6	43 ± 7	4.8 ± 0.7
12	Mizujinja	Mar. 8, 2007	−7.8	−48	2.5	70 ± 6	2.9 ± 0.2
13	Hiyoshijinja	Aug. 21, 2006	−7.4	−46	5.9	217 ± 12	21.7 ± 1.2
14	Hara	Aug. 21, 2006	−7.6	−48	4.5	113 ± 10	8.7 ± 0.7
15	Iouji	Aug. 23, 2006	−8.0	−50	6.8	42 ± 6	4.8 ± 0.7
16	Kansekien	Aug. 21, 2006	−8.4	−54	3.6	67 ± 8	4.1 ± 0.5
17	Takifudou	Aug. 21, 2006	−8.5	−54	3.5	61 ± 7	3.7 ± 0.4
18	Youmeiji	Aug. 21, 2006	−8.5	−55	3.4	78 ± 8	4.5 ± 0.5
19	Hounji	Aug. 23, 2006	−8.2	−52	5.1	52 ± 7	4.4 ± 0.6
20	Sugita (1)	Mar. 8, 2007	−7.6	−49	8.3	39 ± 4	5.5 ± 0.6
21	Sugita (2)	Mar. 8, 2007	−7.7	−50	7.2	42 ± 4	5.1 ± 0.5
22	Izurimizu	Aug. 22, 2006	−7.8	−49	5.8	62 ± 7	6.1 ± 0.7
23	Kamikoizumi	Aug. 22, 2006	−8.4	−54	3.4	121 ± 10	7.0 ± 0.6
24	Wakutamaike	Aug. 22, 2006	−8.5	−55	4.6	96 ± 9	7.5 ± 0.7
25	Hagoromo	Aug. 23, 2006	−8.6	−55	5.3	65 ± 6	5.9 ± 0.6
26	Yoshimaike	Aug. 23, 2006	−9.3	−61	6.6	53 ± 7	5.9 ± 0.7
27	Shiraitonotaki	Mar. 7, 2007	−9.5	−63	4.2	129 ± 8	9.3 ± 0.5
28	Shiraitoyusui	Mar. 7, 2007	−9.2	−61	5.2	109 ± 7	9.6 ± 0.6
29	Inokashira	Aug. 22, 2006	−9.3	−61	3.6	130 ± 11	8.0 ± 0.7
30	Jinbanotaki	Mar. 7, 2007	−8.7	−57	2.7	124 ± 7	5.8 ± 0.3

Table 10
Chemical composition of the Mt. Fuji spring waters and groundwaters

No.	Na^+ (mg/L)	K^+ (mg/L)	Mg^{2+} (mg/L)	Ca^{2+} (mg/L)	Cl^- (mg/L)	SO_4^{2-} (mg/L)	NO_3^- (mg/L)	HCO_3^- (mg/L)	SiO_2 (mg/L)
1	4.7	1.1	5.3	10.2	2.8	3.4	2.2	58.6	52.7
2	4.5	1.0	3.7	13.8	2.5	4.6	3.0	58.6	40.3
3	11.3	1.8	4.8	14.5	2.1	18.2	0.6	72.6	25.2
4	6.8	1.6	4.7	12.8	2.5	7.0	3.7	63.4	36.6
5	8.4	1.5	5.6	15.0	2.6	14.3	1.9	71.4	32.7
6	7.8	1.5	5.1	13.4	2.2	12.7	2.1	65.9	32.8
7	7.5	1.5	4.0	12.4	5.7	9.0	5.7	52.5	39.6
8	11.2	2.1	5.9	16.8	7.5	10.9	3.4	82.4	44.9
9	9.7	1.8	5.0	14.9	6.9	15.4	6.2	60.4	41.4
10	8.2	1.9	4.3	12.4	7.7	9.3	6.3	51.2	42.8
11	9.6	1.9	4.8	14.5	6.6	17.0	4.7	58.6	41.1
12	3.4	1.1	0.9	3.6	2.5	1.4	2.3	16.5	30.6
13	7.3	1.2	4.9	11.2	5.9	1.1	2.6	63.4	46.3
14	7.2	1.0	2.1	7.0	4.5	2.6	0.5	39.7	39.3
15	7.1	2.7	5.0	12.5	6.8	13.6	16.7	40.3	45.6
16	6.3	1.5	2.7	7.8	3.6	6.3	5.0	36.0	38.9
17	6.3	1.6	2.7	7.8	3.5	6.4	5.2	36.0	38.2
18	6.7	1.4	2.7	7.7	3.4	6.5	5.1	36.0	37.6
19	8.0	2.3	5.3	14.9	5.1	16.4	19.0	47.6	40.5
20	6.4	5.5	8.2	28.0	8.3	39.7	64.1	22.6	38.1
21	6.6	3.8	6.2	21.2	7.2	31.1	40.6	25.6	38.7
22	7.0	2.5	4.9	19.1	5.8	18.9	24.0	47.6	43.7
23	6.8	1.6	5.1	12.9	3.4	14.2	9.4	50.6	43.6
24	7.5	2.0	4.0	11.7	4.6	9.0	9.4	48.8	43.1
25	7.7	2.1	3.5	11.4	5.3	7.4	8.2	48.2	44.3
26	14.2	1.7	4.4	12.6	6.6	18.4	7.6	58.0	44.5
27	8.6	1.6	3.5	9.7	4.2	8.9	7.1	44.5	37.0
28	9.2	1.9	3.7	10.5	5.2	10.9	8.3	45.8	35.0
29	5.9	1.0	2.4	8.2	3.6	7.7	3.2	32.9	24.6
30	4.0	0.9	1.7	7.8	2.7	5.9	3.0	27.5	20.0

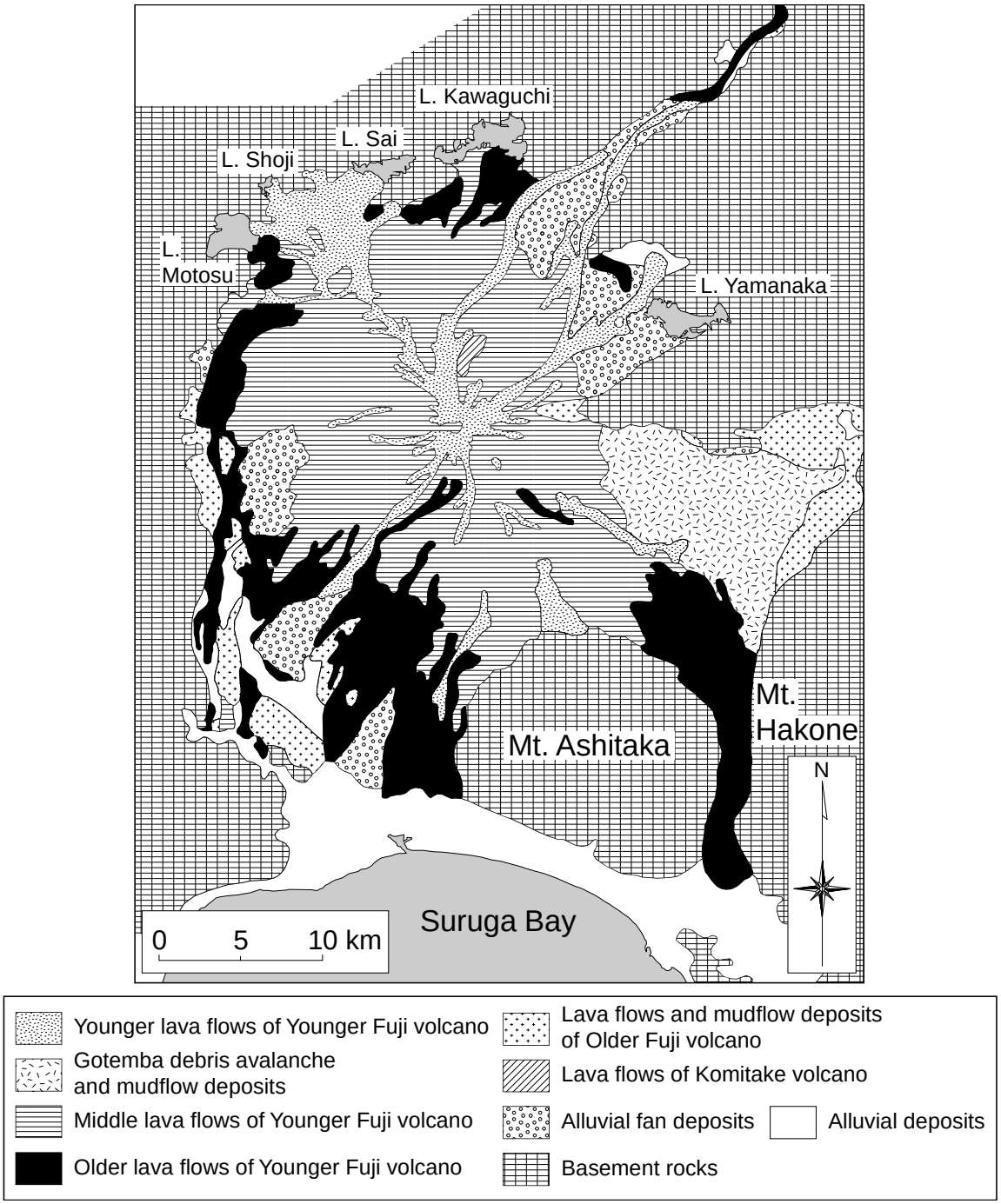

Figure 24 General surface geology of Mt. Fuji (after Tsuya, 1968; Machida, 1977, p. 51).

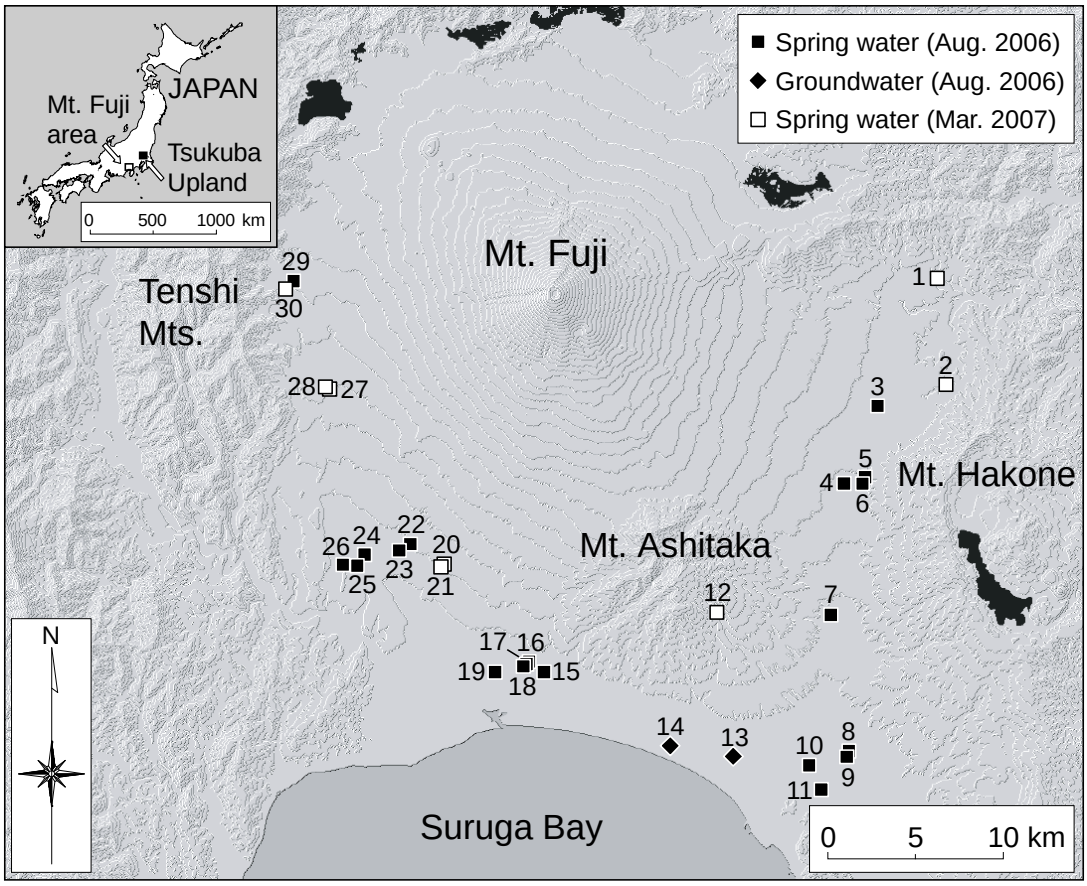

Figure 25 Location of sampling points in the Mt. Fuji area (based on the Digital Map 50 m Grid (Elevation) published by the Geographical Survey Institute). Sampling points include 28 spring waters and two groundwaters from artesian flowing wells.

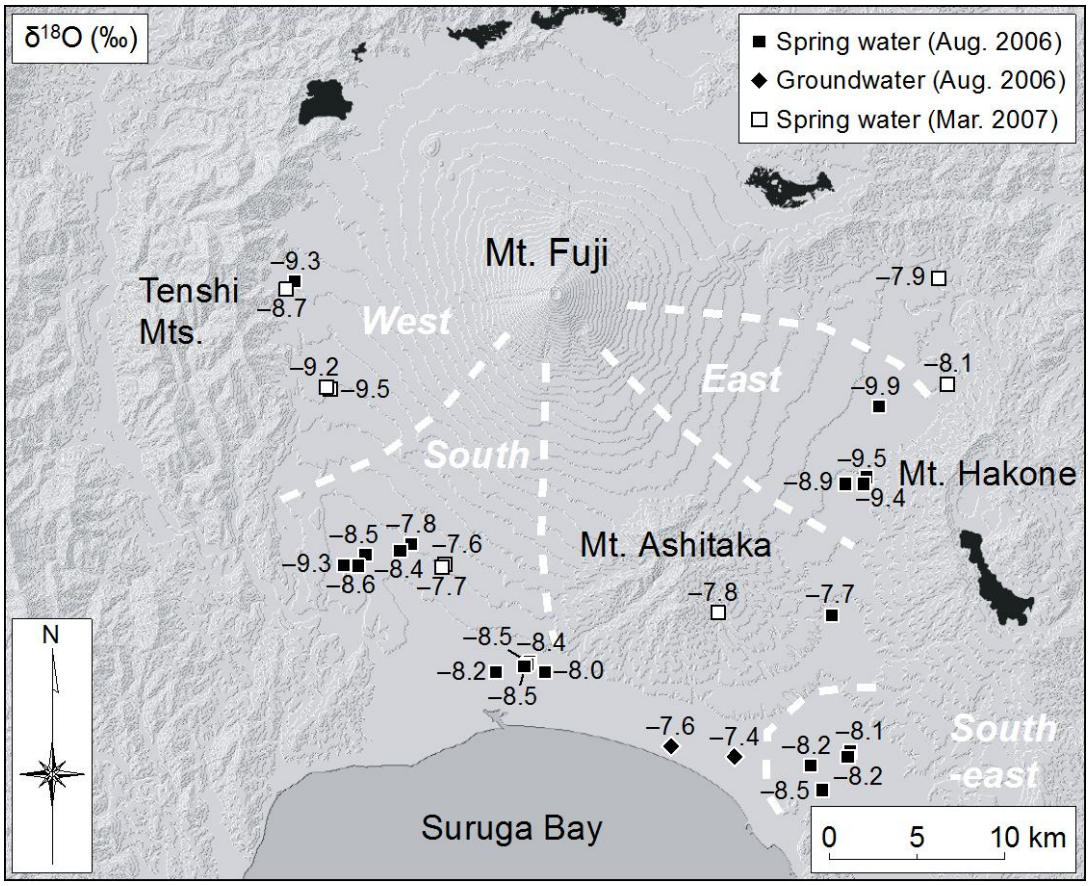

Figure 26 Spatial distribution of $\delta^{18}O$ values in spring waters and groundwaters in the Mt. Fuji area.

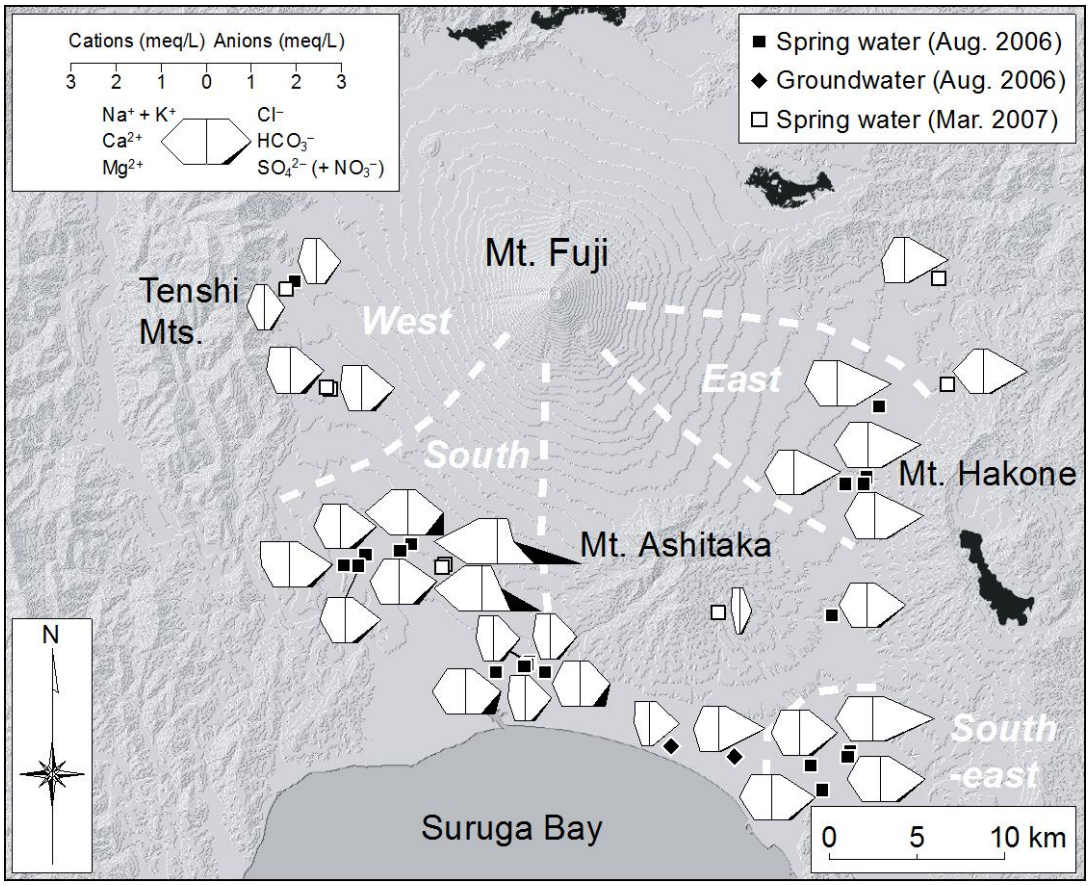

Figure 27 Spatial distribution of water chemistry in the Mt. Fuji area.

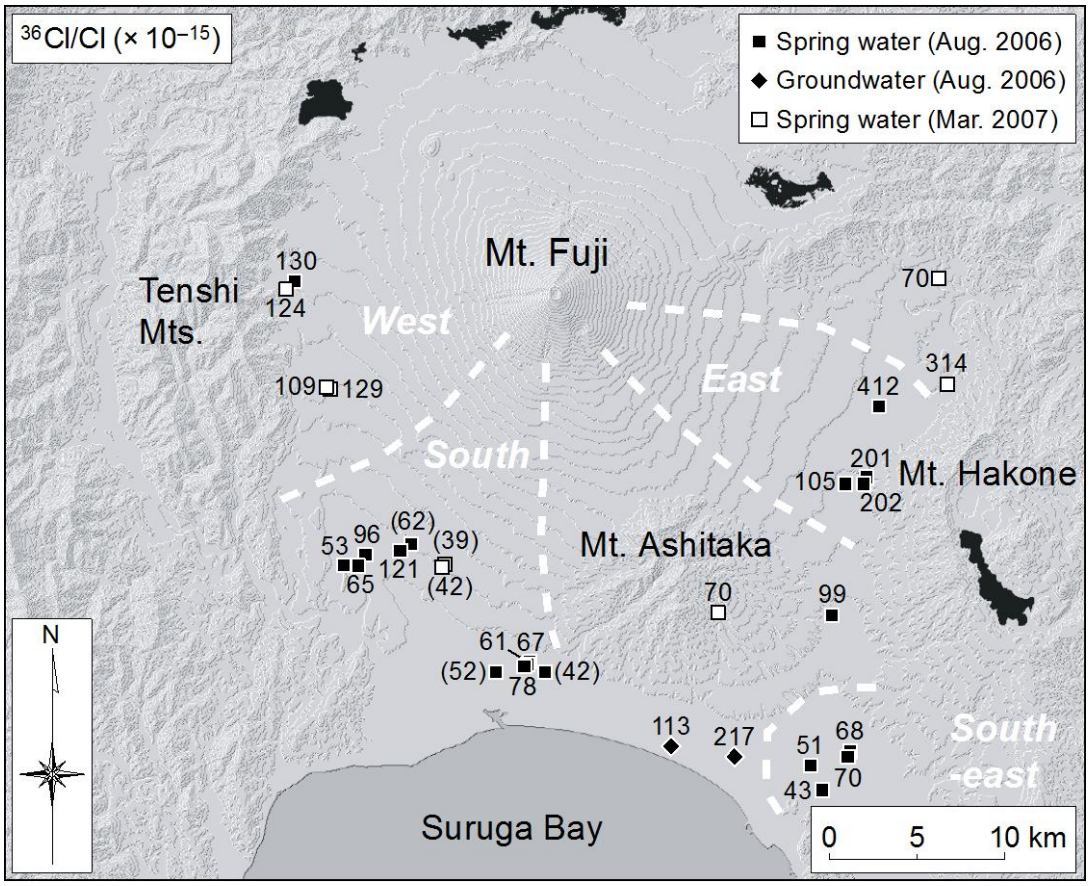

Figure 28 Spatial distribution of ^{36}Cl/Cl ratios in spring waters and groundwaters in the Mt. Fuji area. Values in parentheses represent the samples with high NO_3^- concentration (>10 mg/L).

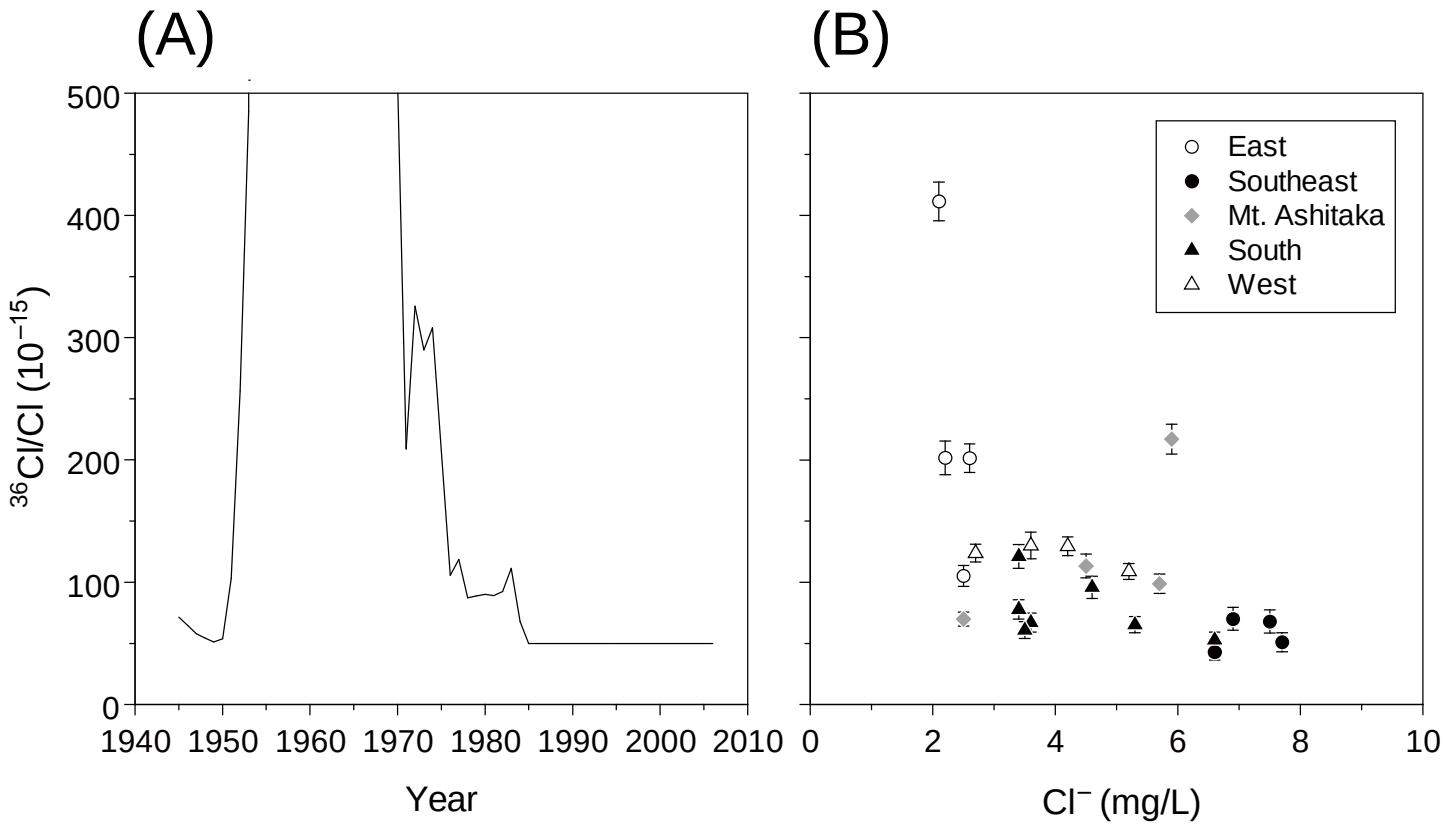

Figure 29 Estimation of residence time of spring waters and groundwaters using bomb-produced ^{36}Cl. (A) Predicted time-series variation of ^{36}Cl/Cl in the Mt. Fuji area. (B) Measured ^{36}Cl/Cl ratios in spring waters and groundwaters.

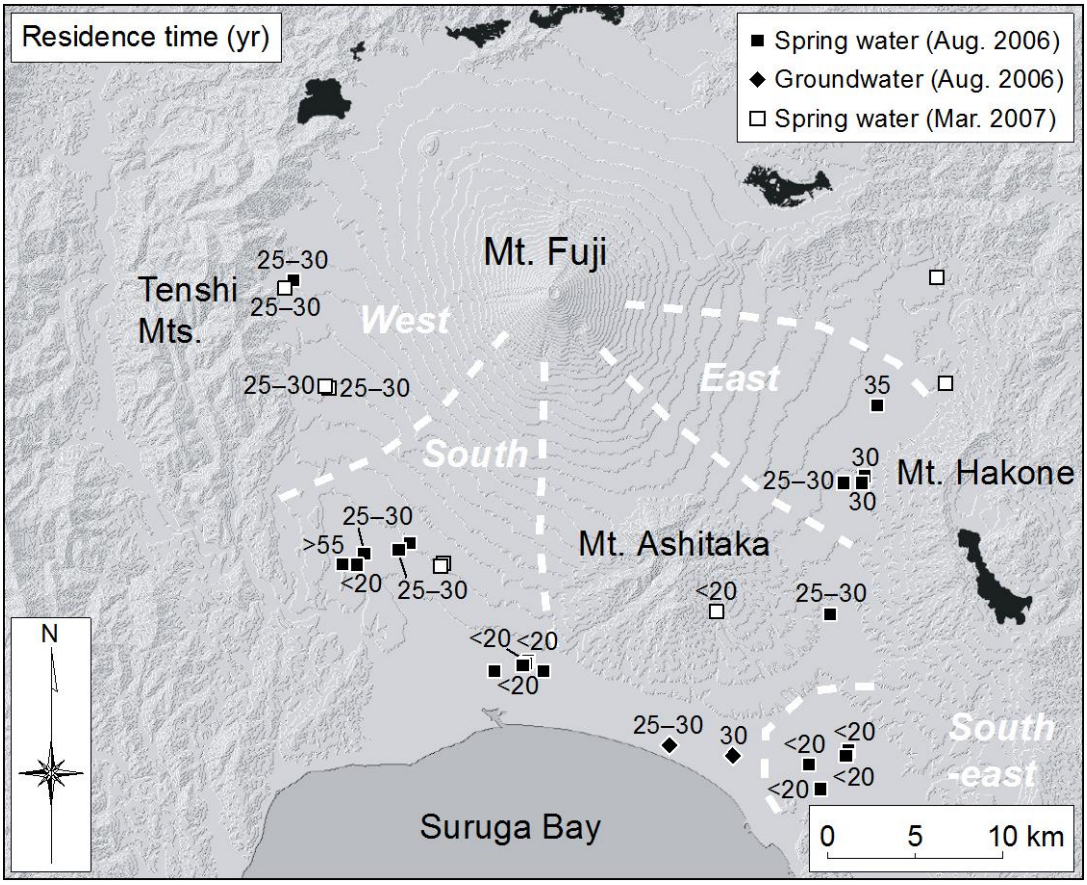

Figure 30 Spatial distribution of residence time of spring waters and groundwaters in the Mt. Fuji area, estimated from ^{36}Cl.

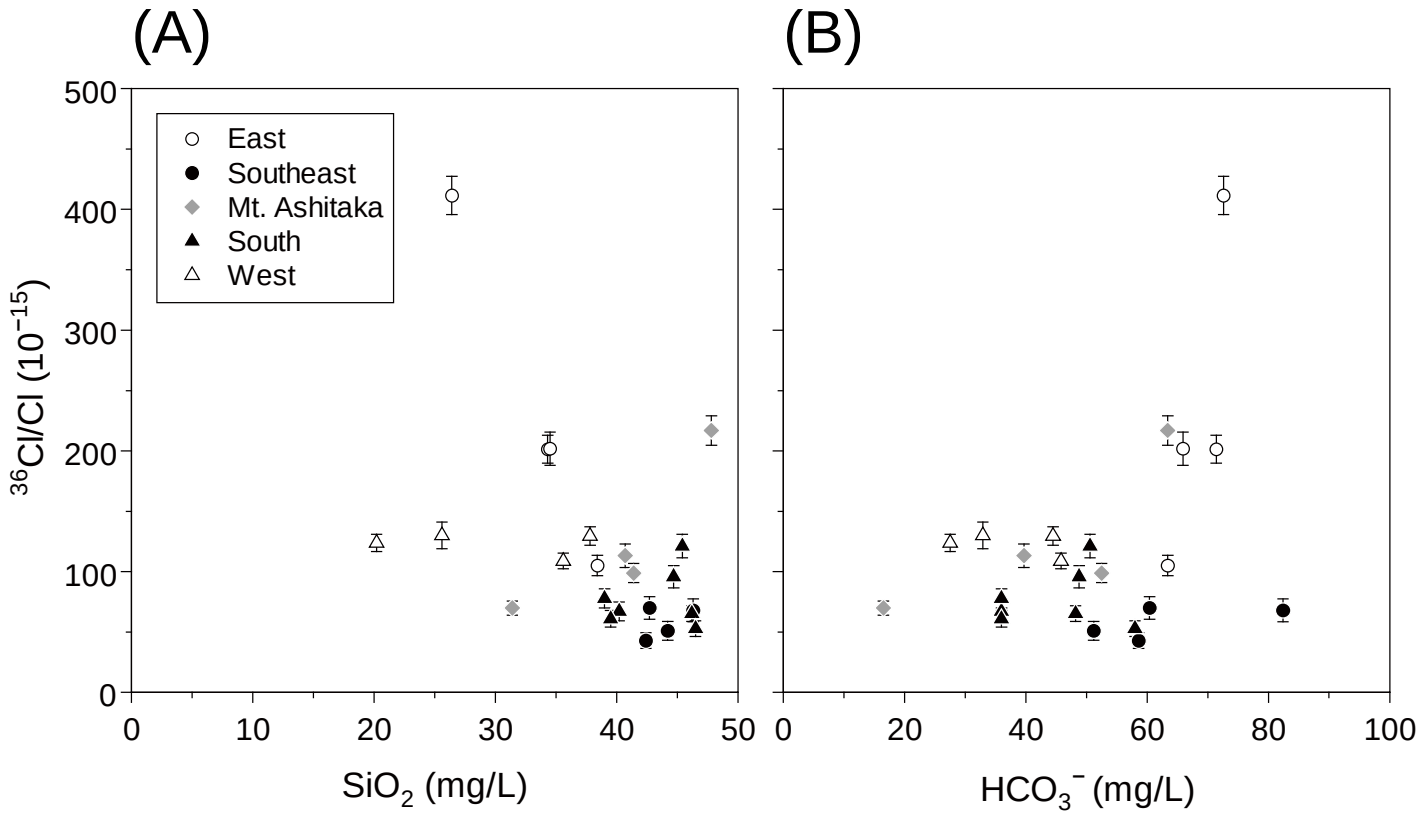

Figure 31 ^{36}Cl ratios in spring waters and groundwaters compared with (A) SiO_2 and (B) HCO_3^- concentrations.

Chapter 7 Conclusions

This study has presented a methodology for quantitatively estimating residence time of modern groundwater by using bomb-produced ^{36}Cl. Total deposition of bomb-produced ^{36}Cl was estimated for the Oderbruch region, Germany and the Tsukuba Upland, Japan, from measured ^{36}Cl concentrations in groundwater. The proposed method was then applied to the springs around Mt. Fuji, Japan.

The $^{36}Cl/Cl$ distribution in groundwater was investigated in the Oderbruch aquifer. The Oderbruch groundwaters appeared to be affected by saline water. The effect of its mixing was corrected using a two-component mixing model. Simulation of tracer transport for ^{3}H and ^{36}Cl derived scaling factors in the range of 0.3–1.22 (c.f. 2.5 based on the latitudinal distribution model). Estimated time-series variation of $^{36}Cl/Cl$ in the Oder River basin is in satisfactory agreement with the $^{36}Cl/Cl$ ratios in wine samples from the Rheingau, Germany. This suggests that an over-simplified model such as the latitudinal distribution model is not suitable for estimating the fallout pattern of bomb-produced ^{36}Cl. The results also imply that the scaling factor can be obtained by measuring ^{36}Cl in systematically-sampled groundwaters.

Depth profile of $^{36}Cl/Cl$ ratio in groundwater was investigated in the Tsukuba Upland. From the vertical distribution of ^{36}Cl, the total bomb-produced ^{36}Cl fallout over the upland is 2.3×10^{12} atoms/m^2, which corresponds to a scaling factor of 0.96. The ratio of the maximum bomb-peak fallout to the average natural background flux for the estimated local fallout history is consistent with measured data in Nepal. This agreement supports the validity of the obtained scaling factor. The results also confirmed that the local fallout history of ^{36}Cl can be estimated from a groundwater profile.

Residence time of spring waters around Mt. Fuji was estimated using bomb-produced

^{36}Cl. To estimate time-series variation of ^{36}Cl/Cl ratio in the Mt. Fuji area, the Dye-3 fallout data was scaled using a scaling factor obtained for the Tsukuba Upland. Measured ^{36}Cl/Cl ratios in spring waters were compared to the estimated time-series variation under the assumption of piston flow. Distribution of spring water residence time is reasonably consistent with previous studies. However, residence time in the western foot obviously disagrees with previous one. This may be due to the difference in the natural background ^{36}Cl/Cl ratio among different slopes. It can be caused by the difference in the Cl^- concentration in precipitation.

Condition of the recharge area (i.e. the natural background level of ^{36}Cl/Cl, chloride concentration in precipitation, and mean annual precipitation) has to be known correctly, otherwise errors may be directly enlarged in estimating residence times. However, the results obtained show the fundamental effectiveness of the method proposed in this study.

Acknowledgements

I am deeply indebted to my supervisor Dr. Norio Tase (Professor, University of Tsukuba) for offering me the opportunity to carry out this work. Without his continuous advice, guidance and encouragement, I would not have been able to complete this work. Many thanks are expressed to Dr. Yasuo Nagashima (Professor Emeritus, University of Tsukuba) for guiding me to the field of accelerator mass spectrometry (AMS). The manuscript of this thesis was reviewed by Dr. Tadashi Tanaka (Professor, University of Tsukuba), Dr. Maki Tsujimura (Associate Professor, University of Tsukuba), Dr. Tsutomu Yamanaka (Assistant Professor, University of Tsukuba) and Dr. Kimikazu Sasa (Assistant Professor, University of Tsukuba). Their careful reading and critical comments considerably improved this thesis.

I am grateful to Dr. Yasuo Nagashima, Dr. Kimikazu Sasa, Mr. Tsutomu Takahashi (University of Tsukuba), and all the members of the AMS Group, University of Tsukuba, for their continuous support and contributions during ^{36}Cl measurements. Development of the sample preparation scheme for ^{36}Cl-AMS was contributed by Dr. Riki Seki (Former Professor, University of Tsukuba), Ms. Michiko Tamari (University of Tsukuba), Dr. Yuki Matsushi (The University of Tokyo) and Dr. Keisuke Sueki (Associate Professor, University of Tsukuba). I would like to express my gratitude to Dr. Kunihiko Nishiizumi (University of California, Berkeley) for his detailed advice on sample preparation using ion exchange resin.

Dr. Gudrun Massmann (Free University of Berlin) conducted groundwater sampling in the Oderbruch polder. She provided valuable data including the ^{3}H/^{3}He data. Groundwater sampling in the Tsukuba Upland was assisted by Dr. Masaya Yasuhara (Geological Survey of Japan), Dr. Makoto Takahashi (Geological Survey of Japan) and Mr. Seongwon Lee (University of Tsukuba). Monthly precipitation sampling was designed upon the advice of Dr.

Shiho Yabusaki (Rissho University). She also kindly supported $\delta^{18}O$ and δD analyses using a mass spectrometer. I am thankful to Dr. Alfred Priller (University of Vienna) for providing the ^{36}Cl data of wine samples from the Rheingau.

Invaluable suggestions and continuous encouragement from Dr. Yuki Matsushi have helped me to complete this thesis. Encouragement from my colleague Mr. Seongwon Lee also helped me to continue my research. I appreciate all the staff and colleagues at the Laboratory of Hydrological Science, University of Tsukuba for their fruitful discussion and valuable comments during the group seminar.

References

Absalon, D. and Matysik, M. (2007): Change in water quality and runoff in the Upper Oder River Basin. *Geomorphology*, **92**, 106–118.

Alley, W.M., Healy, R.W., LaBaugh, J.W. and Reilly, T.E. (2002): Flow and storage in groundwater systems. *Science*, **296**, 1985–1990.

Andrews, J.N., Edmunds, W.M., Smedley, P.L., Fontes, J.-Ch., Fifield, L.K. and Allan, G.L. (1994): Chlorine-36 in groundwater as a palaeoclimatic indicator: The East Midlands Triassic sandstone aquifer (UK). *Earth and Planetary Science Letters*, **122**, 159–171.

Andrews, J.N., Florkowski, T., Lehmann, B.E. and Loosli, H.H. (1991): Underground production of radionuclides in the Milk River aquifer, Alberta, Canada. *Applied Geochemistry*, **6**, 425–434.

Andrews, J.N. and Fontes, J.-Ch. (1992): Importance of the in situ production of ^{36}Cl, ^{36}Ar and ^{14}C in hydrology and hydrogeochemistry. In *Isotope Techniques in Water Resources Development 1991*, IAEA, Vienna, pp. 245–269.

Andrews, J.N., Fontes, J.-Ch., Michelot, J.-L. and Elmore, D. (1986): In-situ neutron flux, ^{36}Cl production and groundwater evolution in crystalline rocks at Stripa, Sweden. *Earth and Planetary Science Letters*, **77**, 49–58.

Bagge, E. and Willkomm, H. (1966): Geologische Altersbestimmung mit ^{36}Cl (Geologic age determination with ^{36}Cl). *Atomkernenergie*, **11**, 176–184 (in German with English abstract).

Balderer, W., Synal, H.-A. and Deak, J. (2004): Application of the chlorine-36 method for the delineation of groundwater infiltration of large river systems: Example of the Danube River in western Hungary (Szigetköz area). *Environmental Geology*, **46**, 755–762.

Baumgartner, A. and Reichel, E. (1975): *The World Water Balance: Mean Annual Global, Continental and Maritime Precipitation, Evaporation, and Runoff*. Elsevier, Amsterdam, 179 pp.

Baumgartner, S., Beer, J., Masarik, J., Wagner, G., Meynadier, L. and Synal, H.-A. (1998): Geomagnetic modulation of the ^{36}Cl flux in the GRIP ice core. *Science*, **279**, 1330–1332.

Bear, J. (1979): *Hydraulics of Groundwater*. McGraw-Hill, New York, 567 pp.

Beasley, T.M., Cecil, L.D., Sharma, P., Kubik, P.W., Fehn, U., Mann, L.J. and Gove, H.E. (1993): Chlorine-36 in the Snake River Plain aquifer at the Idaho National Engineering Laboratory: Origin and implications. *Ground Water*, **31**, 302–310.

Beasley, T.M., Elmore, D., Kubik, P.W. and Sharma, P. (1992): Chlorine-36 release from the Savannah River Site nuclear fuel reprocessing facilities. *Ground Water*, **30**, 539–548.

Bennett, C.L., Beukens, R.P., Clover, M.R., Gove, H.E., Liebert, R.B., Litherland, A.E., Purser, K.H. and Sondheim, W.E. (1977): Radiocarbon dating using electrostatic accelerators: Negative ions provide the key. *Science*, **198**, 508–510.

Bentley, H.W., Phillips, F.M. and Davis, S.N. (1986a): Chlorine-36 in the terrestrial environment. In *Handbook of Environmental Isotope Geochemistry*, Vol. 2, Fritz, P. and Fontes, J.-Ch. (eds.), Elsevier, Amsterdam, pp. 427–480.

Bentley, H.W., Phillips, F.M., Davis, S.N., Gifford, S., Elmore, D., Tubbs, L.E. and Gove, H.E. (1982): Thermonuclear ^{36}Cl pulse in natural water. *Nature*, **300**, 737–740.

Bentley, H.W., Phillips, F.M., Davis, S.N., Habermehl, M.A., Airey, P.L., Calf, G.E., Elmore, D., Gove, H.E. and Torgersen, T. (1986b): Chlorine 36 dating of very old groundwater 1. The Great Artesian Basin, Australia. *Water Resources Research*, **22**, 1991–2001.

Bird, J.R., Davie, R.F., Chivas, A.R., Fifield, L.K., Ophel, T.R. (1991): Chlorine-36 production and distribution in Australia. *Palaeogeography, Palaeoclimatology,*

Palaeoecology, **84**, 299–307.

Bleichrodt, J.F. (1978): Mean tropospheric residence time of cosmic-ray-produced beryllium 7 at north temperate latitudes. *Journal of Geophysical Research*, **83**(C6), 3058–3062.

Blinov, A. (1988): The dependence of cosmogenic isotope production rate on solar activity and geomagnetic field variations. In *Secular Solar and Geomagnetic Variations in the Last 10,000 Years*. Stephenson, F.R. and Wolfendale, A.W. (eds.), Kluwer, Dordrecht, pp. 329–340.

Blinov, A., Massonet, S., Sachsenhauser, H., Stan-Sion, C., Lazarev, V., Beer, J., Synal, H.-A., Kaba, M., Masarik, J. and Nolte, E. (2000): An excess of ^{36}Cl in modern atmospheric precipitation. *Nuclear Instruments and Methods in Physics Research B*, **172**, 537–544.

Bonner, F.T., Roth, E., Schaeffer, O.A. and Thompson, S.O. (1961): Chlorine-36 and deuterium study of Great Basin lake waters. *Geochimica et Cosmochimica Acta*, **25**, 261–266.

Busenberg, E. and Plummer, L.N. (1992): Use of chlorofluorocarbons (CCl_3F and CCl_2F_2) as hydrologic tracers and age-dating tools: The alluvium and terrace system of Central Oklahoma. *Water Resources Research*, **28**, 2257–2283.

Busenberg, E. and Plummer, L.N. (2000): Dating young groundwater with sulfur hexafluoride: Natural and anthropogenic sources of sulfur hexafluoride. *Water Resources Research*, **36**, 3011–3030.

Cecil, L.D., Green, J.R., Vogt, S., Frape, S.K., Davis, S.N., Cottrell, G.L. and Sharma, P. (1999): Chlorine-36 in water, snow, and mid-latitude glacial ice of North America: Meteoric and weapons-tests production in the vicinity of the Idaho National Engineering and Environmental Laboratory, Idaho. *U.S. Geological Survey Water Resources Investigations Report*, **99-4037**, 27 pp.

Cecil, L.D., Green, J.R., Vogt, S., Michel, R. and Cottrell, G. (1998): Isotopic composition of ice cores and meltwater from Upper Fremont Glacier and Galena Creek rock glacier, Wyoming. *Geografiska Annaler*, **80A**, 287–292.

Cecil, L.D., Pittman, J.R., Beasley, T.M., Michel, R.L., Kubik, P.W., Sharma, P., Fehn, U. and Gove, H.E. (1992): Water infiltration rates in the unsaturated zone at the Idaho National Engineering Laboratory estimated from chlorine-36 and tritium profiles, and neutron logging. In *Proceedings of the 7th International Symposium on Water–Rock Interaction*, Kharaka, Y.K. and Maest, A.S. (eds.), Balkema, Rotterdam, pp. 709–714.

Cecil, L.D. and Vogt, S. (1997): Identification of bomb-produced chlorine-36 in mid-latitude glacial ice of North America. *Nuclear Instruments and Methods in Physics Research B*, **123**, 287–289.

Chapelle, F.H. and Knobel, L.L. (1983): Aqueous geochemistry and the exchangeable cation composition of glauconite in the Aquia aquifer, Maryland. *Ground Water*, **21**, 343–352.

Clark, I. and Fritz, P. (1997): *Environmental Isotopes in Hydrogeology.* Lewis, Boca Raton, 328 pp.

Conard, N.J., Elmore, D., Kubik, P.W., Gove, H.E., Tubbs, L.E., Chrunyk, B.A. and Wahlen, M. (1986): The chemical preparation of AgCl for measuring ^{36}Cl in polar ice with accelerator mass spectrometry. *Radiocarbon*, **28**, 556–560.

Cook, P.G., Jolly, I.D., Leaney, F.W. and Walker, G.R. (1994): Unsaturated zone tritium and chlorine 36 profiles from southern Australia: Their use as tracers of soil water movement. *Water Resources Research*, **30**, 1709–1719.

Cook, P.G. and Robinson, N.I. (2002): Estimating groundwater recharge in fractured rock from environmental ^{3}H and ^{36}Cl, Clare Valley, South Australia. *Water Resources Research*, **38**(8), 1136, doi:10.1029/2001WR000772.

Corcho Alvarado, J.A., Purtschert, R., Hinsby, K., Troldborg, L., Hofer, M., Kipfer, R., Aeschbach-Hertig, W. and Synal, H.-A. (2005): ^{36}Cl in modern groundwater dated by a multi-tracer approach (^{3}H/^{3}He, SF_6, CFC-12 and ^{85}Kr): A case study in quaternary sand aquifers in the Odense Pilot River Basin, Denmark. *Applied Geochemistry*, **20**, 599–609.

Cornett, R.J.J., Andrews, H.R., Chant, L.A., Davies, W.G., Greiner, B.F., Imahori, Y., Koslowsky, V.T., Kotzer, T., Milton, J.C.D. and Milton, G.M. (1997): Is ^{36}Cl from weapons' test fallout still cycling in the atmosphere? *Nuclear Instruments and Methods in Physics Research B*, **123**, 378–381.

Davie, R.F., Kellett, J.R., Fifield, L.K., Evans, W.R., Calf, G.E., Bird, J.R., Topham, S. and Ophel, T.R. (1989): Chlorine-36 measurements in the Murray Basin: Preliminary results from the Victorian and South Australian Mallee region. *BMR Journal of Australian Geology and Geophysics*, **11**, 261–272.

Davis, R., Jr. and Schaeffer, O.A. (1955): Chlorine-36 in nature. *Annals of the New York Academy of Sciences*, **62**, 105–122.

Davis, S.N. and Bentley, H.W. (1982): Dating groundwater, a short review. In *Nuclear and Chemical Dating Technique—Interpreting the Environmental Records*, Currie, L.A. (ed.), American Chemical Society Symposium Series, Vol. 176, pp. 187–222.

Davis, S.N., Cecil, L.D., Zreda, M. and Sharma, P. (1998): Chlorine-36 and the initial value problem. *Hydrogeology Journal*, **6**, 104–114.

Davis, S.N. and DeWiest, R.J.M. (1966): *Hydrogeology*. John Wiley & Sons, New York, 463 pp.

Davis, S.N., Moysey, S., Cecil, L.D. and Zreda, M. (2003): Chlorine-36 in groundwater of the United States: Empirical data. *Hydrogeology Journal*, **11**, 217–227.

Delmas, R.J., Beer, J., Synal, H.-A., Muscheler, R., Petit, J.-R. and Pourchet, M. (2004):

Bomb-test ^{36}Cl measurements in Vostok snow (Antarctica) and the use of ^{36}Cl as a dating tool for deep ice cores. *Tellus*, **56B**, 492–498.

Dyrssen, D. and Nyman, P.O. (1955): Slow-neutron-induced radioactivity of sea-water. *Acta Radiologica*, **43**, 421–427.

Edmunds, W.M. (2005): Groundwater as an archive of climatic and environmental change. In *Isotopes in the Water Cycle: Past, Present and Future of a Developing Science*, Aggarwal, P.K., Gat, J.R. and Froehlich, K.F.O. (eds.), Springer, Dordrecht, p. 341–352.

Edmunds, W.M. and Walton, N.R.G. (1983): The Lincolnshire Limestone—Hydrogeochemical evolution over a ten-year period. *Journal of Hydrology*, **61**, 201–211.

Egboka, B.C.E., Cherry, J.A., Farvolden, R.N. and Frind, E.O. (1983): Migration of contaminants in groundwater at a landfill: A case study. 3. Tritium as an indicator of dispersion and recharge. *Journal of Hydrology*, **63**, 51–80.

Elmore, D., Fulton, B.R., Clover, M.R., Marsden, J.R., Gove, H.E., Naylor, H., Purser, K.H., Kilius, L.R., Beukens, R.P. and Litherland, A.E. (1979): Analysis of ^{36}Cl in environmental water samples using an electrostatic accelerator. *Nature*, **277**, 22–25.

Elmore, D. and Phillips, F.M. (1987): Accelerator mass spectrometry for measurement of long-lived radioisotopes. *Science*, **236**, 543–550.

Elmore, D., Tubbs, L.E., Newman, D., Ma, X.Z., Finkel, R., Nishiizumi, K., Beer, J., Oeschger, H. and Andree, M. (1982): ^{36}Cl bomb pulse measured in a shallow ice core from Dye 3, Greenland. *Nature*, **300**, 735–737.

Eriksson, E. (1960): The yearly circulation of chloride and sulfur in nature; meteorological, geochemical and pedological implications. Part II. *Tellus*, **12**, 63–109.

Fabryka-Martin, J., Davis, S.N. and Elmore, D. (1987): Applications of ^{129}I and ^{36}Cl in hydrology. *Nuclear Instruments and Methods in Physics Research B*, **29**, 361–371.

Fabryka-Martin, J., Whittemore, D.O., Davis, S.N., Kubik, P.W. and Sharma, P. (1991): Geochemistry of halogens in the Milk River aquifer, Alberta, Canada. *Applied Geochemistry*, **6**, 447–464.

Feige, Y., Oltman, B.G. and Kastner, J. (1968): Production rates of neutrons in soils due to natural radioactivity. *Journal of Geophysical Research*, **73**, 3135–3142.

Feth, J.H. (1981): Chloride in natural continental water—a review. *U.S. Geological Survey Water-Supply Paper*, **2176**, 30 pp.

Fifield, L.K. (1999): Accelerator mass spectrometry and its applications. *Reports on Progress in Physics*, **62**, 1223–1274.

Finkel, R.C., Nishiizumi, K., Elmore, D., Ferraro, R.D. and Gove, H.E. (1980): ^{36}Cl in polar ice, rainwater and seawater. *Geophysical Research Letters*, **7**, 983–986.

Finkel, R.C. and Suter, M. (1993): AMS in the earth sciences: Technique and applications. *Advances in Analytical Geochemistry*, **1**, 1–114.

Firestone, R.B. and Shirley, V.S. (eds.) (1996): *Table of Isotopes*. 8th Edition, Vol. 1, John Wiley & Sons, New York, 1531 pp.

Florkowski, T. and Schuszler, Ch. (1986): Attempt to determine the environmental ^{36}Cl concentration in water by liquid scintillation counting. *Nuclear Instruments and Methods in Physics Research B*, **17**, 515–518.

Fontes, J.-Ch. (1989): The chlorine-36 method: Dating of natural waters. In *Nuclear Methods of Dating*, Roth, E. and Poty, B. (eds.), CEA, Paris, pp. 379–398.

Fontes, J.-Ch. and Andrews, J.N. (1994): Accelerator mass spectrometry in hydrology. *Nuclear Instruments and Methods in Physics Research B*, **92**, 367–375.

Funakura, T., Okochi, H., Nagoya, T., Inazu, K., Minami, Y. and Igarashi, Y. (2007): Development of solar-powered rainwater collector and observation of wet deposition

fluxes on the mountainside of Mt. Fuji. *Bunseki Kagaku*, **56**, 805–811 (in Japanese with English abstract).

Green, J.R., Cecil, L.D., Synal, H.-A., Kreutz, K.J., Wake, C.P., Naftz, D.L. and Frape, S.K. (2000): Chlorine-36 and cesium-137 in ice-core samples from mid-latitude glacial sites in the Northern Hemisphere. *Nuclear Instruments and Methods in Physics Research B*, **172**, 812–816.

Green, J.R., Cecil, L.D., Synal, H.-A., Santos, J., Kreutz, K.J. and Wake, C.P. (2004): A high resolution record of chlorine-36 nuclear-weapons-tests fallout from Central Asia. *Nuclear Instruments and Methods in Physics Research B*, **223–224**, 854–857.

Hainsworth, L.J., Mignerey, A.C., Helz, G.R., Sharma, P. and Kubik, P.W. (1994): Modern chlorine-36 deposition in southern Maryland, USA. *Nuclear Instruments and Methods in Physics Research B*, **92**, 345–349.

Helios Rybicka, E. (1996): Impact of mining and metallurgical industries on the environment in Poland. *Applied Geochemistry*, **11**, 3–9.

Hem, J.D. (1985): Study and interpretation of the chemical characteristics of natural water. 3rd edition, *U.S. Geological Survey Water-Supply Paper*, **2254**, 263 pp.

Hendry, M.J. and Schwartz, F.W. (1988): An alternative view on the origin of chemical and isotopic patterns in groundwater from the Milk River aquifer, Canada. *Water Resources Research*, **24**, 1747–1763.

Herczeg, A.L. and Edmunds, W.M. (2000): Inorganic ions as tracers. In *Environmental Tracers in Subsurface Hydrology*, Cook, P.G. and Herczeg, A.L. (eds.), Kluwer, Boston, pp. 31–77.

Hiyama, T., Sato, A., Yasuhara, M., Marui, A., Suzuki, Y. and Takayama, S. (1995): Water quality of the precipitation around the Mt. Fuji. *Bulletin of the Environmental Research*

Center, the University of Tsukuba, **20**, 45–54 (in Japanese with English title).

Holton, J.R., Haynes, P.H., McIntyre, M.E., Douglass, A.R., Rood, R.B. and Pfister, L. (1995): Stratosphere–troposphere exchange, *Reviews of Geophysics*, **33**, 403–439.

Huggle, D., Blinov, A., Stan-Sion, C., Korschinek, G., Scheffel, C., Massonet, S., Zerle, L., Beer, J., Parrat, Y., Gaeggeler, H., Hajdas, W. and Nolte, E. (1996): Production of cosmogenic ^{36}Cl on atmospheric argon. *Planetary and Space Science*, **44**, 147–151.

IAEA/WMO (2004): Global Network of Isotopes in Precipitation. The GNIP Database, Accessible at: http://isohis.iaea.org.

Ikeda, K. (1982): A study on chemical characteristics of ground water in Fuji area. *Journal of the Japanese Association of Groundwater Hydrology*, **24**, 77–93 (in Japanese with English abstract).

Ikeda, K. (1989): Chemical evolution of groundwater quality in the southern foot of Mount Fuji. *Bulletin of the Geological Survey of Japan*, **40**, 331–404.

Ikeda, K. (1995): A hydrogeochemical study on the groundwater in the southern foot of Mount Fuji —Changes in the groundwater quality, related to hydrological changes before and after salinization of groundwater—. *Hydrology (Journal of Japanese Association of Hydrological Sciences)*, **25**, 57–70 (in Japanese with English abstract).

Ino, M. (1976): The quantity of water in each spring on the west and south slope of Mt. Fuji. *Journal of the Japanese Association of Groundwater Hydrology*, **18**, 1–8 (in Japanese with English abstract).

Ino, M. (1987): Springs at the eastern, southern and western foots of Mt. Fuji. *Hydrology (Journal of Japanese Association of Hydrological Sciences)*, **17**, 63–74 (in Japanese with English abstract).

Inoue, K., Yokota, N., Murai, H., Kumagai, N. and Mochizuki, J. (1993): Rain and

percolation waters of beech and Japanese cypress forests in the foot of Mt. Fuji and neutralization of acid rain by a beech tree. *Japanese Journal of Soil Science and Plant Nutrition*, **64**, 265–274 (in Japanese with English abstract).

Itadera, K. and Shimada, J. (1992): Evaluation of the surface runoff at the ERC experimental field. *Bulletin of the Environmental Research Center, the University of Tsukuba*, **16**, 55–61 (in Japanese with English title).

Jiang, S., Lin, Y. and Zhang, H. (2004): Improvement of the sample preparation method for AMS measurement of ^{36}Cl in natural environment. *Nuclear Instruments and Methods in Physics Research B*, **223–224**, 318–322.

Jiang, S.S., Hemmick, T.K., Kubik, P.W., Elmore, D., Gove, H.E., Tullai-Fitzpatrick, S. and Hossain, T.Z. (1990): Measurement of the ^{36}Ar(n, p)^{36}Cl cross section at thermal energies using the AMS technique. *Nuclear Instruments and Methods in Physics Research B*, **52**, 608–611.

Kakiuchi, M. (1995): Tritium concentration of surface waters in the Mt. Fuji area. In *Study on Groundwater Flow System in Mt. Fuji*, Takayama, S. (ed.), Research Report to the Ministry of Education, Science, Sports and Culture for 1992–1994 Grant-in-Aid for Scientific Research, No. 04302064, pp. 56–64 (in Japanese).

Kayane, I. (1980): *Hydrology*. Taimei-Do, Tokyo, 272 pp. (in Japanese).

Kayane, I. and Li, B.-C. (1983): Groundwater ages in the Tsukuba Science City estimated from tritium concentrations. *Tsukuba Environmental Studies*, **7**, 124–127 (in Japanese).

Kazahaya, K. and Yasuhara, M. (1994): A hydrogen isotopic study of spring waters in Mt. Yatsugatake, Japan: Application to groundwater recharge and flow processes. *Hydrology (Journal of Japanese Association of Hydrological Sciences)*, **24**, 107–119 (in Japanese with English abstract).

Kazemi, G.A., Lehr, J.H. and Perrochet, P. (2006): *Groundwater Age*. John Wiley & Sons, Hoboken, 325 pp.

Keywood, M.D., Chivas, A.R., Fifield, L.K., Cresswell, R.G. and Ayers, G.P. (1997): The accession of chloride to the western half of the Australian continent. *Australian Journal of Soil Research*, **35**, 1177–1190.

Kizawa, T., Iida, M., Matsuyama, S. and Miyawaki, A. (1969): *Mt. Fuji—Solving the Mystery of its Nature*. NHK Books 91, NHK, Tokyo, 253 pp. (in Japanese).

Knies, D.L., Elmore, D., Sharma, P., Vogt, S., Li, R., Lipschutz, M.E., Petty, G., Farrell, J., Monaghan, M.C., Fritz, S. and Agee, E. (1994): ^{7}Be, ^{10}Be and ^{36}Cl in precipitation. *Nuclear Instruments and Methods in Physics Research B*, **92**, 340–344.

Kodama, M. (1968): Geomagnetic and solar modulation effects of sea-level cosmic ray intensity —Summary of cosmic ray latitude surveys aboard the expedition ship SOYA during 1956–1962—. *JARE Scientific Reports, Series A*, No. 5, Department of Polar Research, National Science Museum, Tokyo, 61 pp.

Kondoh, A., Tanaka, T., Tang, C., Sakura, Y., Shimada, J., Shibano, H., Liu, C., Zhang, W., Hu, C., Liu, X., Li, J., Chen, J. and Shen, Y. (2001): Water problems in the North China Plain. *Journal of Japan Society of Hydrology and Water Resources*, **14**, 376–387 (in Japanese).

Kotoda, K. (1968): Field study on rainfall–runoff relations in a small basin —Initial loss and runoff coefficient—. *Tokyo Geography Papers*, **12**, 121–142 (in Japanese with English abstract).

Krupp, H.K., Biggar, J.W. and Nielsen, D.R. (1972): Relative flow rates of salt and water in soil. *Soil Science Society of America Proceedings*, **36**, 412–417.

Kulongoski, J.T., Hilton, D.R., Cresswell, R.G., Hostetler, S. and Jacobson, G. (2008):

Helium-4 characteristics of groundwaters from Central Australia: Comparative chronology with chlorine-36 and carbon-14 dating techniques. *Journal of Hydrology*, **348**, 176–194.

Kurata, N. (1966): *Explanatory Text of the Hydrogeology of Mt. Fuji*. Hydrogeological Maps of Japan No. 14 (Scale 1:50,000), Geological Survey of Japan, Tsukuba, 31 pp. (in Japanese with English abstract).

Lal, D. and Peters, B. (1967): Cosmic ray produced radioactivity on the earth. In *Handbuch der Physik*, Vol. 46/2, Sitte, K. (ed.), Springer, Berlin, pp. 551–612.

Lazarev, V. (2003): The cosmogenic and anthropogenic ^{36}Cl in the environment. Ph.D. Thesis, Technical University of Munich, Munich, 109 pp.

Lehmann, B.E. and Loosli, H.H. (1991): Isotopes formed by underground production. 6.1. Introduction. In *Applied Isotope Hydrogeology: A Case Study in Northern Switzerland*, Studies in Environmental Science 43, Pearson, F.J., Jr., Balderer, W., Loosli, H.H., Lehmann, B.E., Matter, A., Peters, Tj., Schmassmann, H. and Gautschi, A. (eds.), Elsevier, Amsterdam, pp. 239–249.

Lehmann, B.E., Love, A., Purtschert, R., Collon, P., Loosli, H.H., Kutschera, W., Beyerle, U., Aeschbach-Hertig, W., Kipfer, R., Frape, S.K., Herczeg, A., Moran, J., Tolstikhin, I.N. and Gröning, M. (2003): A comparison of groundwater dating with ^{81}Kr, ^{36}Cl and ^{4}He in four wells of the Great Artesian Basin, Australia. *Earth and Planetary Science Letters*, **211**, 237–250.

Lehmann, B.E. and Purtschert, R. (1997): Radioisotope dynamics—The origin and fate of nuclides in groundwater. *Applied Geochemistry*, **12**, 727–738.

Levin, I. and Kromer, B. (1997): $\Delta^{14}CO_2$ record from Schauinsland. In *Trends: A Compendium of Data on Global Change*, Carbon Dioxide Information Analysis Center,

Oak Ridge National Laboratory, U.S. Department of Energy, Oak Ridge.

Levin, I., Kromer, B., Schoch-Fischer, H., Bruns, M., Münnich, M., Berdau, D., Vogel, J.C. and Münnich, K.O. (1994): $\Delta^{14}CO_2$ record from Vermunt. In *Trends: A Compendium of Data on Global Change*, Carbon Dioxide Information Analysis Center, Oak Ridge National Laboratory, U.S. Department of Energy, Oak Ridge.

Liu, B., Phillips, F., Hoines, S., Campbell, A.R. and Sharma, P. (1995): Water movement in desert soil traced by hydrogen and oxygen isotopes, chloride, and chlorine-36, southern Arizona. *Journal of Hydrology*, **168**, 91–110.

Lockhart, L.B., Jr., Baus, R.A., Patterson, R.L., Jr. and Saunders, A.W., Jr. (1959): Contamination of the air by radioactivity from the 1958 nuclear tests in the Pacific. *Science*, **130**, 161–162.

Lucas, L.L. and Unterweger, M.P. (2000): Comprehensive review and critical evaluation of the half-life of tritium. *Journal of Research of the National Institute of Standards and Technology*, **105**, 541–549.

Machida, H. (1964): Tephrochronological study of volcano Fuji and adjacent areas. *Journal of Geography*, **73**, 293–308, 337–350 (in Japanese with English abstract).

Machida, H. (1977): *Tephra: Its Characteristics and Relationship to the Japanese Quaternary Era*. Soju-Shobo, Tokyo, 324 pp. (in Japanese).

Machida, H. (2007): Development of Fuji volcano: A review from Quaternary tephrochronology. In *Fuji Volcano*, Aramaki, S., Fujii, T., Nakada, S. and Miyaji, N. (eds.), Yamanashi Institute of Environmental Sciences, Fujiyoshida, pp. 29–44 (in Japanese with English abstract).

Machta, L. (1959). Transport in the stratosphere and through the troposphere. In *Atmospheric Diffusion and Air Pollution*, Frenkiel, F.N. and Sheppard, P.A. (eds.), Advances in

Geophysics, Vol. 6, Academic Press, New York, pp. 273–288.

Machta, L. (1965): Status of global radioactive-fallout predictions. In *Radioactive Fallout from Nuclear Weapons Tests*, Klement, A.W., Jr. (ed.), CONF-765, U. S. Atomic Energy Commission, Oak Ridge, pp. 369–391.

Mahara, Y., Habermehl, M.A., Miyakawa, K., Shimada, J., Mizuochi, Y. (2007): Can the ^{4}He clock be calibrated by ^{36}Cl for groundwater dating? *Nuclear Instruments and Methods in Physics Research B*, **259**, 536–546.

Mahara, Y., Igarashi, T. and Tanaka, Y. (1993): Groundwater ages of confined aquifer in Mishima lava flow, Shizuoka. *Journal of Groundwater Hydrology*, **35**, 201–215 (in Japanese with English abstract).

Mahara, Y., Nakata, E., Ooyama, T., Miyakawa, K., Igarashi, T., Ichihara, Y. and Matsumoto, H. (2006): Proposal for the methods to characterize fossil seawater —Distribution of anions, cations and stable isotopes, and estimation on the groundwater residence time by measuring ^{36}Cl at the Taiheiyou Coal Mine—. *Journal of Groundwater Hydrology*, **48**, 17–33 (in Japanese with English abstract).

Maloszewski, P. and Zuber, A. (1982): Determining the turnover time of groundwater systems with the aid of environmental tracers. 1. Models and their applicability. *Journal of Hydrology*, **57**, 207–231.

Maruta, E., Dokiya, Y. and Tsuboi, K. (1993): Chemical composition of the precipitation at Mt. Fuji in relation to pressure patterns. *Environmental Science*, **6**, 311–320 (in Japanese with English abstract).

Masarik, J. and Beer, J. (1999): Simulation of particle fluxes and cosmogenic nuclide production in the Earth's atmosphere. *Journal of Geophysical Research*, **104**(D10), 12099–12111.

Masarik, J. and Reedy, R.C. (1995): Terrestrial cosmogenic-nuclide production systematics calculated from numerical simulations. *Earth and Planetary Science Letters*, **136**, 381–395.

Massmann, G. (2002): Infiltration of river water into the groundwater—Investigation and modelling of hydraulic and geochemical processes during bank filtration in the Oderbruch, Germany. Ph.D. Thesis, Free University Berlin, Berlin, 218 pp.

Massmann, G., Pekdeger, A. and Merz, C. (2004): Redox processes in the Oderbruch polder groundwater flow system in Germany. *Applied Geochemistry*, **19**, 863–886.

Massmann, G., Tichomirowa, M., Merz, C. and Pekdeger, A. (2003): Sulfide oxidation and reduction in shallow groundwater system (Oderbruch Aquifer, Germany). *Journal of Hydrology*, **278**, 231–243.

Masuda, T., Murakoshi, K., Saito, M. (1994): Hydrogeological study on springs on the southeastern slope of Mt. Fuji —Study on reduction of spring quantity in Kakita-Gawa river and others—, *Nippon Koei Technical Forum*, **3**, 25–33 (in Japanese with English abstract).

Milton, G.M., Kramer, S.J., Kotzer, T.G., Milton, J.C.D., Andrews, H.R., Chant, L.A., Cornett, R.J., Davies, W.G., Greiner, B.F., Imahori, Y., Koslowsky, V.T. and McKay, J.W. (1997): Cl 36—A potential paleodating tool. *Nuclear Instruments and Methods in Physics Research B*, **123**, 371–377.

Milton, G.M., Milton, J.C.D., Schiff, S., Cook, P., Kotzer, T.G. and Cecil, L.D. (2003): Evidence for chlorine recycling—hydrosphere, biosphere, atmosphere—in a forested wet zone on the Canadian Shield. *Applied Geochemistry*, **18**, 1027–1042.

Milton, J.C.D., Milton, G.M., Andrews, H.R., Chant, L.A., Cornett, R.J.J., Davies, W.G., Greiner, B.F., Imahori, Y., Koslowsky, V.T., Kotzer, T., Kramer, S.J. and McKay, J.W.

(1997): A new interpretation of the distribution of bomb-produced chlorine-36 in the environment, with special reference to the Laurentian Great Lakes. *Nuclear Instruments and Methods in Physics Research B*, **123**, 382–386.

Mitsui, K. (1982): Changes in salt intrusion into ground water and process of river water pollution and its recovery in southern foot of Mount Fuji. *Journal of Geography*, **91**, 378–396 (in Japanese with English abstract).

Miyaji, N., Endo, K., Togashi, S. and Uesugi, Y. (1992): Tephrochronological history of Mt. Fuji. In *Volcanoes and Geothermal Fields of Japan*, 29th IGC Field Trip Guide Book, Vol. 4, Geological Survey of Japan, Tsukuba, pp. 75–109.

Miyake, N. (1978): Runoff characteristics of small watersheds in hilly areas. In *Water Balance in Japan*, Ichikawa, M. and Kayane, I. (eds.), Kokon-Shoin, Tokyo, pp. 77–88 (in Japanese).

Mori, K. (1985): Qualitative changes of groundwater with the movement —A case study in the Nobi and Ise Plains—. *Hydrology*, **15**, 55–59 (in Japanese with English abstract).

Morris, D.A. and Johnson, A.I. (1967): Summary of hydrologic and physical properties or rock and soil materials as analyzed by the Hydrologic Laboratory of the U.S. Geological Survey 1948–1960. *U.S. Geological Survey Water-Supply Paper*, **1839-D**, 42 pp.

Moysey, S., Davis, S.N., Zreda, M. and Cecil, L.D. (2003): The distribution of meteoric $^{36}Cl/Cl$ in the United States: A comparison of models. *Hydrogeology Journal*, **11**, 615–627.

Muller, R.A. (1977): Radioisotope dating with a cyclotron. *Science*, **196**, 489–494.

Nagae, R. (1984): Study on hydrological geology of southern part of Mt. Fuji. *Technical Report of the National Research Institute of Agricultural Engineering WM*, **4**, 23–41 (in Japanese with English title).

Nagashima, Y., Seki, R., Matsuhiro, T., Takahashi, T., Sasa, K., Sueki, K., Hoshi, M., Fujita, S., Shizuma, K. and Hasai, H. (2004): Chlorine-36 in granite samples from the Hiroshima A-bomb site. *Nuclear Instruments and Methods in Physics Research B*, **223–224**, 782–787.

Nagashima, Y., Seki, R., Takahashi, T. and Arai, D. (2000): Status of the ^{36}Cl AMS system at the University of Tsukuba. *Nuclear Instruments and Methods in Physics Research B*, **172**, 129–133.

Nakai, N. (1996): Chemical and isotopic characteristics of groundwater in Fujinomiya city. In *Report on Groundwater in Fujinomiya City*, Tsuchi, R. (ed.), Fujinomiya City Office, Fujinomiya, pp. 21–36 (in Japanese).

Nelson, D.E., Korteling, R.G. and Stott, W.R. (1977): Carbon-14: Direct detection at natural concentrations. *Science*, **198**, 507–508.

Nishiizumi, K., Arnold, J.R., Elmore, D., Ferraro, R.D., Gove, H.E., Finkel, R.C., Beukens, R.P., Chang, K.H. and Kilius, L.R. (1979): Measurements of ^{36}Cl in Antarctic meteorites and Antarctic ice using a Van de Graaff accelerator. *Earth and Planetary Science Letters*, **45**, 285–292.

Nolte, E., Krauthan, P., Heim, U. and Korschinek, G. (1990): ^{36}Cl measurements and dating of groundwater samples from the Milk River aquifer. *Nuclear Instruments and Methods in Physics Research B*, **52**, 477–482.

Nolte, E., Krauthan, P., Korschinek, G., Maloszewski, P., Fritz, P. and Wolf, M. (1991): Measurements and interpretations of ^{36}Cl in groundwater, Milk River aquifer, Alberta, Canada. *Applied Geochemistry*, **6**, 435–445.

Norris, A.E., Wolfsberg, K., Gifford, S.K., Bentley, H.W. and Elmore, D. (1987): Infiltration at Yucca Mountain, Nevada, traced by ^{36}Cl. *Nuclear Instruments and Methods in Physics*

Research B, **29**, 376–379.

Nyberg, L., Rodhe, A. and Bishop, K. (1999): Water transit times and flow paths from two line injections of ^{3}H and ^{36}Cl in a microcatchment at Gårdsjön, Sweden. *Hydrological Processes*, **13**, 1557–1575.

O'Brien, K. (1979): Secular variations in the production of cosmogenic isotopes in the earth's atmosphere. *Journal of Geophysical Research*, **84**(A2), 423–431.

Ochiai, T. (1995): *Analysis of the Groundwater in the Eastern Part of Mt. Fuji*. Liber Press, Tokyo, 206 pp. (in Japanese).

Ochiai, T. and Kawasaki, H. (1970): Behavior of groundwater flowing in lava beds. *Bulletin of the Agricultural Engineering Research Station*, **8**, 67–83 (in Japanese with English summary).

Ochiai, T. and Kawasaki, H. (1972a): Tritium measurements of ground water in Japan (I). *Journal of Water and Waste*, **14**, 255–261 (in Japanese with English title).

Ochiai, T. and Kawasaki, H. (1972b): Tritium measurements of ground water in Japan (II). *Journal of Water and Waste*, **14**, 1383–1388 (in Japanese with English title).

Oeschger, H., Houtermans, J., Loosli, H. and Wahlen, M. (1970): The constancy of cosmic radiation from isotope studies in meteorites and on the Earth. In *Radiocarbon Variations and Absolute Chronology*, Proceedings of the 12th Nobel Symposium, Olsson, I.U. (ed.), John Wiley & Sons, New York, pp. 471–498.

Ogard, A.E., Thompson, J.L., Rundberg, R.S., Wolfsberg, K., Kubik, P.W., Elmore, D. and Bentley, H.W. (1988): Migration of chlorine-36 and tritium from an underground nuclear test. *Radiochimica Acta*, **44/45**, 213–217.

Ozaki, T. (1978): Sea water intrusion into confined water estimated from long-term observations of chloride ion contents, Fuji City, Shizuoka Prefecture. *Bulletin of the*

Geological Survey of Japan, **29**, 645–666 (in Japanese with English abstract).

Parrat, Y. (1997): Cosmogenic radionuclides in the environment: ^{32}Si in precipitation samples from the Jungfraujoch, production cross sections of ^{36}Cl in argon and modeling of the atmospheric ^{36}Cl production. Ph.D. Thesis, University of Berne, Berne, 66 pp.

Patterson, L.J., Sturchio, N.C., Kennedy, B.M., van Soest, M.C., Sultan, M., Lu, Z.-T., Lehmann, B., Purtschert, R., El Alfy, Z., El Kaliouby, B., Dawood, Y. and Abdallah, A. (2005): Cosmogenic, radiogenic, and stable isotopic constraints on groundwater residence time in the Nubian Aquifer, Western Desert of Egypt. *Geochemistry, Geophysics, Geosystems*, **6**(1), Q01005, doi:10.1029/2004GC000779.

Peterson, K.P. (1970): An empirical model for estimating world-wide deposition from atmospheric nuclear detonations. *Health Physics*, **18**, 357–378.

Phillips, F.M. (2000): Chlorine-36. In *Environmental Tracers in Subsurface Hydrology*, Cook, P.G. and Herczeg, A.L. (eds.), Kluwer, Boston, pp. 299–348.

Phillips, F.M., Bentley, H.W., Davis, S.N., Elmore, D. and Swanick, G.B. (1986): Chlorine 36 dating of very old groundwater 2. Milk River aquifer, Alberta, Canada. *Water Resources Research*, **22**, 2003–2016.

Phillips, F.M. and Castro, M.C. (2003): Groundwater dating and residence time measurements. In *Surface and Ground Water, Weathering, and Soils*, Treatise on Geochemistry, Vol. 5, Drever, J.I. (ed.), Elsevier, Oxford, pp. 451–497.

Phillips, F.M., Davis, S.N. and Kubik, P. (1990): A proposal to use chlorine-36 for monitoring the movement of radionuclides from nuclear explosions. *Ground Water Monitoring & Remediation*, **10**(3), 106–113.

Phillips, F.M., Mattick, J.L., Duval, T.A., Elmore, D. and Kubik, P.W. (1988): Chlorine 36 and tritium from nuclear weapons fallout as tracers for long-term and vapor movement in

desert soils. *Water Resources Research*, **24**, 1877–1891.

Plummer, M.A., Phillips, F.M., Fabryka-Martin, J., Turin, H.J., Wigand, P.E. and Sharma, P. (1997): Chlorine-36 in fossil rat urine: An archive of cosmogenic nuclide deposition during the past 40,000 years. *Science*, **277**, 538–541.

Priller, A., Korschinek, G., Nolte, E. and Rühm, W. (1990): A search for correlation between fall-out of cosmogenic chlorine-36 and solar activity. *Nuclear Instruments and Methods in Physics Research B*, **52**, 618–620.

Prych, E.A. (1998): Using chloride and chlorine-36 as soil-water tracers to estimate deep percolation at selected locations on the U.S. Department of Energy Hanford Site, Washington. *U.S. Geological Survey Water-Supply Paper*, **2481**, 67 pp.

Purdy, C.B., Helz, G.R., Mignerey, A.C., Kubik, P.W., Elmore, D., Sharma, P. and Hemmick, T. (1996): Aquia aquifer dissolved Cl^- and $^{36}Cl/Cl$: Implications for flow velocities. *Water Resources Research*, **32**, 1163–1171.

Purdy, C.B., Mignerey, A.C., Helz, G.R., Drummond, D.D., Kubik, P.W., Elmore, D. and Hemmick, T. (1987): ^{36}Cl: A tracer in groundwater in the Aquia Formation of southern Maryland. *Nuclear Instruments and Methods in Physics Research B*, **29**, 372–375.

Purser, K.H., Liebert, R.B., Litherland, A.E., Beukens, R.P., Gove, H.E., Bennett, C.L., Clover, M.R. and Sondheim, W.E. (1977): An attempt to detect stable N^- ions from a sputter ion source and some implications of the results for the design of tandems for ultra-sensitive carbon analysis. *Revue de Physique Appliquée*, **12**, 1487–1492.

Raisbeck, G.M., Yiou, F., Fruneau, M., Loiseaux, J.M., Lieuvin, M. and Ravel, J.C. (1979): Deposition rate and seasonal variations in precipitation of cosmogenic ^{10}Be. *Nature*, **282**, 279–280.

Raisbeck, G.M., Yiou, F., Fruneau, M., Loiseaux, J.M., Lieuvin, M. and Ravel, J.C. (1981):

Cosmogenic $^{10}Be/^{7}Be$ as a probe of atmospheric transport processes. *Geophysical Research Letters*, **8**, 1015–1018.

Rank, D., Adler, A., Araguás Araguás, L., Froehlich, K., Rozanski, K. and Stichler, W. (1996): Hydrological parameters and climatic signals derived from long term tritium and stable isotope time series of the river Danube. In *Isotope Techniques in the Study of Environmental Change*, IAEA, Vienna, pp. 191–205.

Reiter, E.R. (1975): Stratospheric–tropospheric exchange processes. *Reviews of Geophysics and Space Physics*, **13**, 459–474.

Robertson, W.D. and Cherry, J.A. (1989): Tritium as an indicator of recharge and dispersion in a groundwater system in central Ontario. *Water Resources Research*, **25**, 1097–1109.

Roman, D. and Airey, P.L. (1981): The application of environmental chlorine-36 to hydrology—I. liquid scintillation counting. *International Journal of Applied Radiation and Isotopes*, **32**, 287–290.

Ronzani, C. and Tamers, M.A. (1966): Low level chlorine-36 detection with liquid scintillation techniques. *Radiochimica Acta*, **6**, 206–210.

Sasa, K., Nagashima, Y., Takahashi, T., Seki, R., Tosaki, Y., Sueki, K., Bessho, K., Matsumura, H., Miura, T. and He, M. (2007): ^{26}Al and ^{36}Cl AMS system at the University of Tsukuba: A progress report. *Nuclear Instruments and Methods in Physics Research B*, **259**, 41–46.

Sato, A. and Suzuki, Y. (1996): Temperature of spring waters and groundwaters of Mt. Fuji. *Hydrology (Journal of Japanese Association of Hydrological Sciences)*, **26**, 23–34 (in Japanese with English abstract).

Sato, Y., Yasuike, S., Kono, T., Kitagawa, M., Suzuki, Y. and Takayama, S. (1997): Water qualities of spring and groundwater around Mt. Fuji. *Journal of Japanese Association of*

Hydrological Sciences, **27**, 17–25 (in Japanese with English abstract).

Saxena, R.K. and Jarvis, N.J. (1995): Measurements and modeling of tracer transport in a sandy soil. *Water, Air and Soil Pollution*, **79,** 409–424.

Saxena, R.K., Jarvis, N.J. and Bergström, L. (1994): Interpreting non-steady state tracer breakthrough experiments in sand and clay soils using a dual-porosity model. *Journal of Hydrology*, **162**, 279–298.

Scanlon, B.R. (1992): Evaluation of liquid and vapor flow in desert soils based on chlorine 36 and tritium tracers and nonisothermal flow simulations. *Water Resources Research*, **28**, 285–297.

Scanlon, B.R., Kubik, P.W., Sharma, P., Richter, B.C. and Gove, H.E. (1990): Bomb chlorine-36 analysis in the characterization of unsaturated flow at a proposed radioactive waste disposal facility, Chihuahuan Desert, Texas. *Nuclear Instruments and Methods in Physics Research B*, **52**, 489–492.

Schaeffer, O.A., Thompson, S.O. and Lark, N.L. (1960): Chlorine-36 radioactivity in rain. *Journal of Geophysical Research*, **65**, 4013–4016.

Scheffel, C., Blinov, A., Massonet, S., Sachsenhauser, H., Stan-Sion, C., Beer, J., Synal, H.-A., Kubik, P.W., Kaba, M. and Nolte, E. (1999): ^{36}Cl in modern atmospheric precipitation. *Geophysical Research Letters*, **26**, 1401–1404.

Schlesinger, W.H. (1997): *Biogeochemistry: An Analysis of Global Change*, 2nd Edition, Academic Press, San Diego, 588 pp.

Schlosser, P., Stute, M., Dörr, H., Sonntag, C. and Münnich, K.O. (1988): Tritium/^{3}He dating of shallow groundwater. *Earth and Planetary Science Letters*, **89**, 353–362.

Shanley, J.B., Pendall, E., Kendall, C., Stevens, L.R., Michel, R.L., Phillips, P.J., Forester, R.M., Naftz, D.L., Liu, B., Stern, L., Wolfe, B.B., Chamberlain, C.P., Leavitt, S.W.,

Heaton, T.H.E., Mayer, B., Cecil, L.D., Lyons, W.B., Katz, B.G., Betancourt, J.L., McKnight, D.M., Blum, J.D., Edwards, T.W.D., House, H.R., Ito, E., Aravena, R.O. and Whelan, J.F. (1998): Isotopes as indicators of environmental change. In *Isotope Tracers in Catchment Hydrology*, Kendall, C. and McDonnell, J.J. (eds.), Elsevier, Amsterdam, pp. 761–816.

Sharma, P., Kubik, P.W., Fehn, U., Gove, H.E., Nishiizumi, K. and Elmore, D. (1990): Development of ^{36}Cl standards for AMS. *Nuclear Instruments and Methods in Physics Research B*, **52**, 410–415.

Shimada, J. (2000): Proposals for the groundwater preservation toward 21st century through the view point of hydrological cycle. *Journal of Japanese Association of Hydrological Sciences*, **30**, 63–72 (in Japanese with English abstract).

Shimada, J. (2005): Paleo-hydrological information in the subsurface water extracted by environmental isotopes. *Journal of Japanese Association of Hydrological Sciences*, **35**, 103–110 (in Japanese with English abstract).

Shimada, J., Habermehl, M.A., Mahara, Y. and Kayane, I. (1999): Use of ^{36}Cl age to compile recent 200 k year paleohydrological information from artesian groundwater in Great Artesian Basin, Australia. In *Proceedings of the International Symposium on Groundwater in Environmental Problems*, Chiba University, Chiba, pp. 125–131.

Shimada, J., Matsutani, J., Dapaah-Siakwan, S., Yoshihara, M., Miyaoka, K. and Higuchi, A. (1994): Recent trend of tritium concentration in precipitation at Tsukuba, Japan. *Annual Report of the Institute of Geoscience, the University of Tsukuba*, **20**, 11–14.

Shimada, J., Taniguchi, M. and Kawamura, R. (1990): Groundwater recharge mechanism of Tsukuba Upland area. *Bulletin of the Environmental Research Center, the University of Tsukuba*, **14**, 75–79 (in Japanese with English title).

Smethie, W.M., Jr., Solomon, D.K., Schiff, S.L. and Mathieu, G.G. (1992): Tracing groundwater flow in the Borden aquifer using krypton-85. *Journal of Hydrology*, **130**, 279–297.

Staley, D.O. (1962): On the mechanism of mass and radioactivity transport from stratosphere to troposphere. *Journal of the Atmospheric Sciences*, **19**, 450–467.

Sturchio, N.C., Du, X., Purtschert, R., Lehmann, B.E., Sultan, M., Patterson, L.J., Lu, Z.-T., Müller, P., Bigler, T., Bailey, K., O'Connor, T.P., Young, L., Lorenzo, R., Becker, R., El Alfy, Z., El Kaliouby, B., Dawood, Y., Abdallah, A.M.A. (2004): One million year old groundwater in the Sahara revealed by krypton-81 and chlorine-36. *Geophysical Research Letters*, **31**(5), L05503, doi:10.1029/2003GL019234.

Stute, M., Clark, J.F., Phillips, F.M. and Elmore, D. (1993): Reconstruction of late glacial climates from the groundwater archive: Cl^- and ^{36}Cl in the Carrizo aquifer, Texas. In *Isotope Techniques in Studying Past and Current Environmental Changes in the Hydrosphere and the Atmosphere*, IAEA, Vienna, pp. 259–270.

Sugisaki, R. and Shibata, K. (1961): Geochemical study on groundwater (II) —The relationship between the character of the ground water and the geological structure of the Nobi Plain—. *Journal of the Geological Society of Japan*, **67**, 427–439 (in Japanese with English abstract).

Sültenfuß, J. and Massmann, G. (2004): Datierung mit der ^{3}He-Tritium-Methode am Beispiel der Uferfiltration im Oderbruch (Dating with the ^{3}He-tritium-method: An example of bank filtration in the Oderbruch region). *Grundwasser*, **9**, 221–234 (in German with English abstract).

Suter, M., Beer, J., Bonani, G., Hofmann, H.J., Michel, D., Oeschger, H., Synal, H.-A. and Wölfli, W. (1987): ^{36}Cl studies at the ETH/SIN-AMS facility. *Nuclear Instruments and*

Methods in Physics Research B, **29**, 211–215.

Synal, H.-A., Beer, J., Bonani, G., Lukasczyk, Ch. and Suter, M. (1994): ^{36}Cl measurements at the Zürich AMS facility. *Nuclear Instruments and Methods in Physics Research B*, **92**, 79–84.

Synal, H.-A., Beer, J., Bonani, G., Suter, M. and Wölfli, W. (1990): Atmospheric transport of bomb-produced ^{36}Cl. *Nuclear Instruments and Methods in Physics Research B*, **52**, 483–488.

Taguchi, Y. (1981): Annual variation of groundwater level and temperature in the deep observation wells in the Tsukuba Science City. *Water Temperature Research*, **25**(4), 14–23 (in Japanese).

Takahashi, T., Nishida, M., Ohno, S. and Hamada, T. (1969): Tritium concentration in wine, rain and ground water. *Radioisotopes*, **18**, 560–563.

Tamers, M.A., Ronzani, C. and Scharpenseel, H.W. (1969): Observation of naturally occurring chlorine-36. *Atompraxis*, **15**, 433–437.

Tase, N. (2000): Groundwater development and its issues in the High Plains of the United States. *Research Report of Water Resources Research Center, Kyoto University*, **20**, 87–94 (in Japanese with English title).

Todd, D.K. and Mays, L.W. (2005): *Groundwater Hydrology*. 3rd Edition, John Wiley & Sons, Hoboken, 636 pp.

Togo, M., Fujino, K. and Ito, K. (1995): A survey of air borne salts in the vicinity of Mt. Fuji, central Japan —A primary report—. *Bulletin of Hosei University of Tama*, **10**, 21–41 (in Japanese with English title).

Togo, M., Kiso, Y., Suzuki, M. and Kurita, H. (1997): Investigation of air borne salts in the vicinity of Mt. Fuji; Part 2. *Bulletin of Hosei University of Tama*, **12**, 23–31 (in Japanese

with English title).

Tolstikhin, L.N. and Kamenskiy, I.L. (1969): Determination of groundwater ages by the T-^{3}He method. *Geochemistry International*, **6**, 810–811.

Torgersen, T., Habermehl, M.A., Phillips, F.M., Elmore, D., Kubik, P., Jones, B.G., Hemmick, T. and Gove, H.E. (1991): Chlorine 36 dating of very old groundwater 3. Further studies in the Great Artesian Basin, Australia. *Water Resources Research*, **27**, 3201–3213.

Tosaki, Y., Tase, N., Massmann, G., Nagashima, Y., Seki, R., Takahashi, T., Sasa, K., Sueki, K., Matsuhiro, T., Miura, T., Bessho, K., Matsumura, H. and He, M. (2007): Application of ^{36}Cl as a dating tool for modern groundwater. *Nuclear Instruments and Methods in Physics Research B*, **259**, 479–485.

Tsuchi, R. (1992): Where is the groundwater in Mt. Fuji?—Searching for the unknown mechanism. In *Mt. Fuji—All About its Nature*, Suwa, A. (ed.), Dobun-Shoin, Tokyo, pp. 225–249 (in Japanese).

Tsuchi, R. (1996): Topography, geology and water resources in Fujinomiya city. In *Report on Groundwater in Fujinomiya City*, Tsuchi, R. (ed.), Fujinomiya City Office, Fujinomiya, pp. 37–55 (in Japanese).

Tsuchi, R. (2001): *Topography and Geology of Shizuoka Prefecture*. Explanatory Text of the Geologic Map of Shizuoka Prefecture (Scale 1:200,000; Revised Edition 2001), Naigai Map, Tokyo, 92 pp. (in Japanese).

Tsuchi, R. (2002): Groundwater and springs of Fuji Volcano. In *Nature and Society of Mt. Fuji*, Fuji Sabo Work Office, Chubu Regional Bureau, Ministry of Land, Infrastructure and Transport, Fujinomiya, pp. 65–78 (in Japanese).

Tsuchi, R. (2007): Groundwater and springs of Fuji Volcano, Japan. In *Fuji Volcano*, Aramaki, S., Fujii, T., Nakada, S. and Miyaji, N. (eds.), Yamanashi Institute of Environmental

Sciences, Fujiyoshida, pp. 375–387 (in Japanese with English abstract).

Tsuya, H. (1940): Geological and petrological studies of Volcano Fuji. *Journal of Geography*, **52**, 347–361 (in Japanese).

Tsuya, H. (1968): *Geology of Volcano Mt. Fuji*. Explanatory Text of the Geologic Map of Mt. Fuji (Scale 1:50,000), Geological Survey of Japan, Tsukuba, 24 pp.

Tsuya, H., Machida, H. and Shimozuru, D. (1988): *Explanatory Note for Geologic Map of Mt. Fuji (Scale 1:50,000; Second Printing)*. Miscellaneous Map Series No. 12, Geological Survey of Japan, Tsukuba, 22 pp.

Tuniz, C., Bird, J.R., Fink, D. and Herzog, G.F. (1998): *Accelerator Mass Spectrometry: Ultrasensitive Analysis for Global Science*. CRC Press, Boca Raton, 371 pp.

Turekian, K.K., Nozaki, Y. and Benninger, L.K. (1977): Geochemistry of atmospheric radon and radon products. *Annual Review of Earth and Planetary Sciences*, **5**, 227–255.

Unozawa, A., Isobe, I., Endo, H., Taguchi, Y., Nagai, S., Ishii, T., Aihara, T. and Oka, S. (1988): *Explanatory Text of the Environmental Geologic Map of the Tsukuba Science City and its Surroundings (Scale 1:25,000)*. Miscellaneous Map Series No. 23-2, Geological Survey of Japan, Tsukuba, 139 pp. (in Japanese with English abstract).

Viezee, W. and Singh, H.B. (1980): The distribution of beryllium-7 in the troposphere: Implications on stratospheric/tropospheric air exchange. *Geophysical Research Letters*, **7**, 805–808.

Vogt, S., Elmore, D. and Fritz, S.J. (1994): ^{36}Cl in shallow, perched aquifers from central Indiana. *Nuclear Instruments and Methods in Physics Research B*, **92**, 398–403.

Vogt, S. and Herpers, U. (1988): Radiochemical separation techniques for the determination of long-lived radionuclides in meteorites by means of accelerator-mass-spectrometry. *Fresenius' Zeitschrift für Analytische Chemie*, **33**, 186–188.

Wahlen, M., Deck, B., Weyer, H., Kubik, P., Sharma, P. and Gove, H. (1991): ^{36}Cl in the stratosphere. *Radiocarbon*, **33**, 257–258 (abstract only).

Walker, G.R., Jolly, I.D., Stadter, M.H., Leaney, F.W., Davie, R.F., Fifield, L.K., Ophel, T.R. and Bird, J.R. (1992): Evaluation of the use of ^{36}Cl in recharge studies. In *Isotope Techniques in Water Resources Development 1991*, IAEA, Vienna, pp. 19–29.

Yabusaki, S., Tsujimura, M. and Tase, N. (2003): Recent trend of tritium concentration in precipitation in Kanto Plain, Japan. *Bulletin of the Terrestrial Environment Research Center, the University of Tsukuba*, **4**, 119–124 (in Japanese with English abstract).

Yamamoto, S. (1970): Hydrologic study of volcano Fuji and its adjacent areas —A tentative approach to volcano hydrology—. *Geographical Review of Japan*, **43**, 267–284 (in Japanese with English abstract).

Yamamoto, S. (1971): Hydrologic study of volcano Fuji and its adjacent areas. In *Mt. Fuji*, Research Report of the Co-operative Scientific Survey of Mt. Fuji, Fuji Kyuko, Tokyo, pp. 151–209 (in Japanese with English abstract).

Yamamoto, S. (1995): *Volcano Body Springs in Japan*. Kokon-Shoin, Tokyo, 264 pp.

Yamamoto, S. (1996): Springs of Japan. *Environmental Geology*, **27**, 118–119.

Yamamoto, S, Takamura, H. and Higuchi, M. (1981): A note on the volcano slope springs, eastern part of Mt. Fuji, Japan. *Hydrology*, **11**, 47–52 (in Japanese with English title).

Yasuhara, M., Kazahaya, K. and Marui, A. (2007): An isotopic study on where, when, and how groundwater is recharged in Fuji Volcano, central Japan. In *Fuji Volcano*, Aramaki, S., Fujii, T., Nakada, S. and Miyaji, N. (eds.), Yamanashi Institute of Environmental Sciences, Fujiyoshida, pp. 389–405 (in Japanese with English abstract).

Yasuhara, M., Marui, A., Fuseya, M. and Ishii, T. (1991): Physical properties of the Joso Clay in the Tsukuba Upland from the hydrological point of view. *Geographical Review of*

Japan, **64A**, 719–727 (in Japanese with English abstract).

Yasuhara, M., Marui, A. and Kazahaya, K. (1997): Stable isotopic composition of groundwater from Mt. Yatsugatake and Mt. Fuji, Japan. In *Hydrochemistry*, Peters, N.E. and Coudrain-Ribstein, A. (eds.), IAHS Publication 244, pp. 335–344.

Yasuhara, M., Marui, A., Kazahaya, K., Suzuki, Y. and Takayama, S. (1995): An isotopic study toward the protection of groundwater resources in Mt. Fuji, Japan. In *Solutions '95—Managing the Effects of Man's Activities on Groundwater*, Proceedings of the XXVI IAH Congress, pp. 1224–1229.

Yasuhara, M., Marui, A., Tanaka, T. and Ishii, T. (1990): Physical properties of soils and vertical groundwater movement in upper parts of the Tsukuba Upland —A case study at Higashi, Tsukuba City—. *Bulletin of the Geological Survey of Japan*, **41**, 507–516 (in Japanese with English abstract).

Yoshioka, R., Kitaoka, K. and Koizumi, N. (1993): Groundwater flow systems inferred from isotopic compositions —A case study of Mishima city and its vicinity—. *Journal of Groundwater Hydrology*, **35**, 271–285 (in Japanese with English abstract).

Zerle, L., Faestermann, T., Knie, K., Korschinek, G., Nolte, E., Beer, J. and Schotterer, U. (1997): The ^{41}Ca bomb pulse and atmospheric transport of radionuclide. *Journal of Geophysical Research*, **102**(D16), 19517–19527.